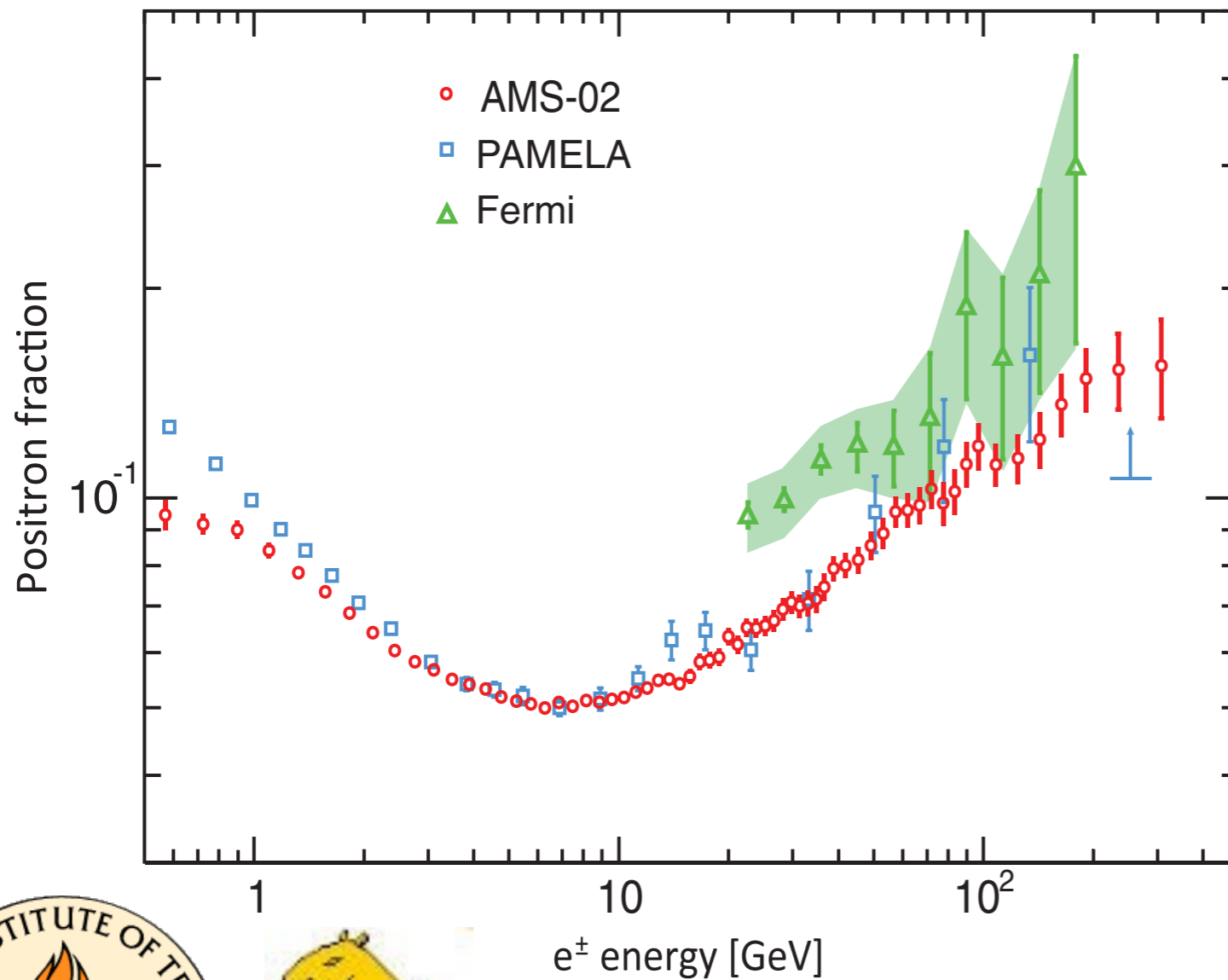


Update after AMS: implications on Dark Matter, local pulsar and supernova remnant sources



The AMS-02 experiment on ISS

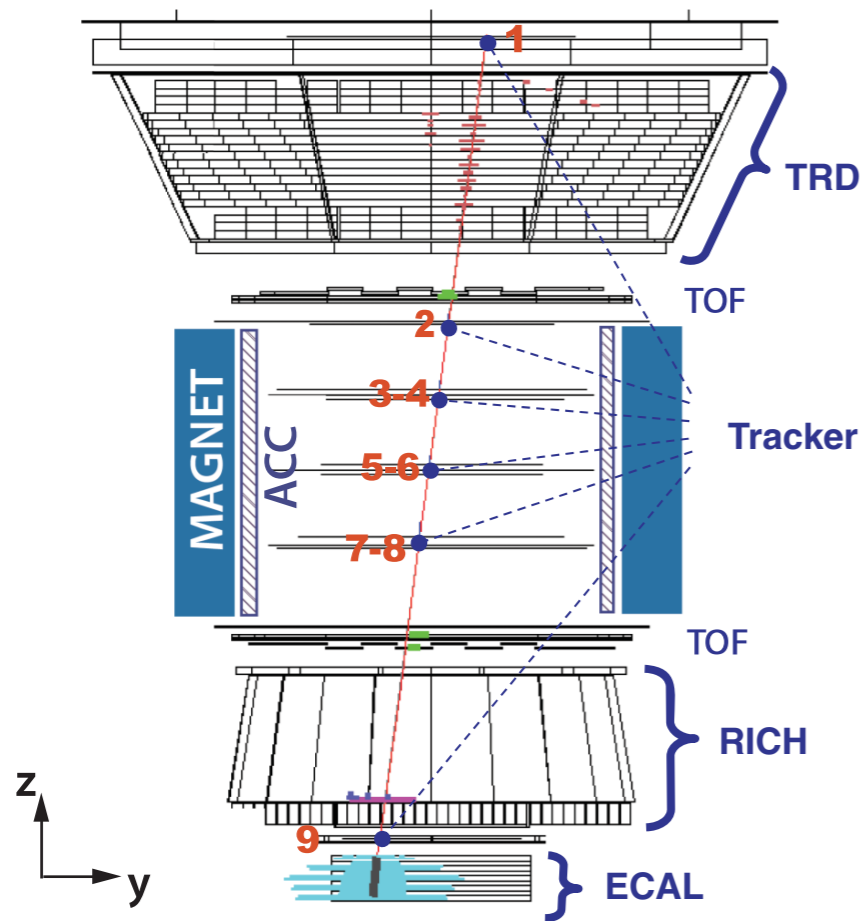
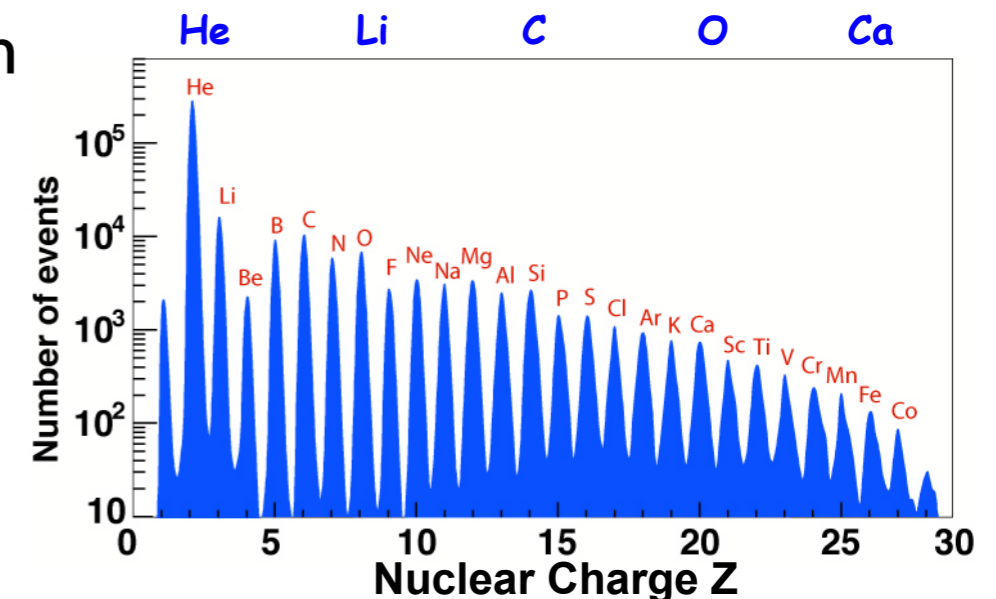
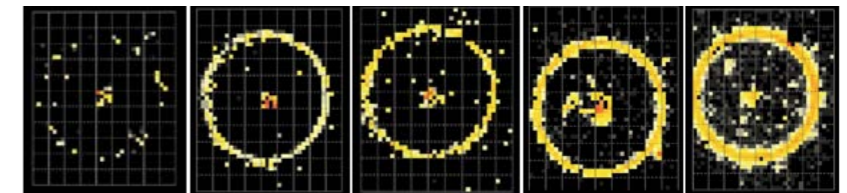


FIG. 1 (color). A 1.03 TeV electron event as measured by the AMS detector on the ISS in the bending (y - z) plane. Tracker planes 1–9 measure the particle charge and momentum. The TRD identifies the particle as an electron. The TOF measures the charge and ensures that the particle is downward-going. The RICH independently measures the charge and velocity. The ECAL measures the 3D shower profile, independently identifies the particle as an electron, and measures its energy. An electron is identified by (i) an electron signal in the TRD, (ii) an electron signal in the ECAL, and (iii) the matching of the ECAL shower energy and the momentum measured with the tracker and magnet.

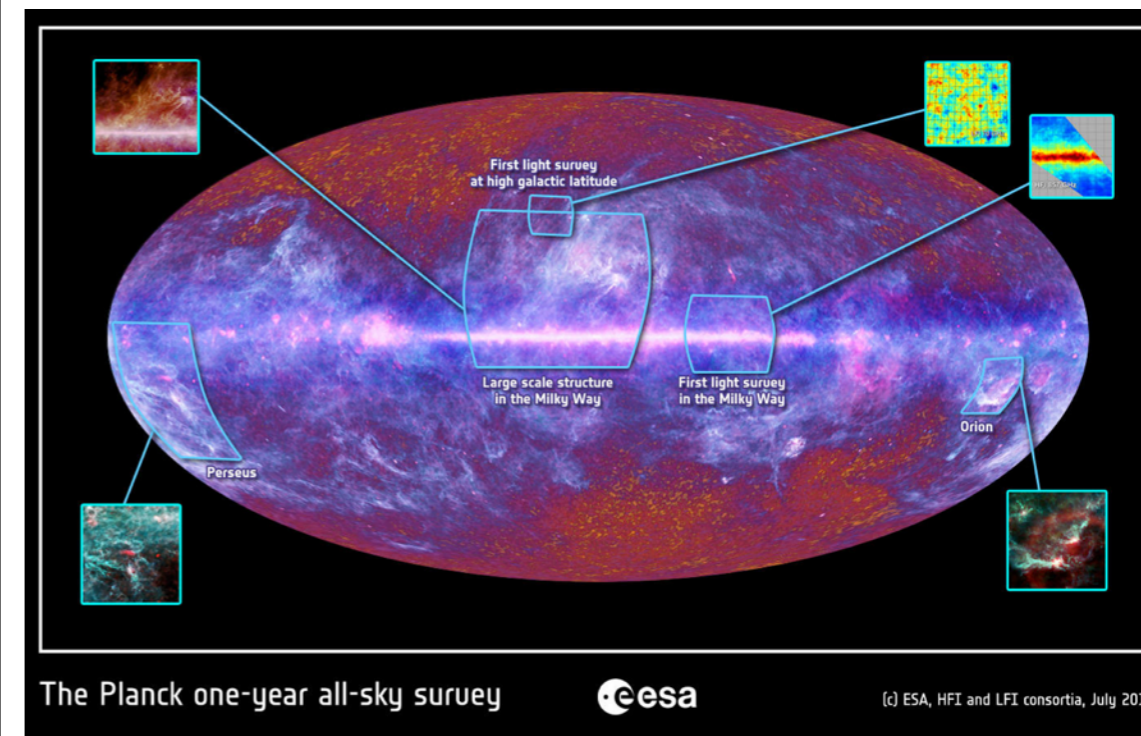
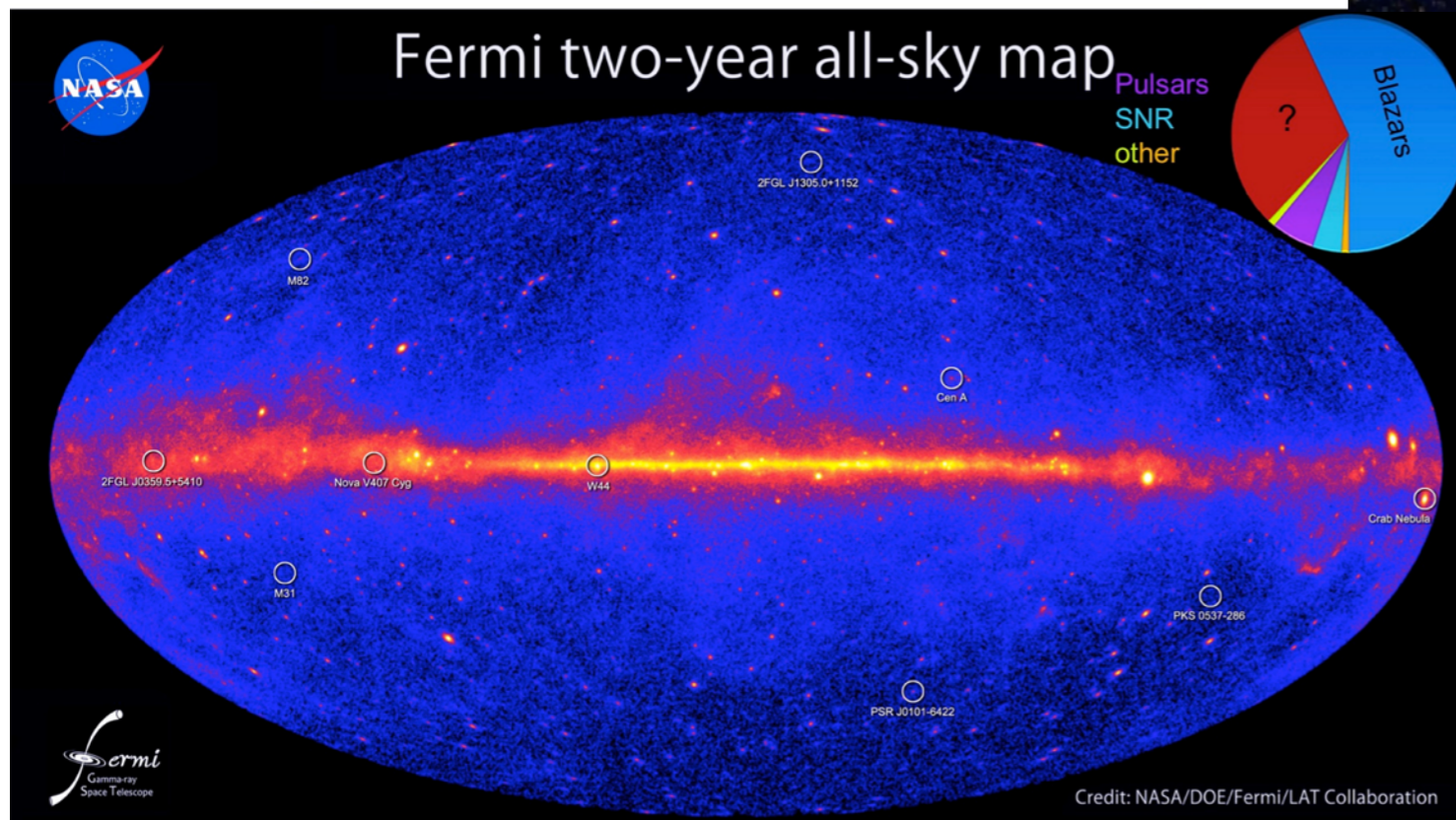
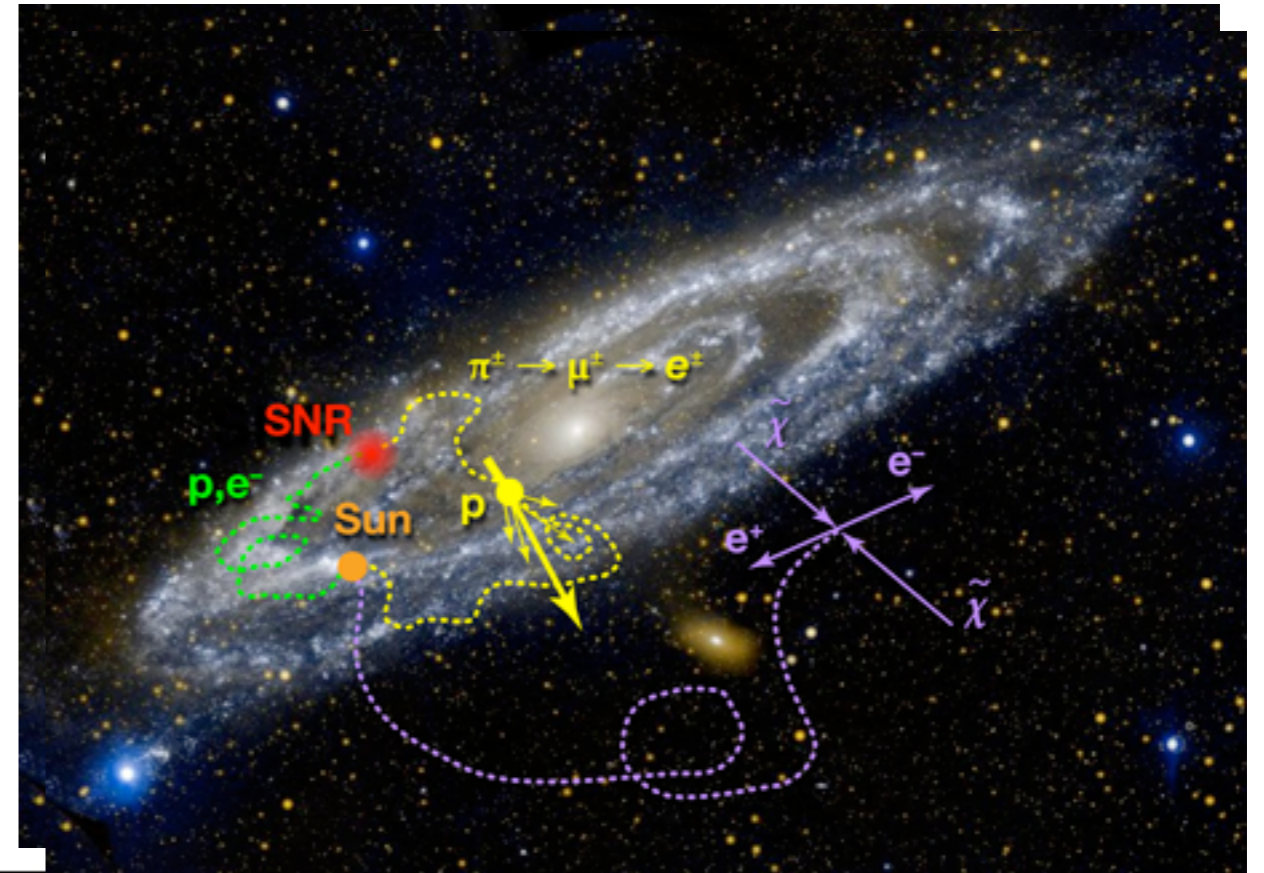
Lunched on May 2011, will collect data for 20 yrs.
Will measure all CR nuclei species up to Ni.

positron fraction,
positrons, electrons
spectra,
antiproton/proton
B/C, Be 10/Be 9



Relevance of CR measurements

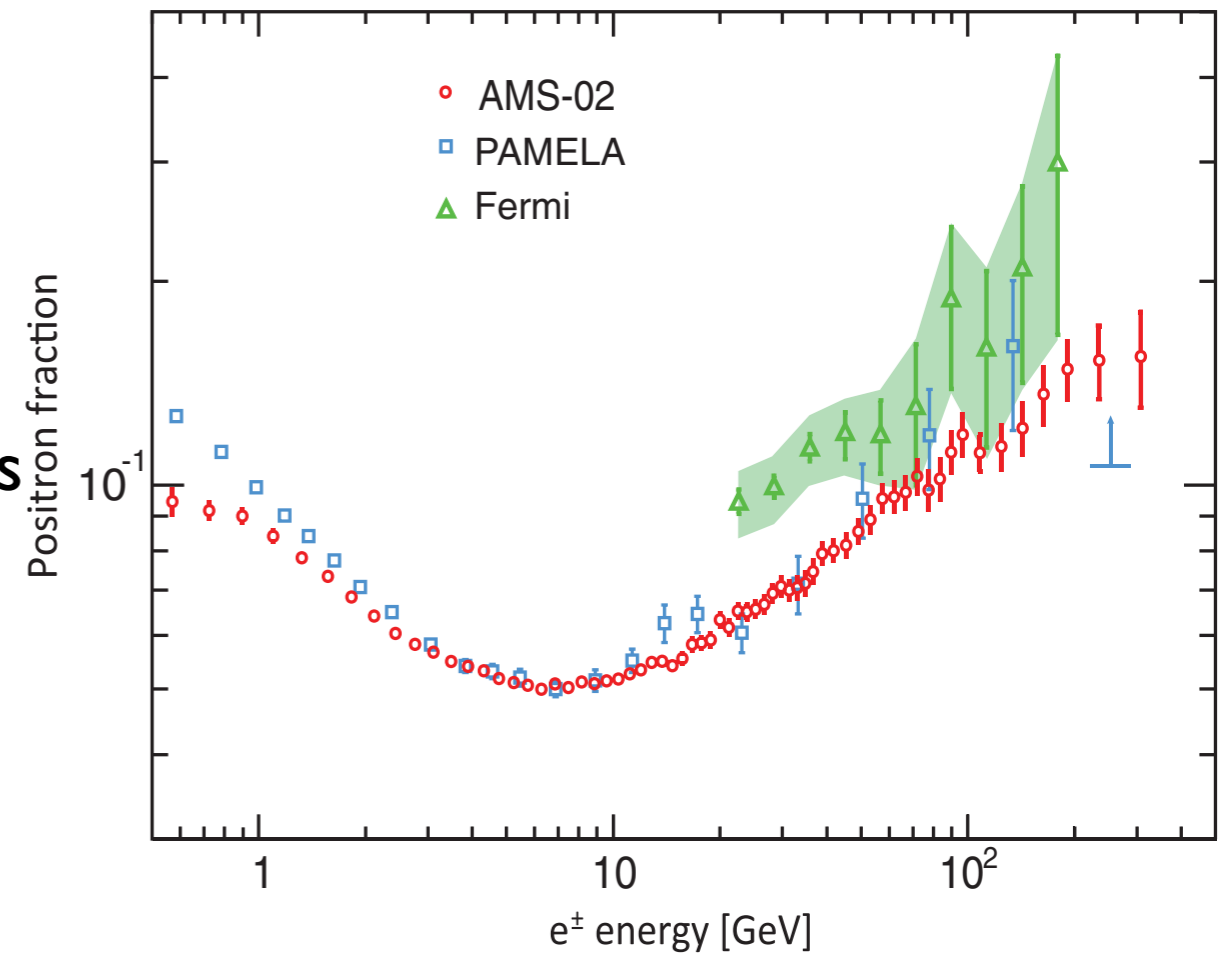
With CR spectral measurements we can understand the properties of the ISM, and probe sources of high energy CRs. Antimatter CRs indirectly also probe Dark Matter (DM). Combine with gamma-ray and radio observations.



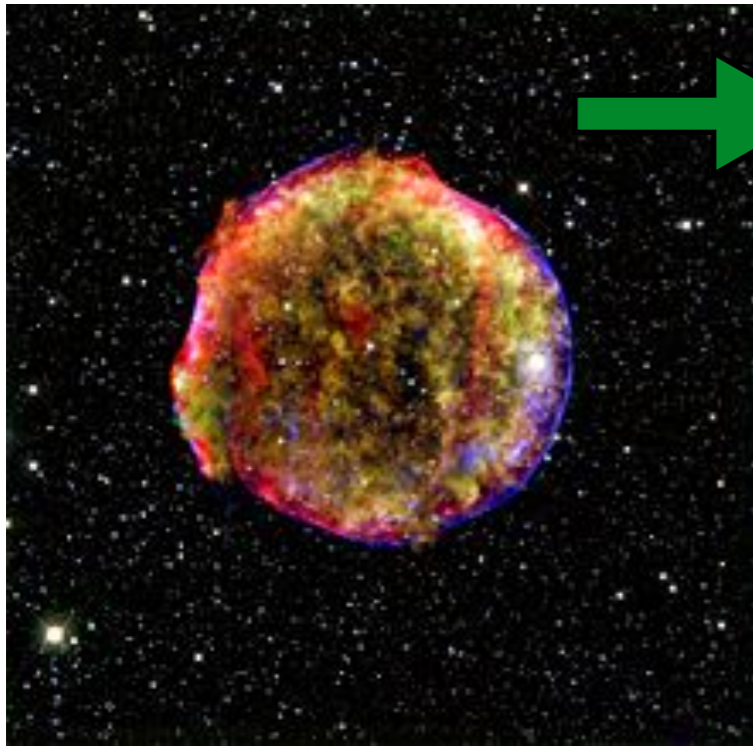
AMS-02 positron fraction results

Positron Fraction: $e^+/(e^- + e^+)$

- Decrease of positron fraction at low energies in agreement with earlier measurements and theoretical expectations (we expected that: standard secondary/primary CRs)
- Further confirmation of the rise of the positron fraction above 10 GeV (seen by HEAT/PAMELA) with great accuracy (good to know)
- Change in the “slope” of the positron fraction between 20 and 250 GeV (interesting for DM)
- No obvious deviation from a smooth rise of the fraction above 10 GeV (interesting as well but needs further analysis; we will revisit that)
- Upper limit on anisotropy of CR positron fraction. Only in very extreme scenarios did we expect to see an anisotropy (see discussion later)



Why the *Rise* of the positron fraction is interesting:



For all *primary* *CRs:

$$q(E)^{inj} \sim E^{-\gamma} \quad \text{at injection into the ISM}$$

For CR protons: $n(E)^p = q(E)\tau_{Diff}$

with $\tau_{Diff} \sim E^{-\delta}$ Thus: $n(E)^p \sim E^{-\gamma-\delta}$

For CR electrons: $n(E)^{e^-} \sim \frac{q(E)\tau_{loss}}{\sqrt{D(E)\tau_{loss}}}$

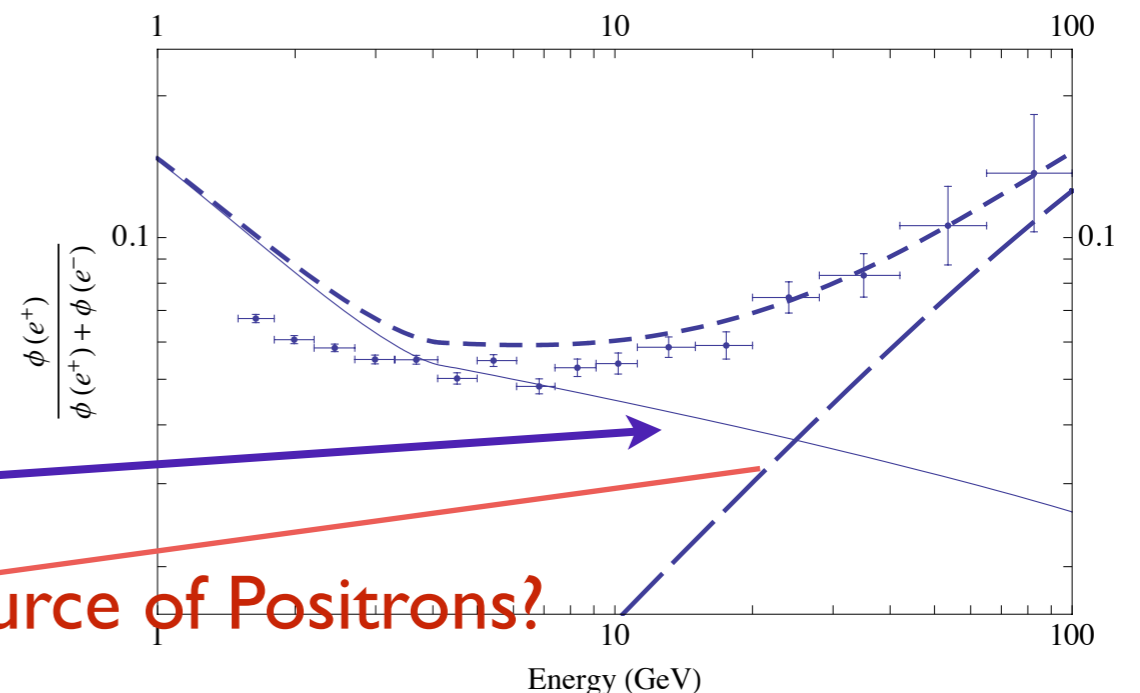
with: $\tau_{loss} \sim E^{-1}$ Thus: $n(E)^{e^-} \sim E^{-\gamma-1+1/2-\delta/2}$

For CR positrons (secondary CRs):

$$pp \rightarrow K^\pm \pi^\pm \rightarrow e^\pm$$

Thus: $n(E)^{e^+} \sim E^{-\gamma-\delta-1+1/2-\delta/2}$

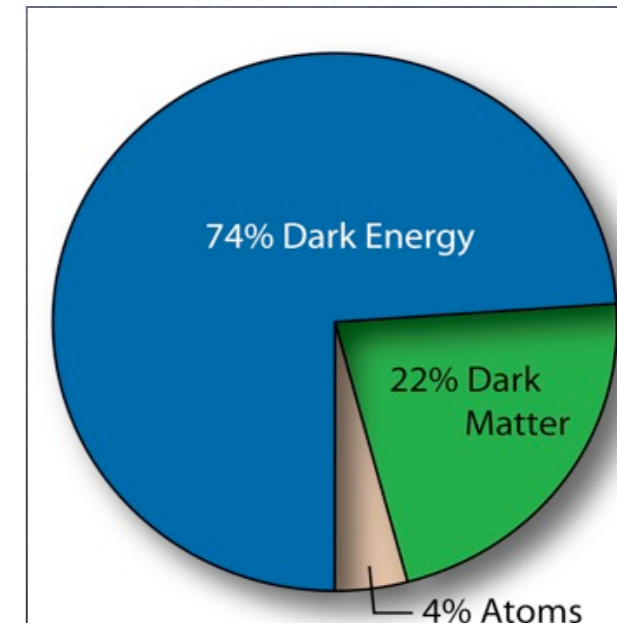
Expect: $\frac{n(E)^{e^+}_{sec}}{n(E)^{e^-}_{prim}} \sim E^{-\delta}$

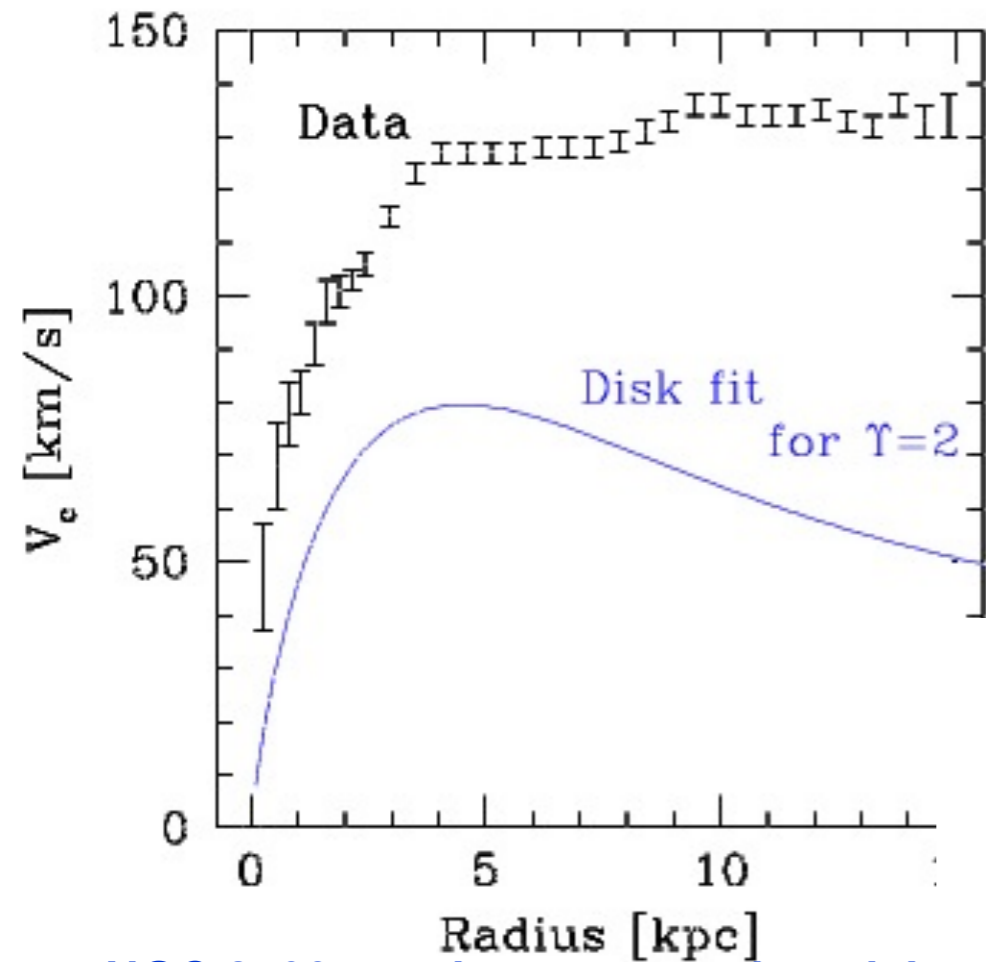


Additional Source of Positrons?

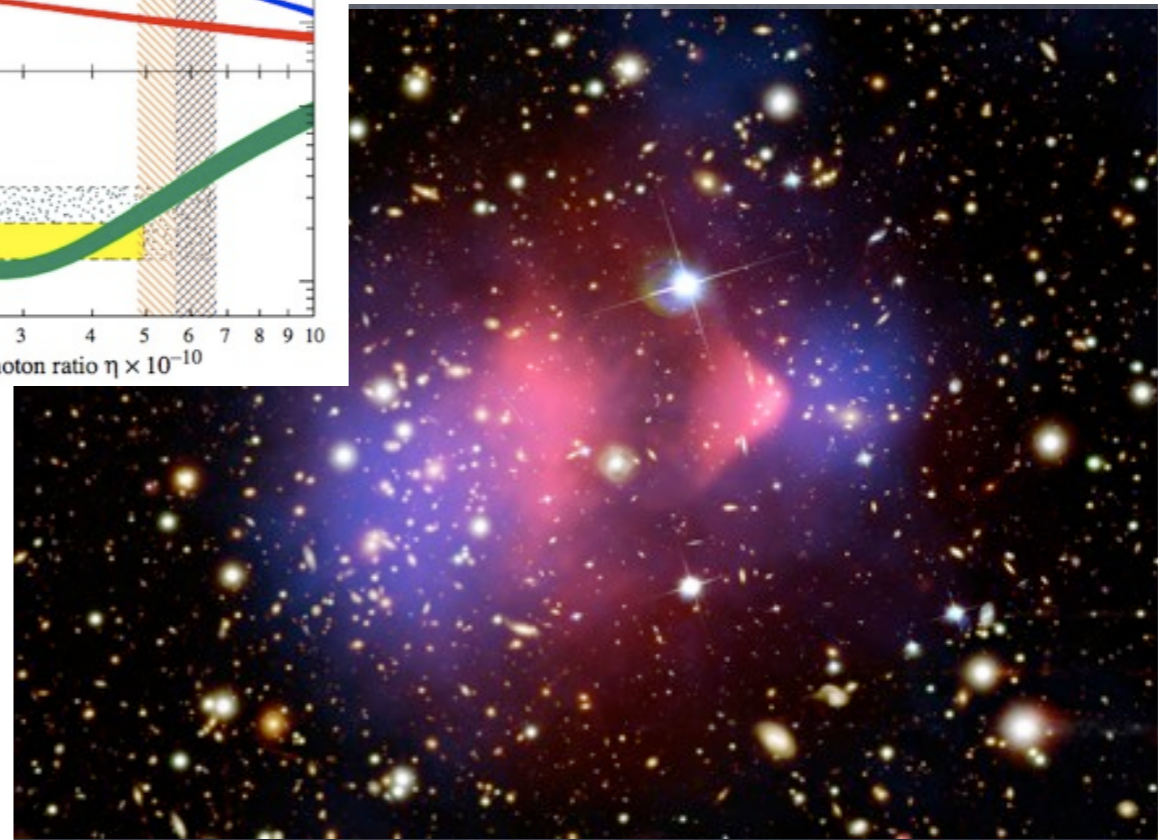
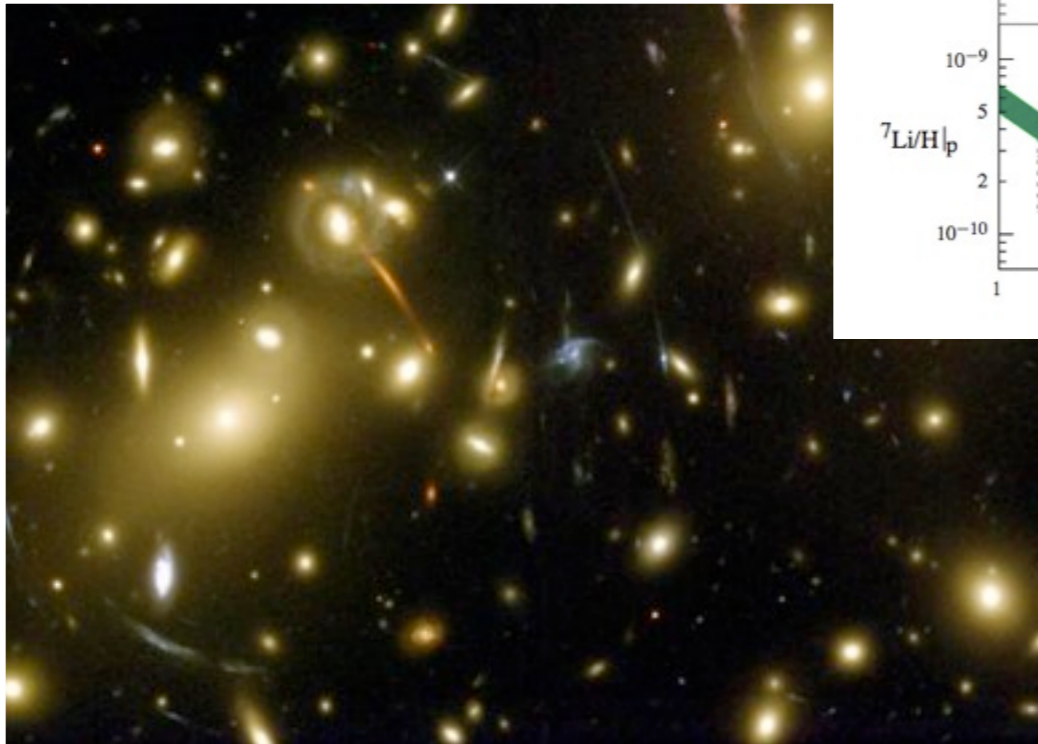
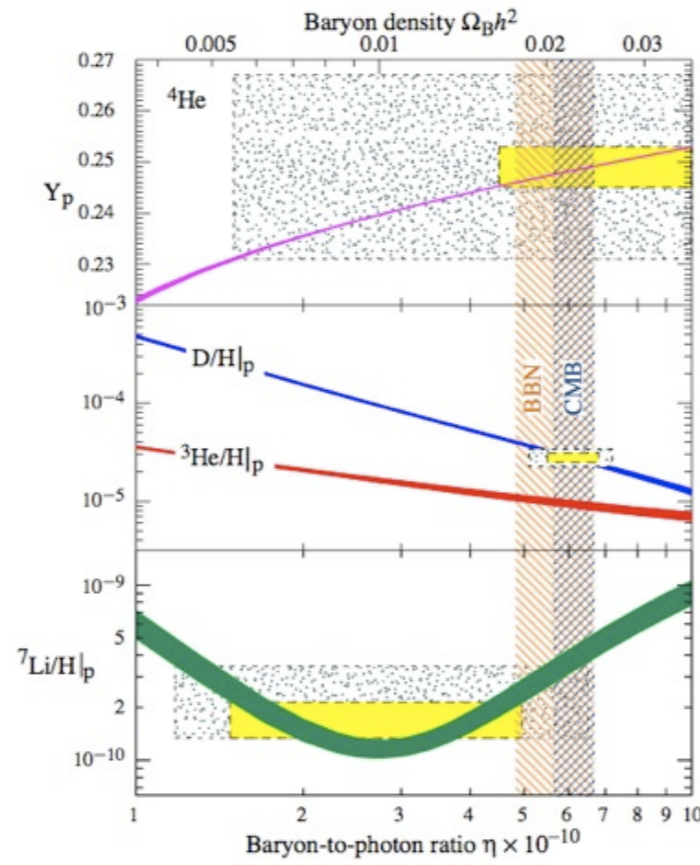
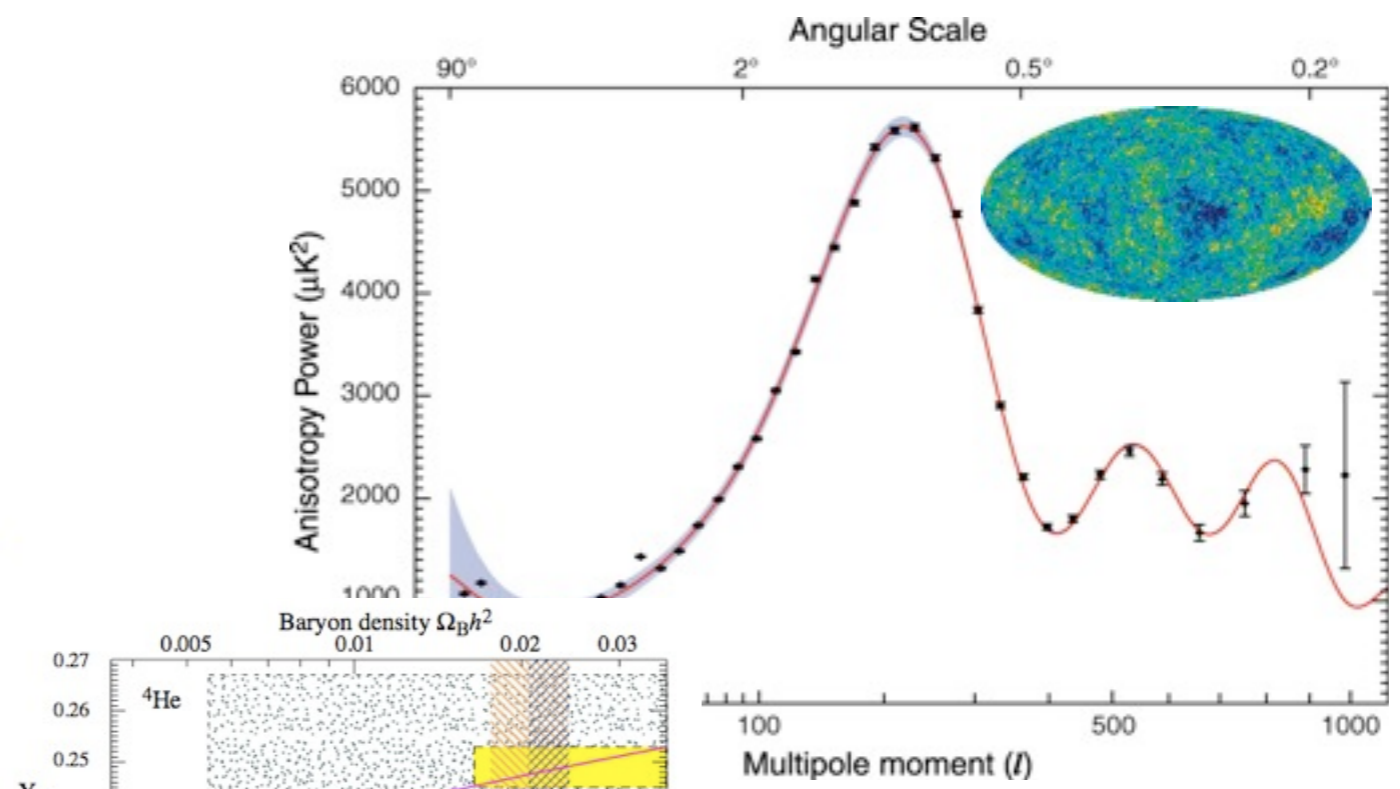
evidence for CDM

- galactic rotation curves
- velocity dispersion of galaxies in clusters
- CMB data and SN Ia data
- distribution of galaxies
- strong lensing measurements of background objects (usually galaxies)
- “collisions” of galaxy clusters (bullet cluster)
- success of BBN (DM is non-baryonic)
- growth of structure (cold DM)

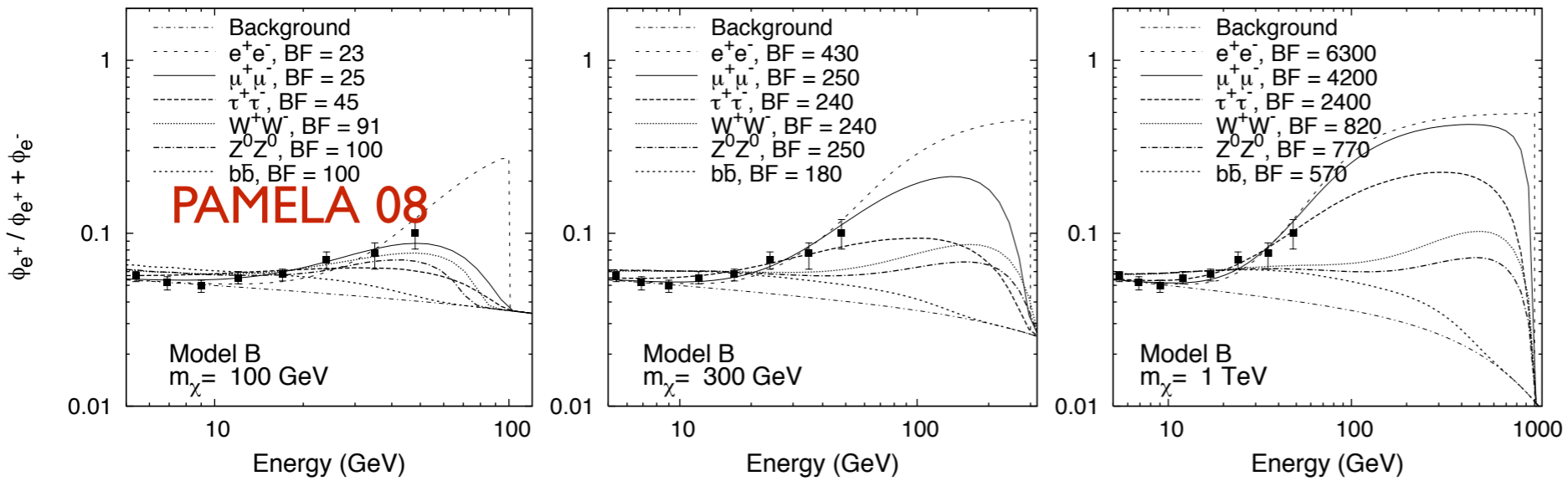




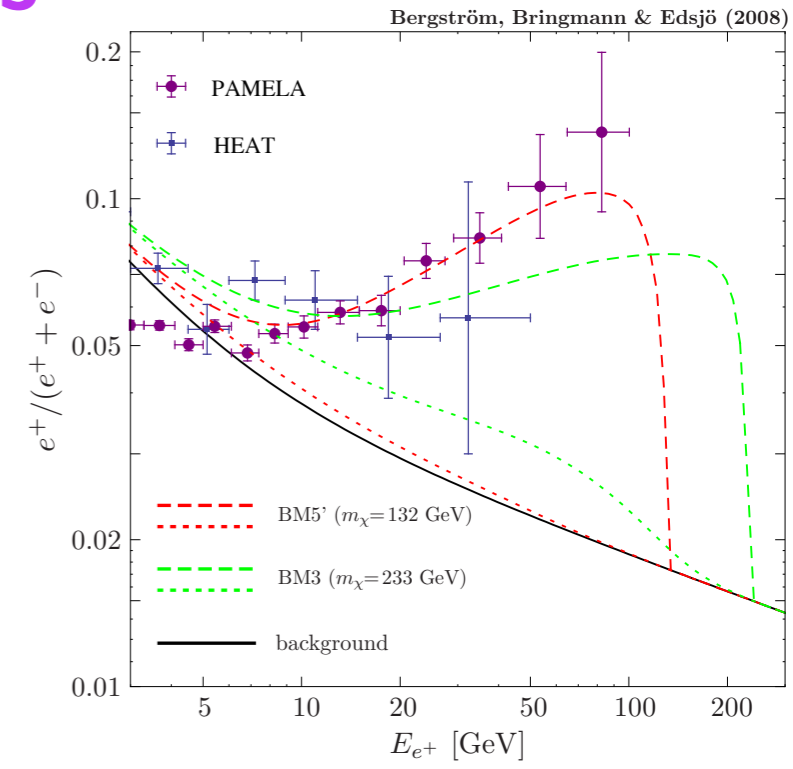
NGC 2403 rotation curve and model



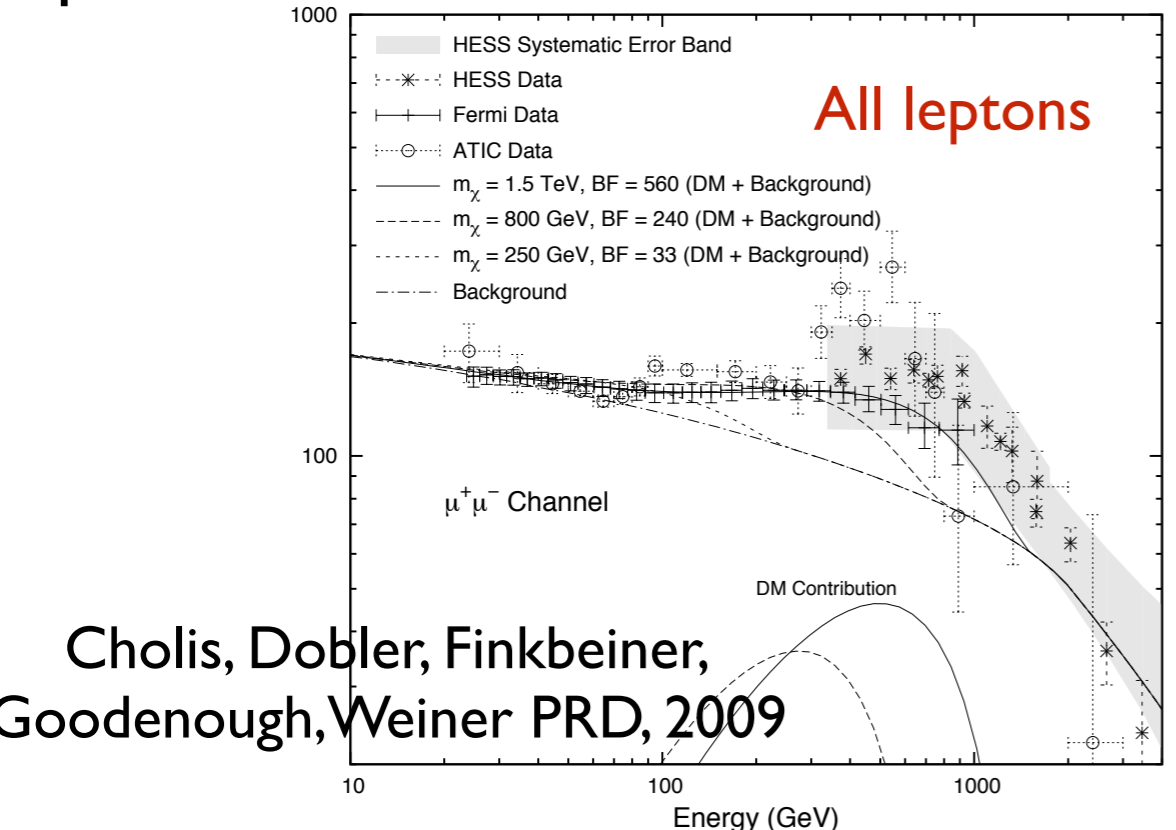
Implications of the positron fraction for Dark Matter annihilation models



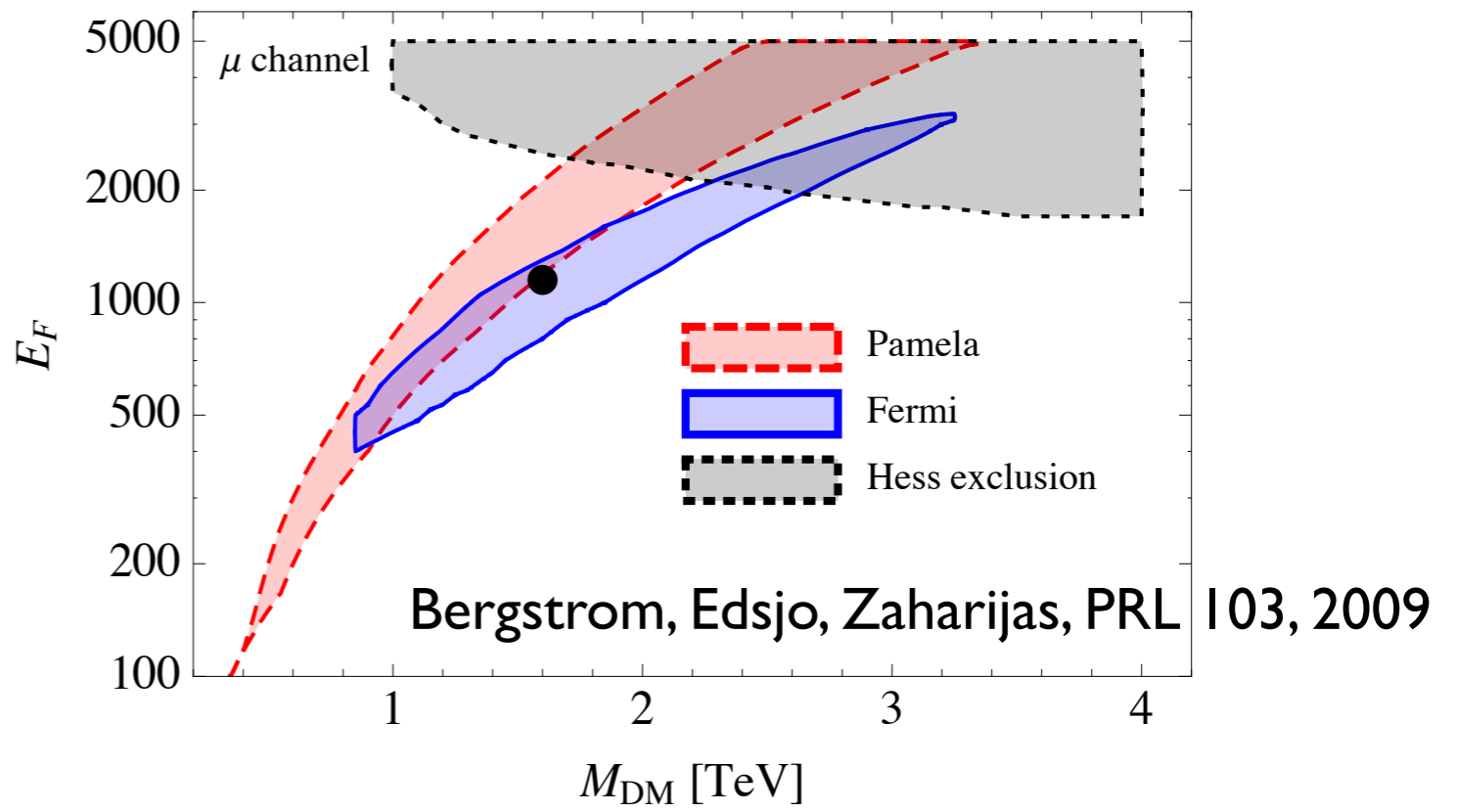
Cholis, Goodenough, Hooper, Simet, Weiner PRD, 2009



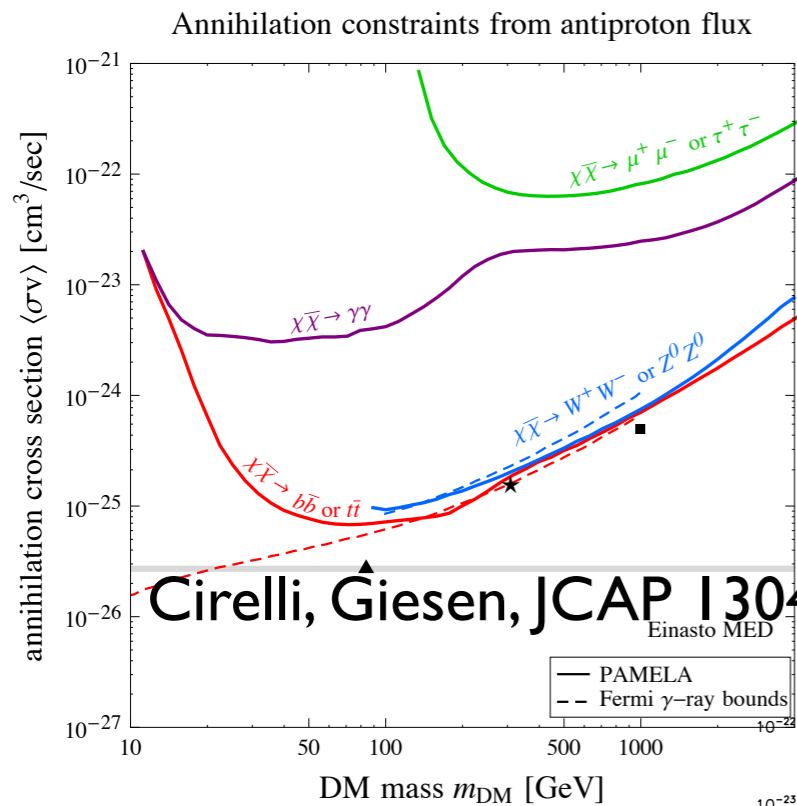
Clear preference for leptophilic DM to account for the rise of the positron fraction spectrum



Cholis, Dobler, Finkbeiner, Goodenough, Weiner PRD, 2009

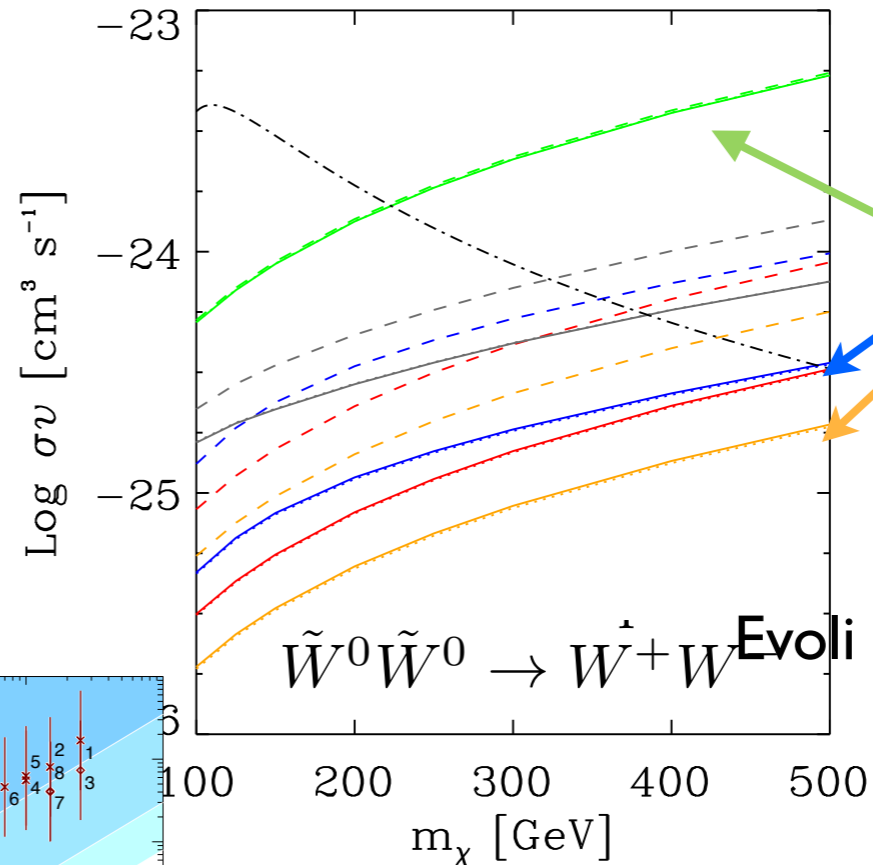


Antiprotons/Gamma-Rays/CMB



Cirelli, Giesen, JCAP 1304 (2013) 015

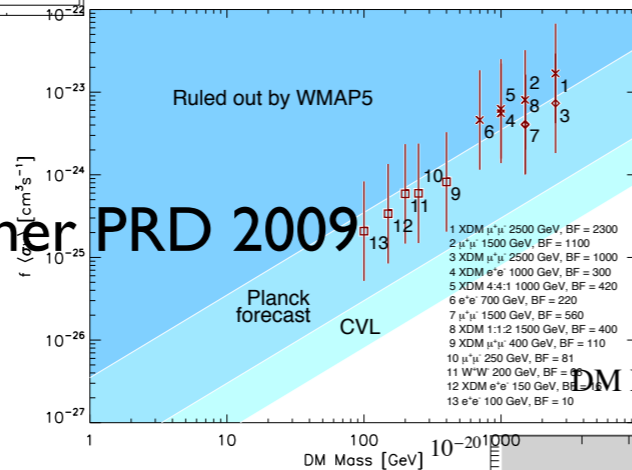
Einasto MED



Different astrophysical assumptions on the properties of the ISM

Evoli et al. PRD 2012

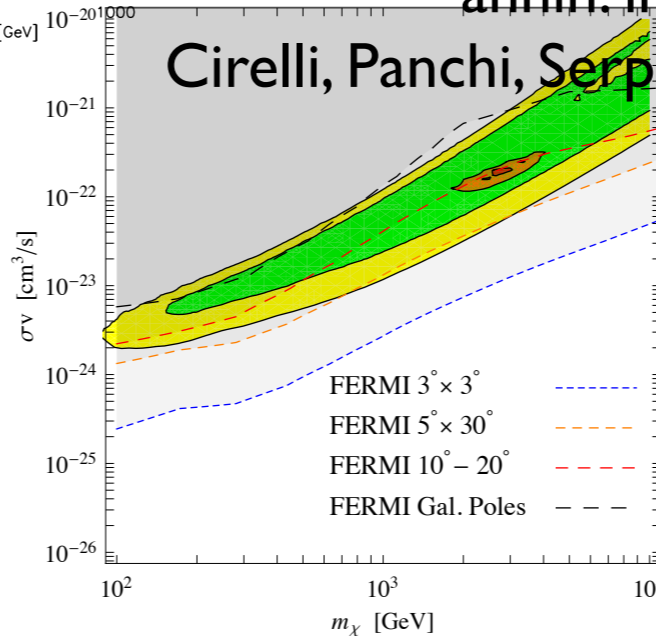
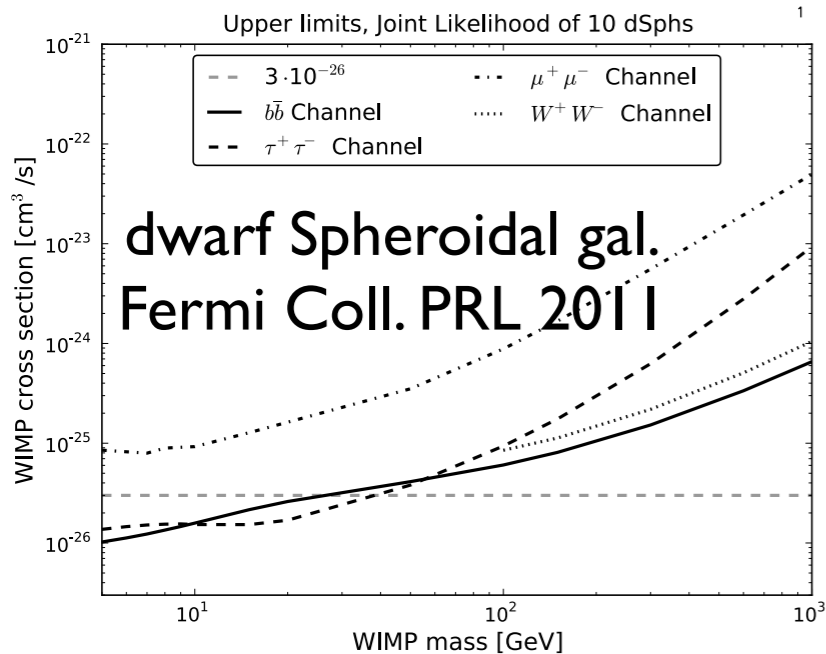
Slatyer, Padmanabhan, Finkbeiner PRD 2009



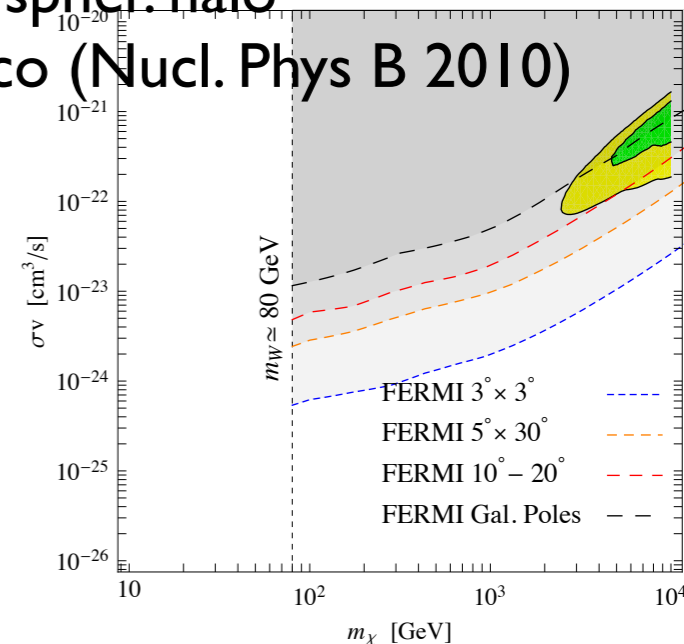
DM DM $\rightarrow \tau\tau$, Einasto profile

DM DM $\rightarrow WW$, Einasto profile

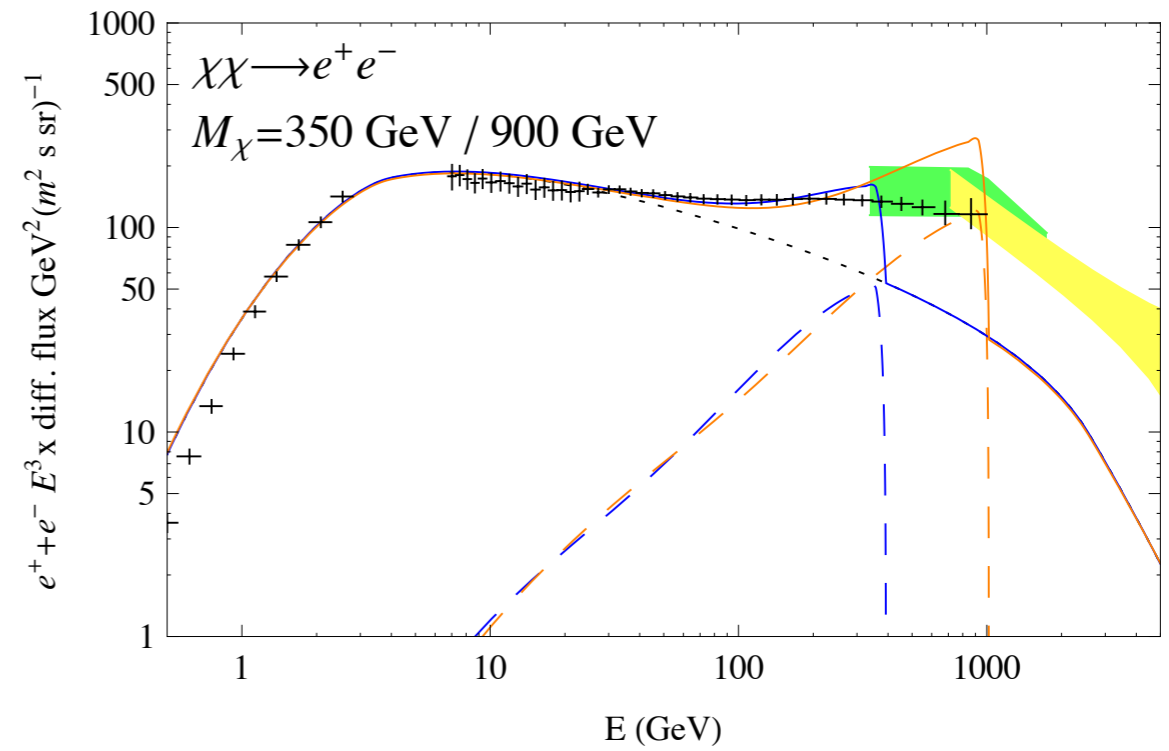
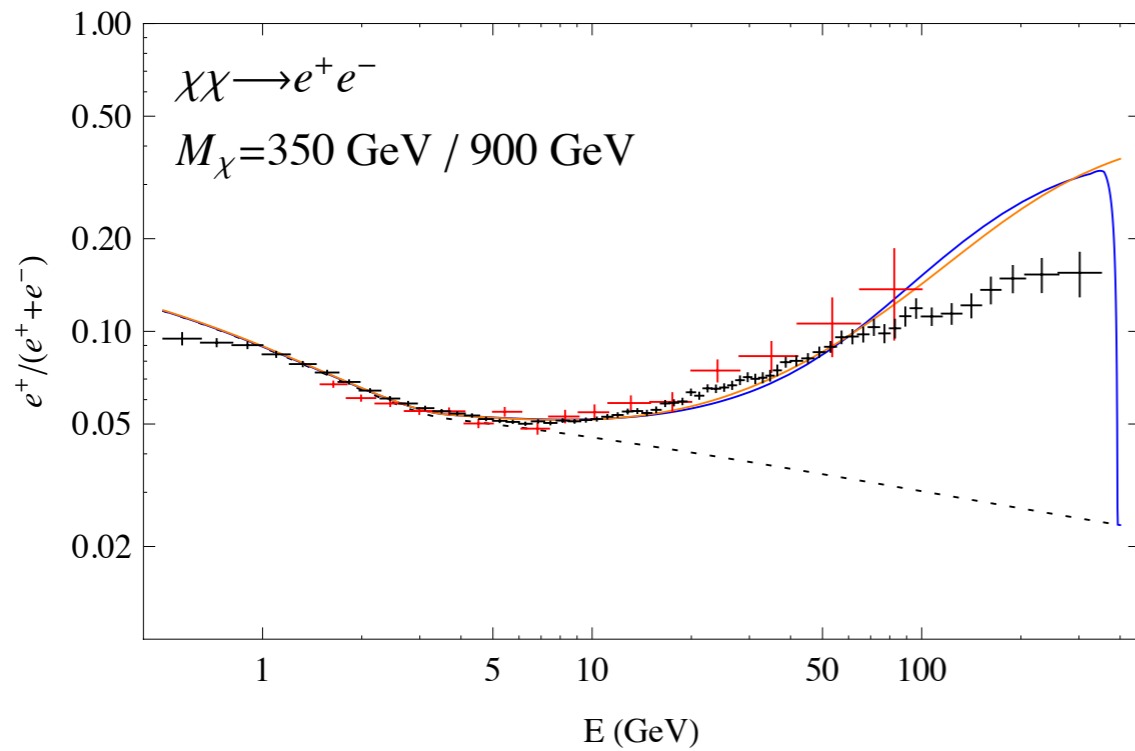
annih. in spher. halo



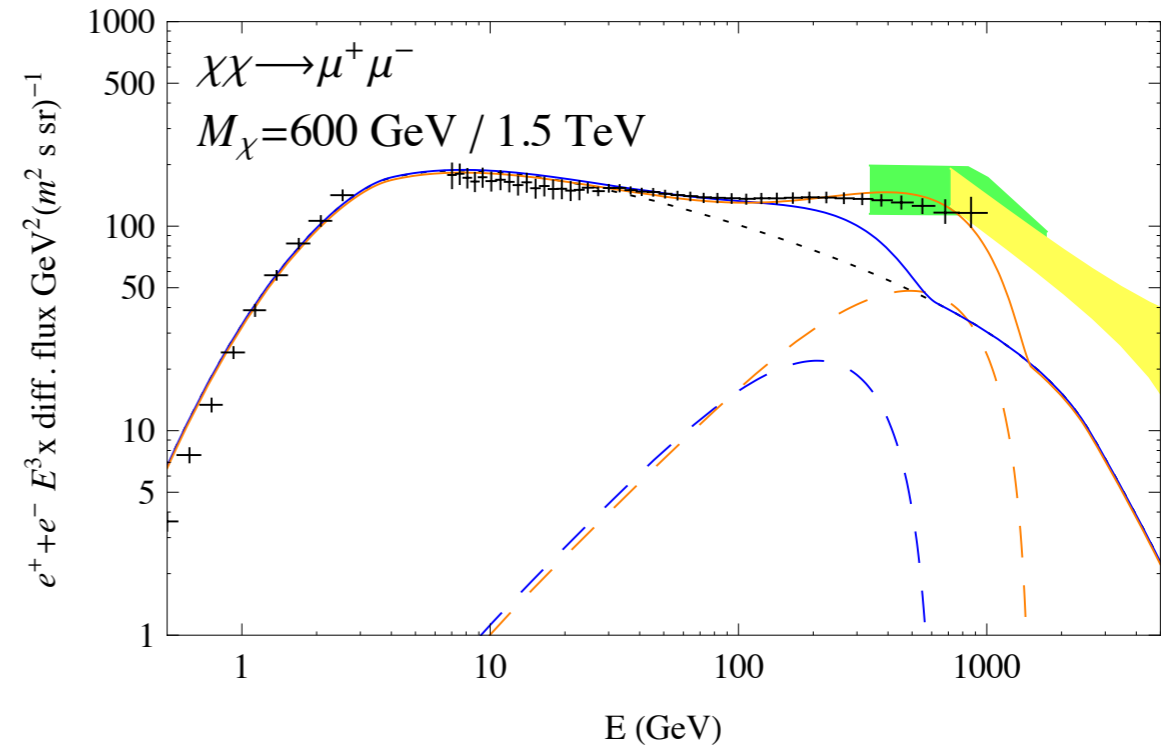
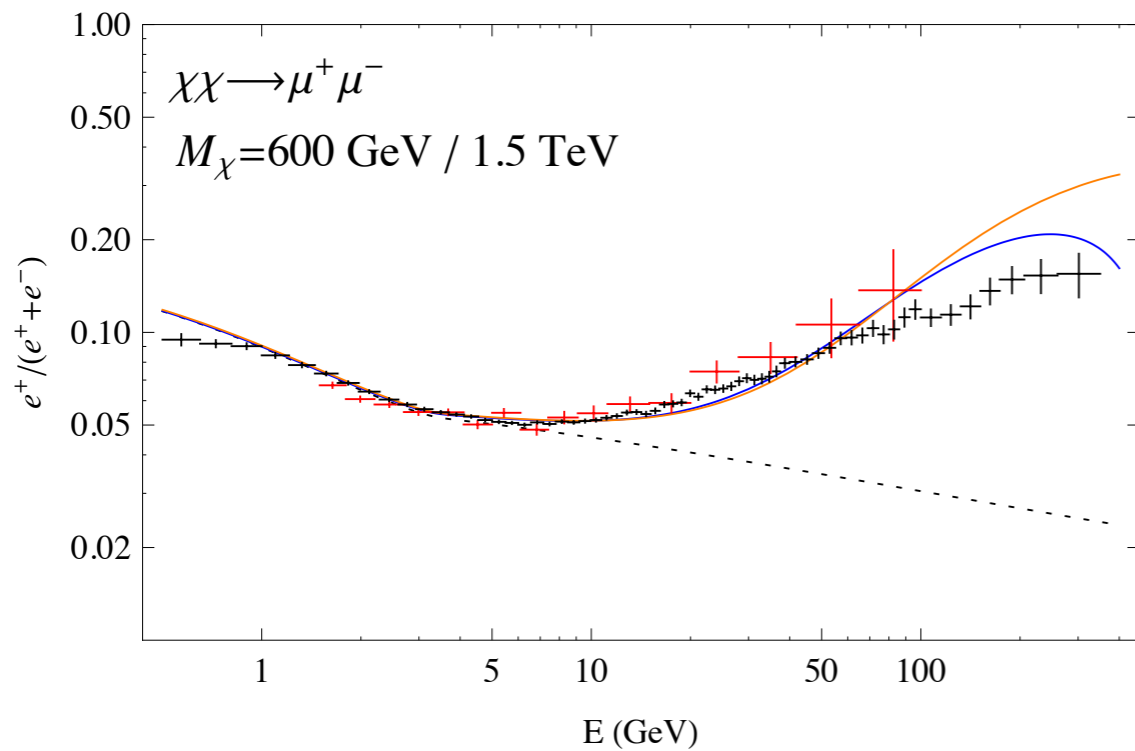
Cirelli, Panichi, Serpico (Nucl. Phys B 2010)



Adding AMS-02

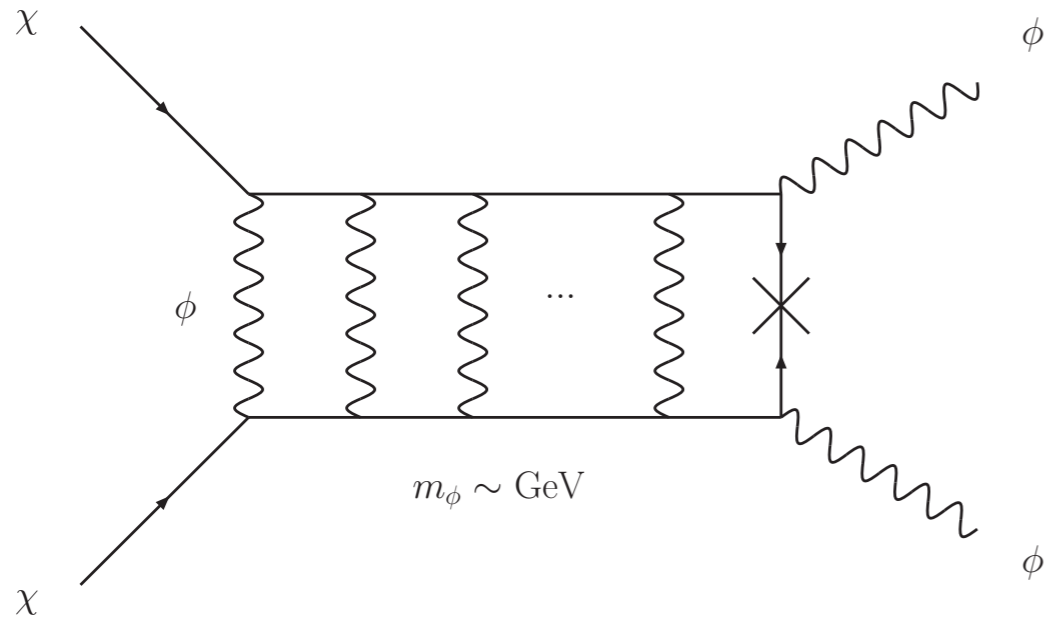


IC, Dan Hooper, PRD 88 023013, 2013



Very poor fit, and clearly inconsistent with the change of the positron fraction slope.

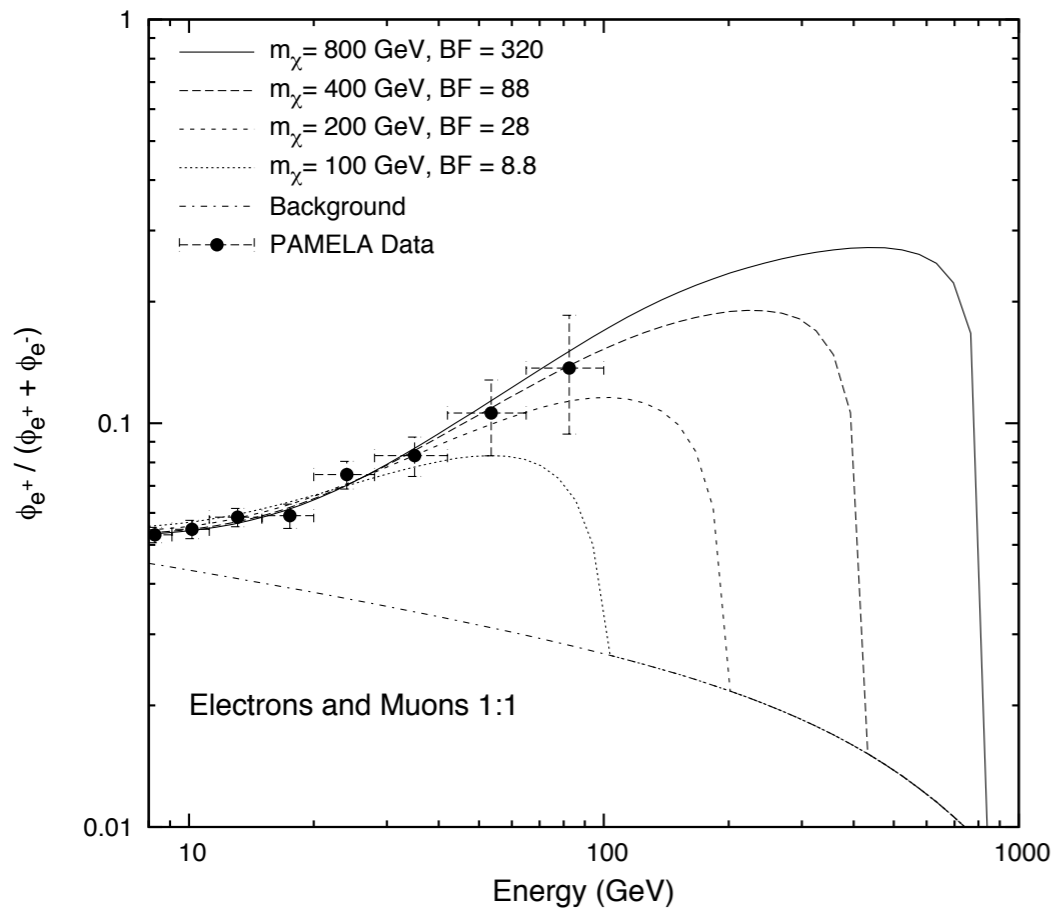
Models with Sommerfeld annihilation (Arkani-Hamed et al. 2008)



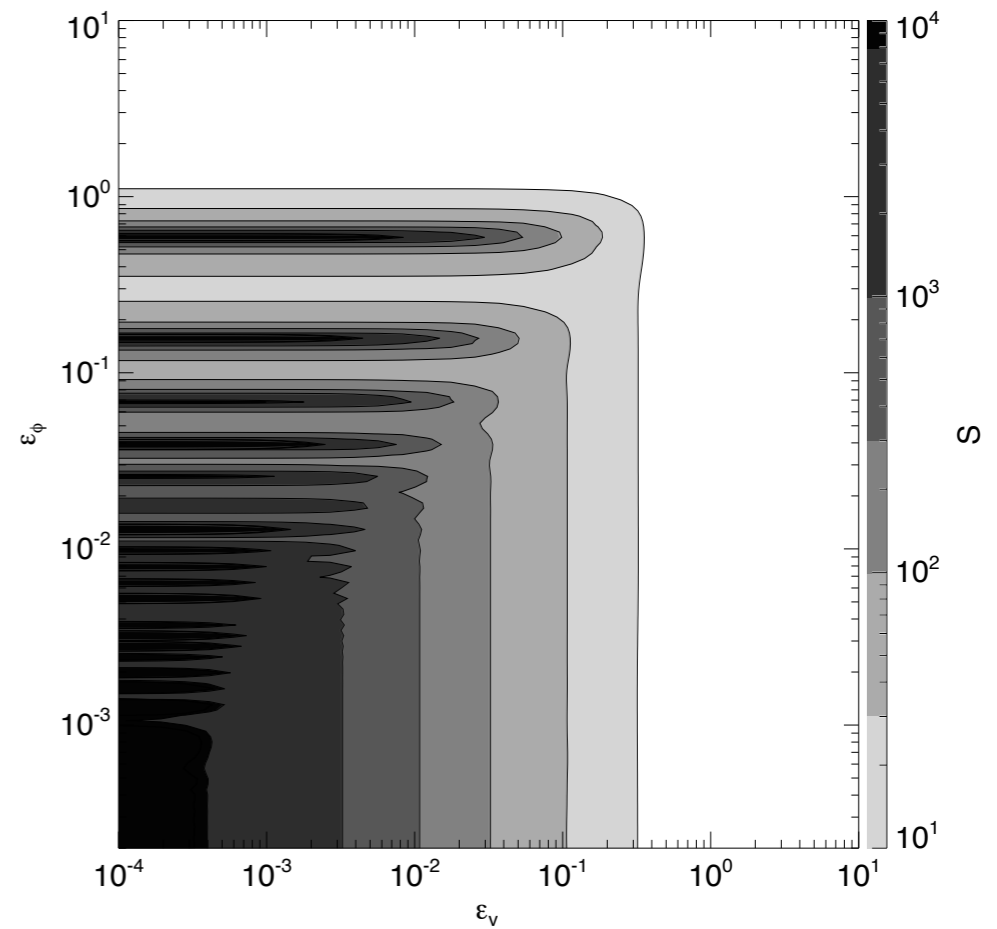
phi mixing with the SM higgs $\kappa\phi^2 h^\dagger h$

$$\langle\phi\rangle \sim m_\phi$$

or mix with EM $F'_{\mu\nu} F^{\mu\nu}$

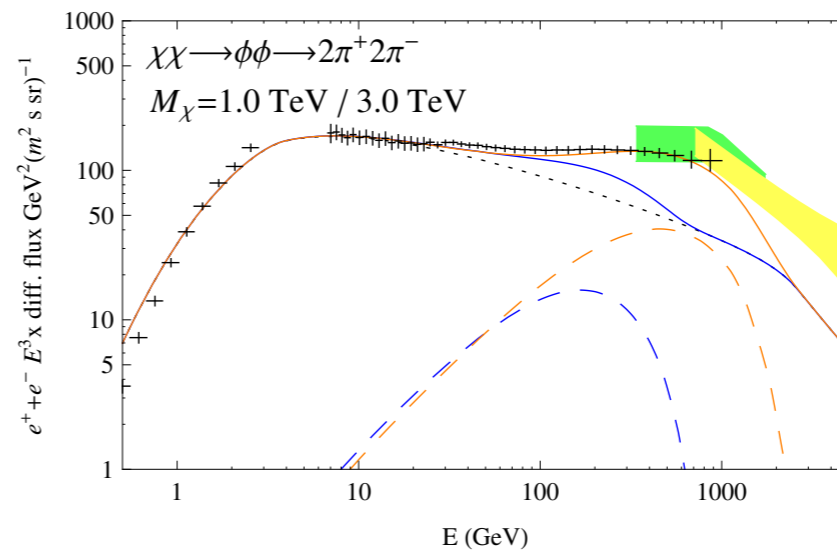
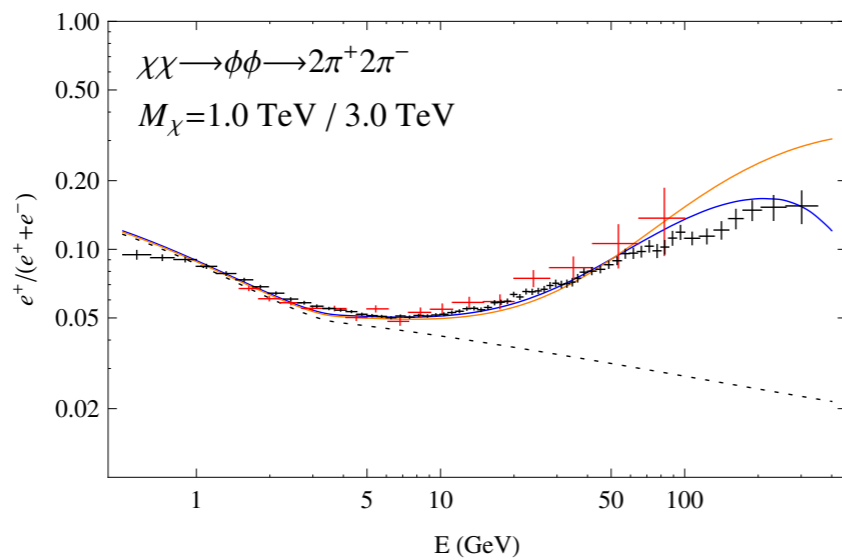
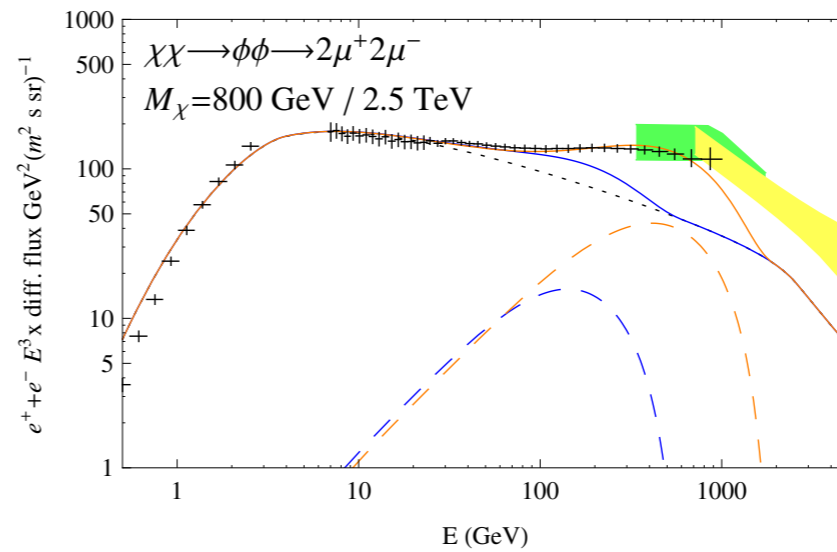
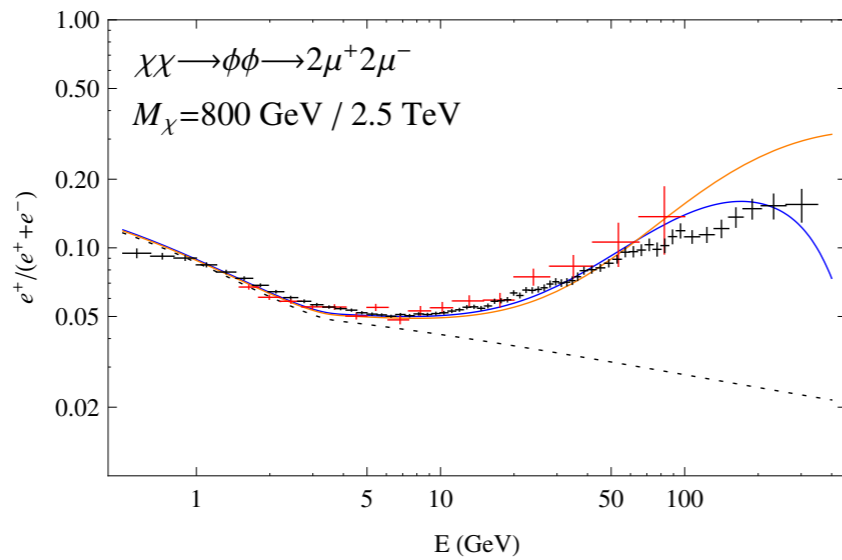
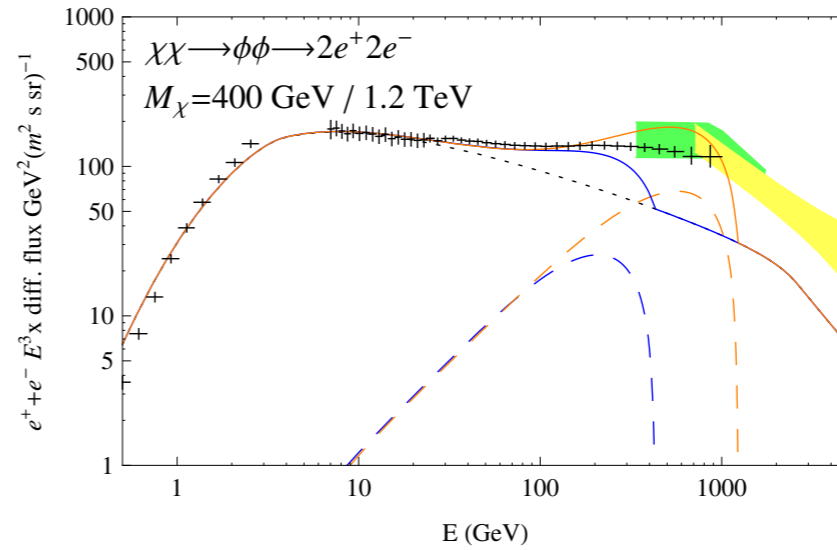
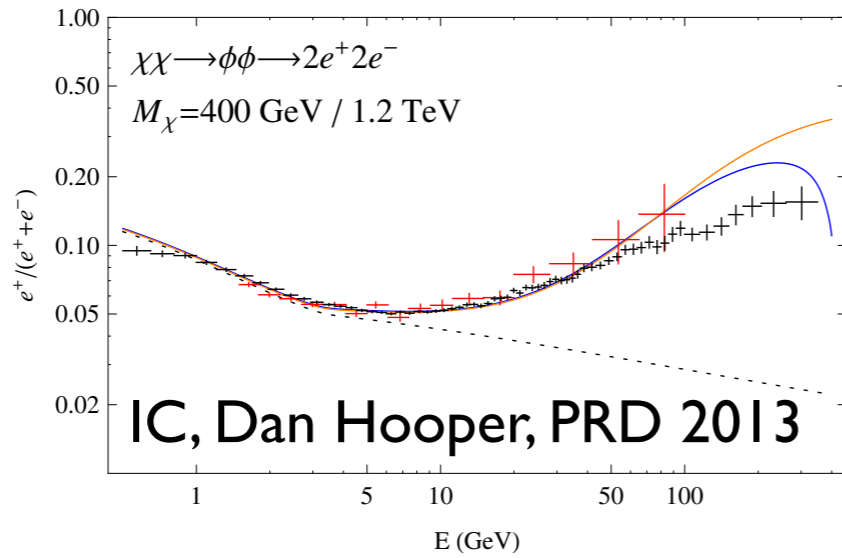


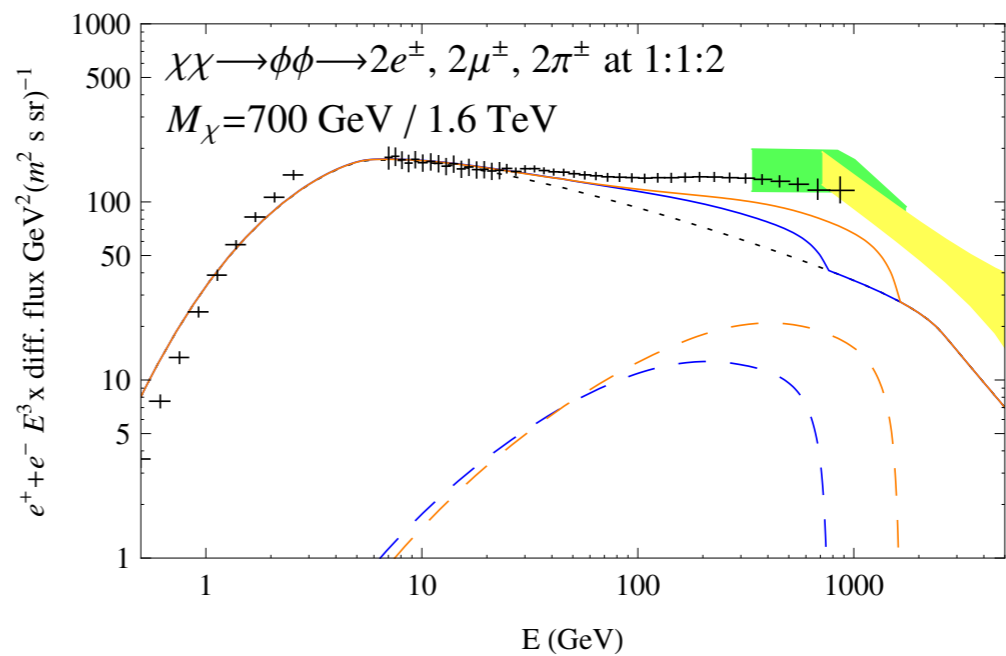
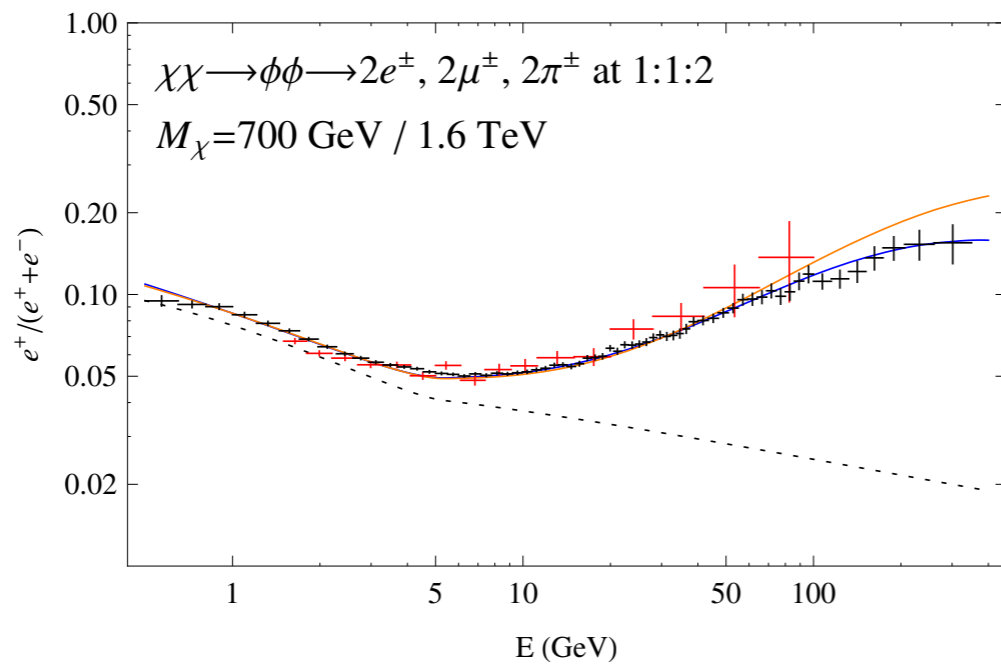
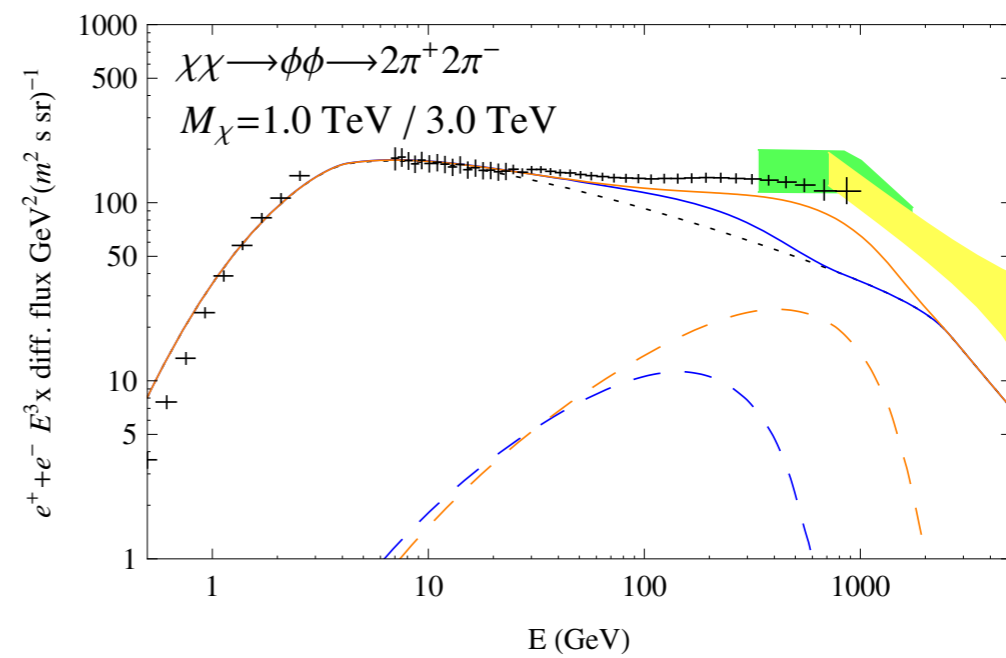
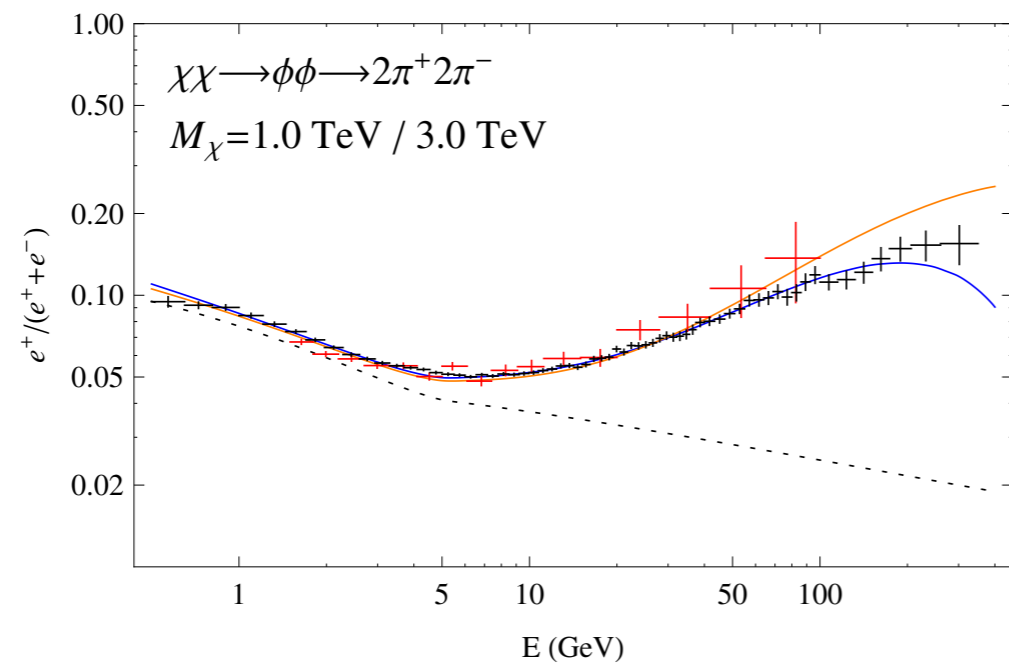
$$S \sim \frac{1}{\epsilon_\phi} \sim \frac{\alpha M}{m_\phi}$$



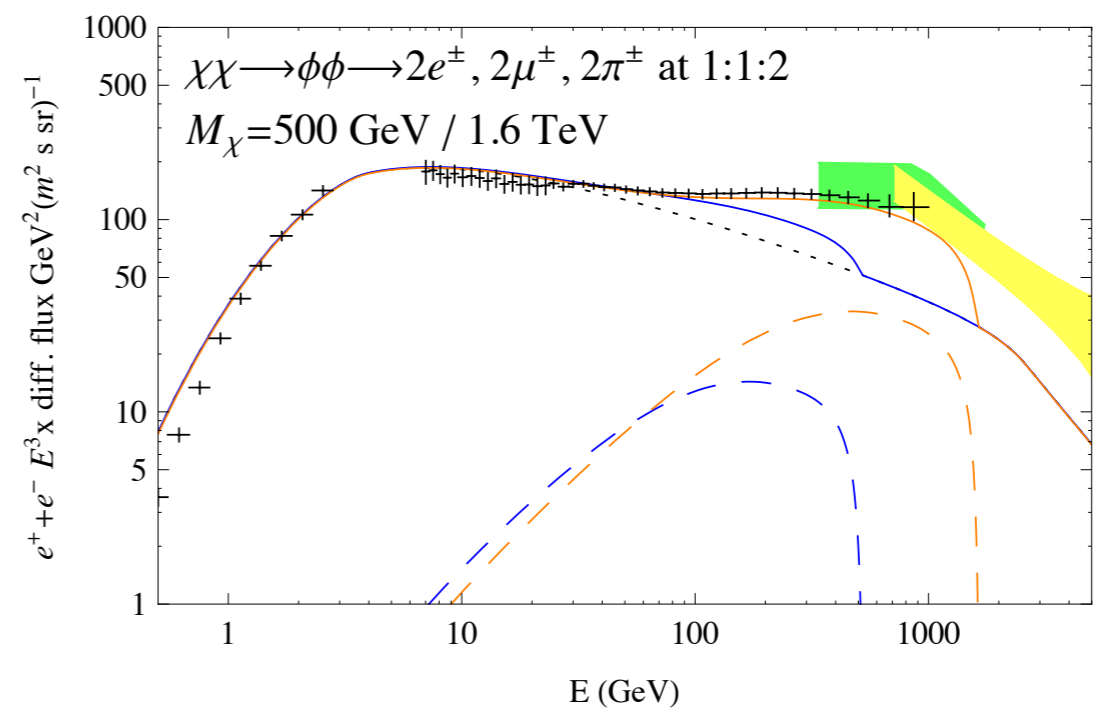
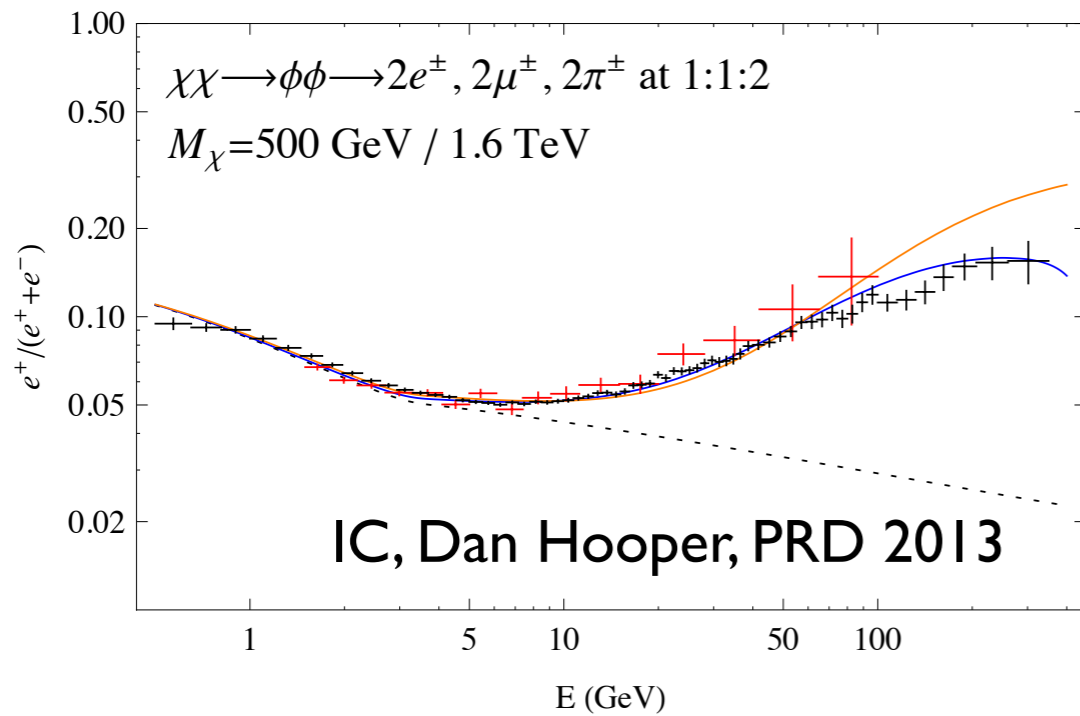
$$\epsilon_\nu \equiv \frac{v}{\alpha}$$

Models with Sommerfeld annihilation

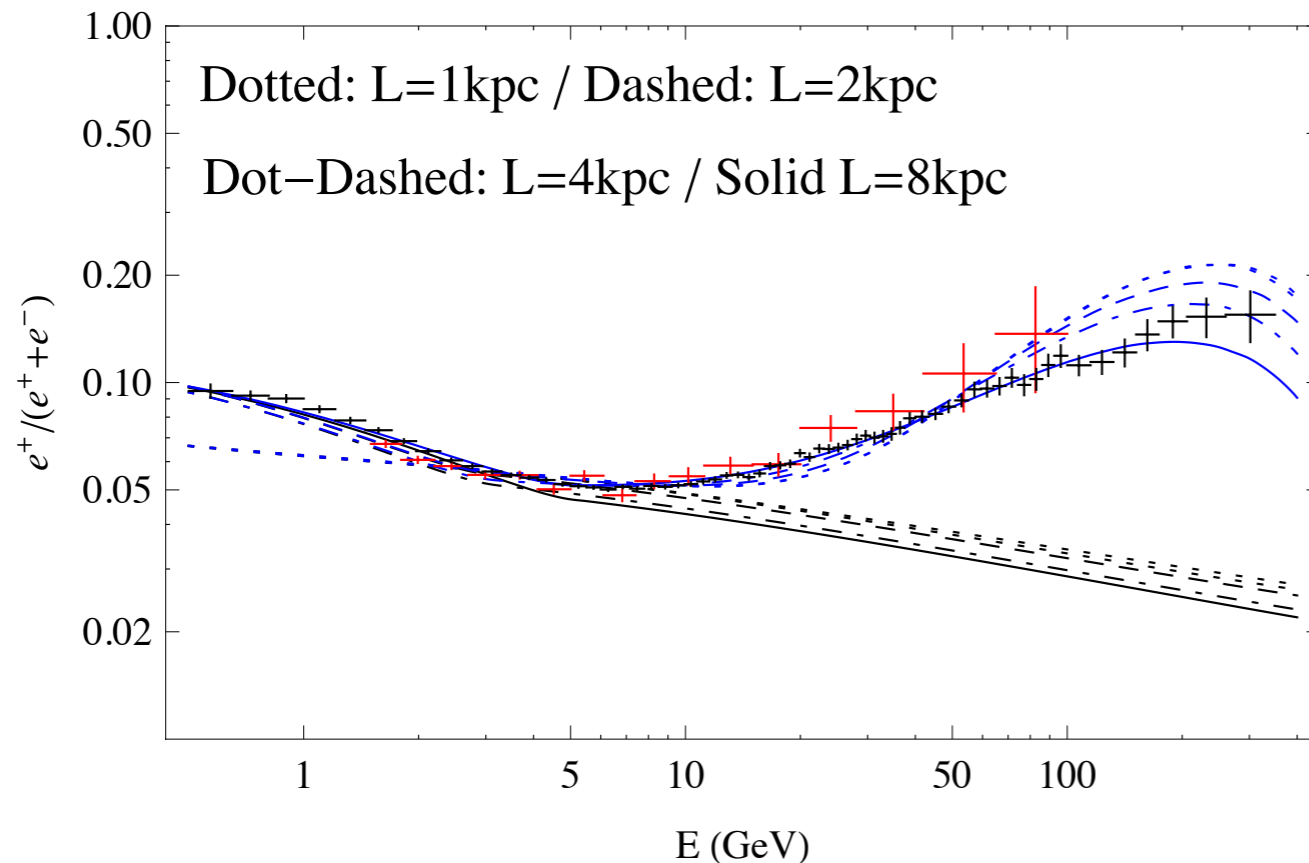




Some inconsistency between AMS and Fermi leptonic data, suggesting the need of more high energy electrons above $\sim 100 \text{ GeV}$.



Softer annihilation spectra are preferred from the combined CR lepton spectra
 Also thinner diffusion halos demand even softer annihilation spectra. Thicker diffusion halos are somewhat preferred in agreement with indications from gamma-rays.



Still some degeneracy between propagation properties and DM annihilation products. With AMS to release heavier nuclei CR spectra, these degeneracies will strongly be reduced.

Physical models that work with all data (leptons/ antiprotons/ gamma-rays/ microwave)

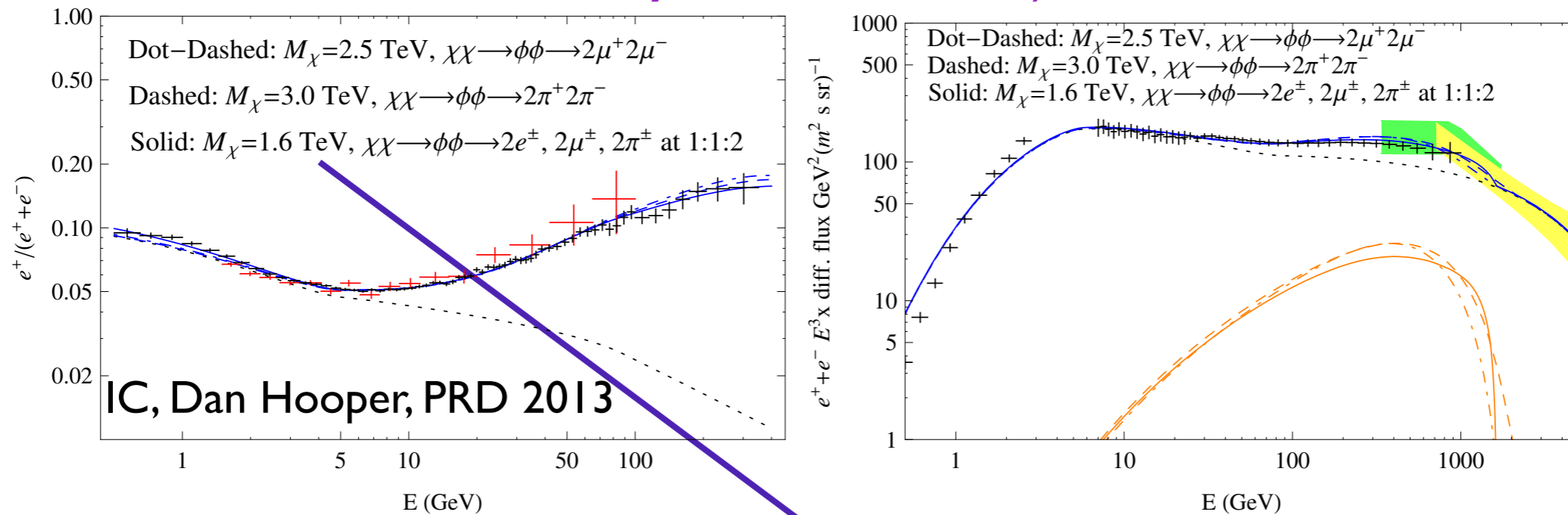
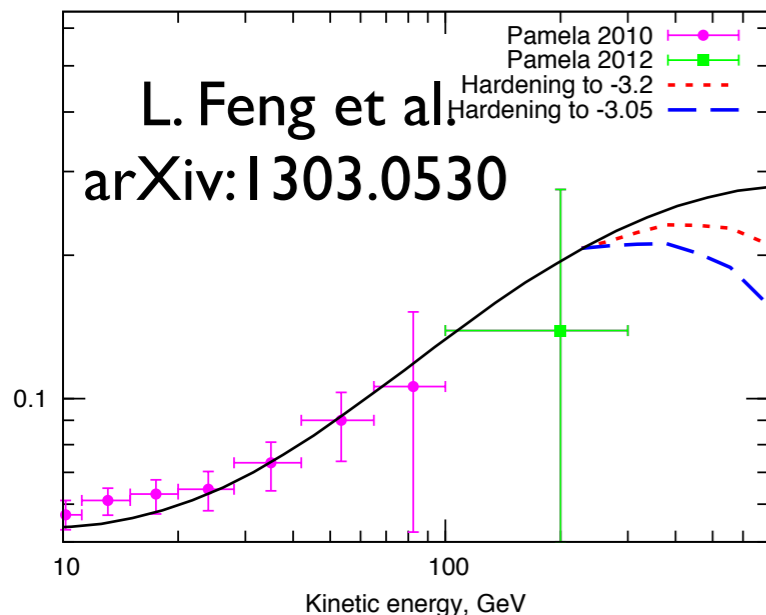
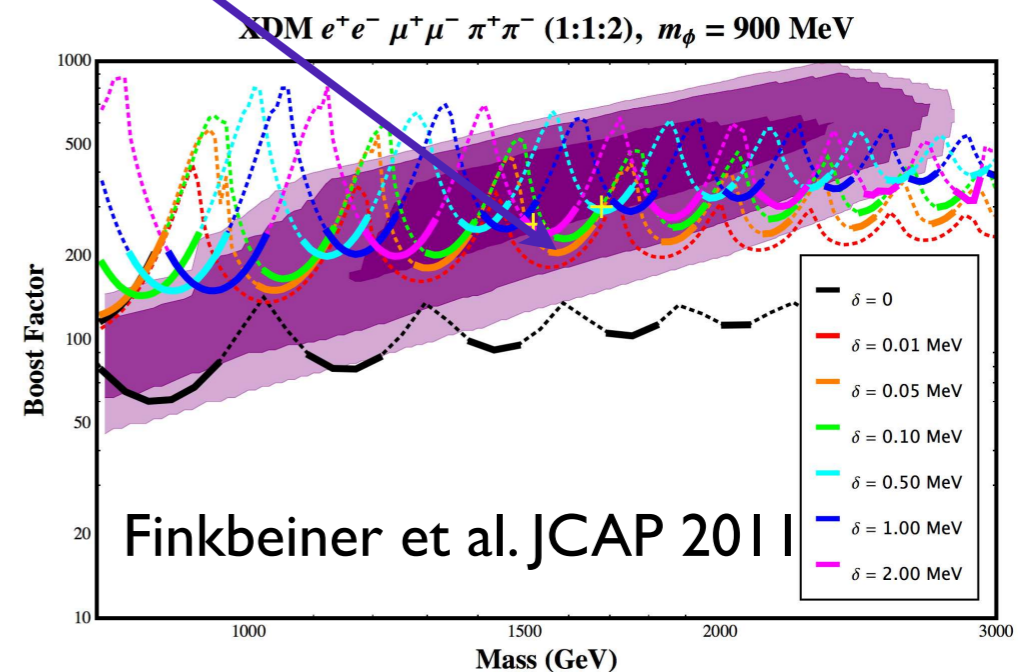


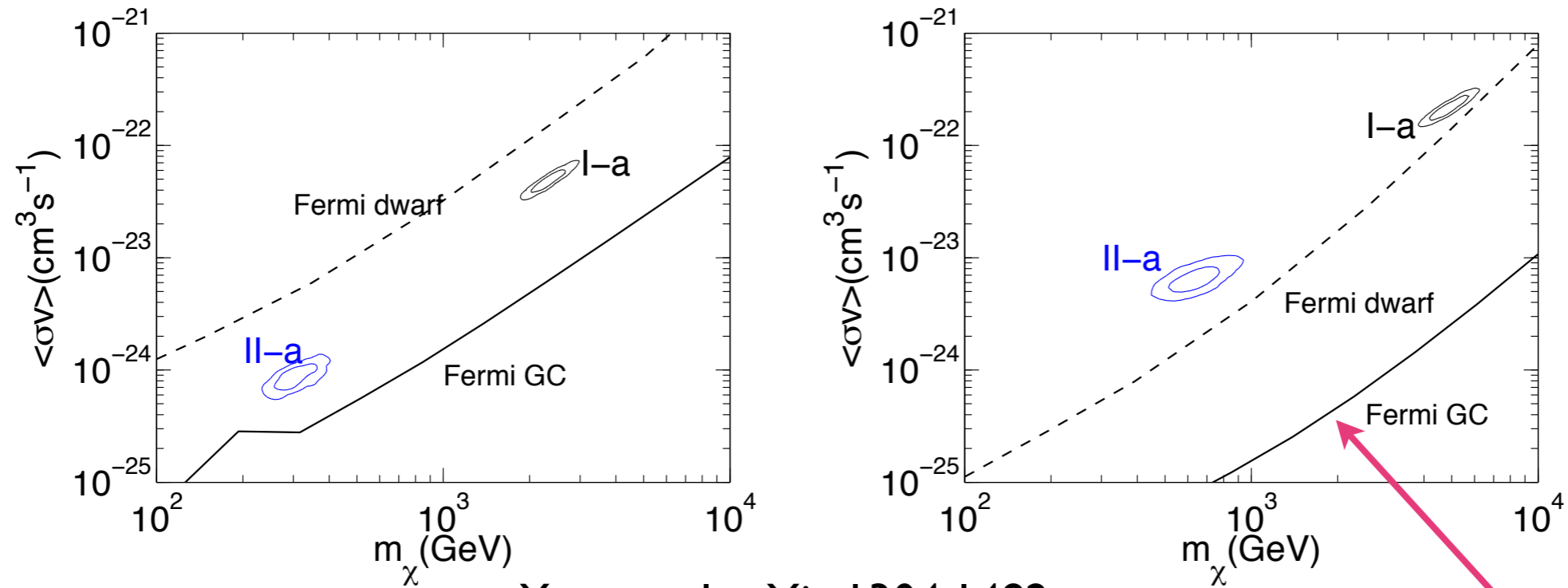
FIG. 6: The same as in Figs. 1, 2, 4 and 5 but for a diffusion zone half-width of $L = 8$ kpc, and for broken power-law spectrum of electrons injected from cosmic ray sources ($dN_{e^-}/dE_{e^-} \propto E_{e^-}^{-2.65}$ below 85 GeV and $dN_{e^-}/dE_{e^-} \propto E_{e^-}^{-2.3}$ above 85 GeV). The cross sections are the same as given in the caption of Fig. 5. With this cosmic ray background, we show the dark matter models compared to the measurements of the cosmic ray positron fraction and the overall leptonic spectrum. Even with the presence of a break, there is a preference towards models with softer injection e^\pm spectra; with the 1.6 TeV to e^\pm, μ^\pm, π^\pm case providing the best $\chi^2/d.o.f.$ fit to the *AMS (Fermi)* lepton data of 0.82(0.51). The 2.5 TeV to $2\mu^+ 2\mu^-$, gives a $\chi^2/d.o.f.$ fit of 1.32(1.07) and the 3.0 TeV to $2\pi^+ 2\pi^-$ a fit of 1.00(1.03). We remind that in the *Fermi* error-bars we do not include an overall shift from the energy resolution uncertainty.



(See also Hooper,
Zurek PRD 2009)



For dark matter annihilating to taus:

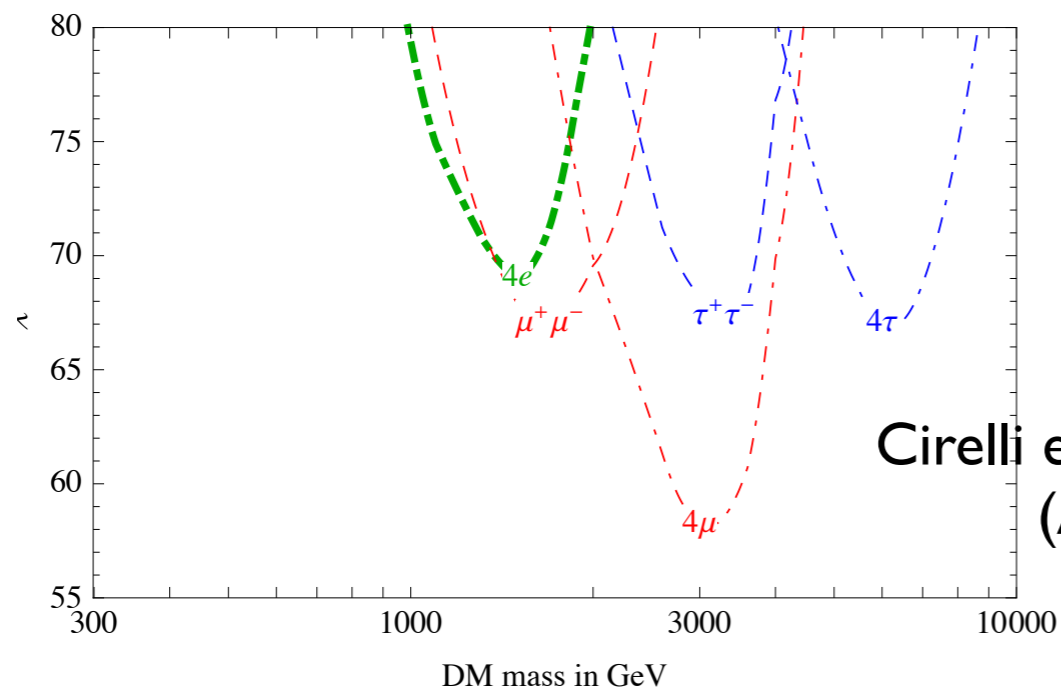


Yuan et al arXiv:1304.1482

FIG. 5: 1σ and 2σ confidence regions on the DM mass and cross section plane, for the fits I-a and II-a respectively. The left panel is for $\mu^+\mu^-$ channel, and the right panel is for $\tau^+\tau^-$ channel. The solid lines show the 95% upper limit of Fermi γ -ray observations of the Galactic center (with normalization of the local density corrected) [59] and dwarf galaxies [60].

Excluded by more than an order of magnitude from gamma-ray data

DM annihilation fit to e^+ and e^+e^- after AMS, FERMI



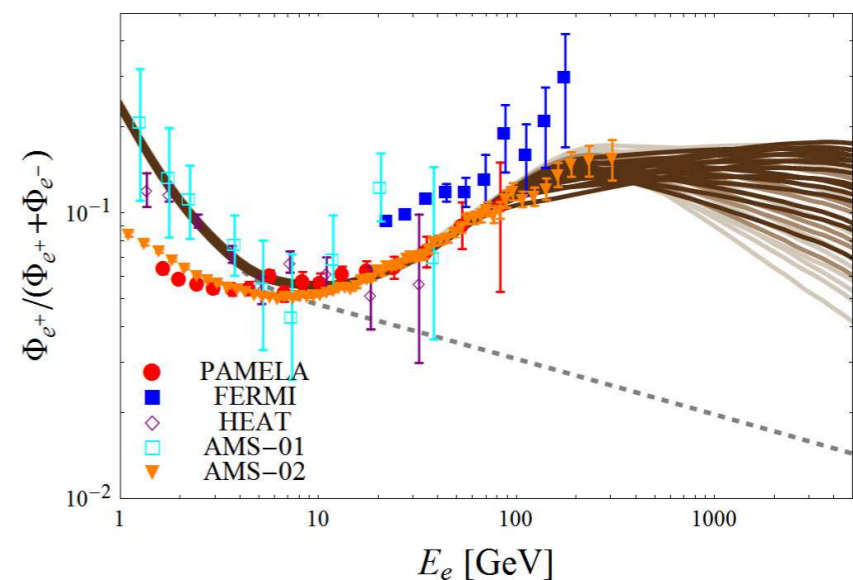
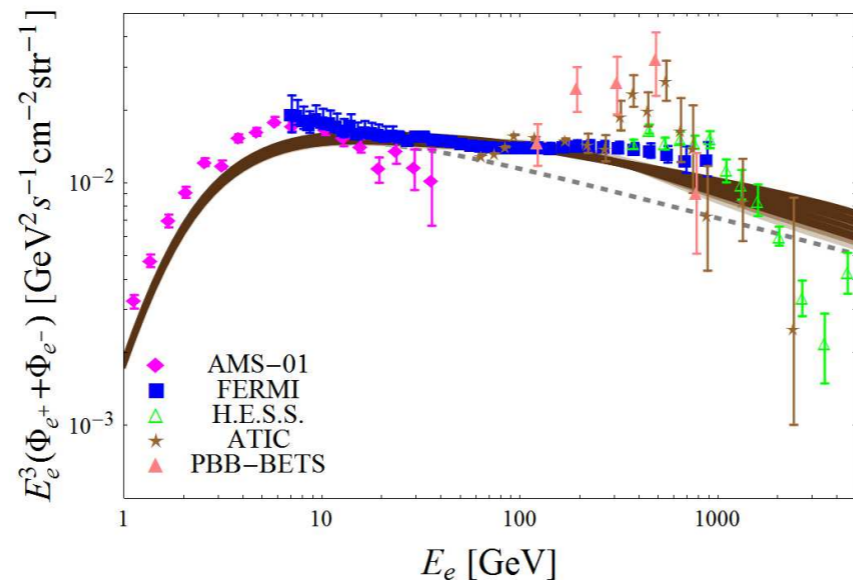
Cirelli et al arXiv:0809.2409
(AMS updated)

Dynamical (decaying) Dark Matter

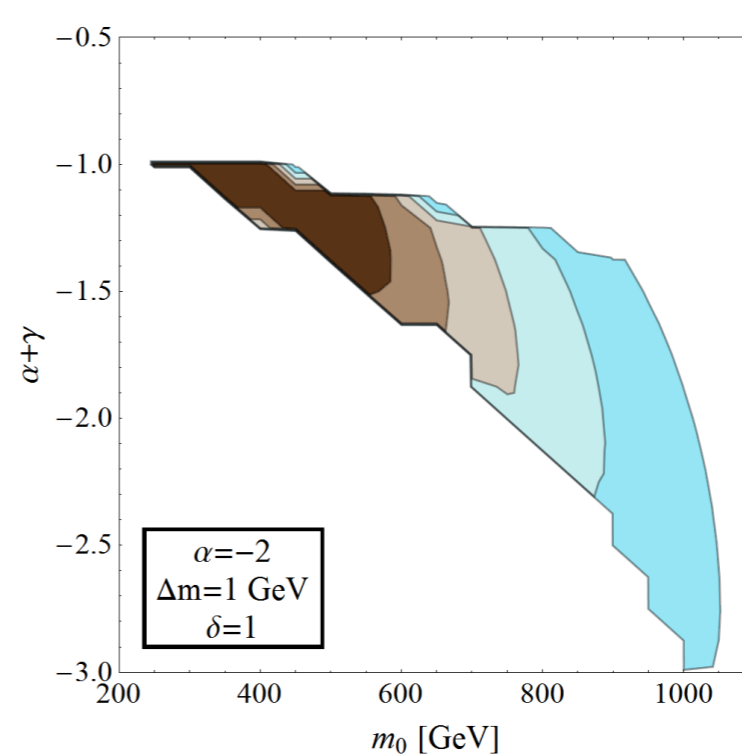
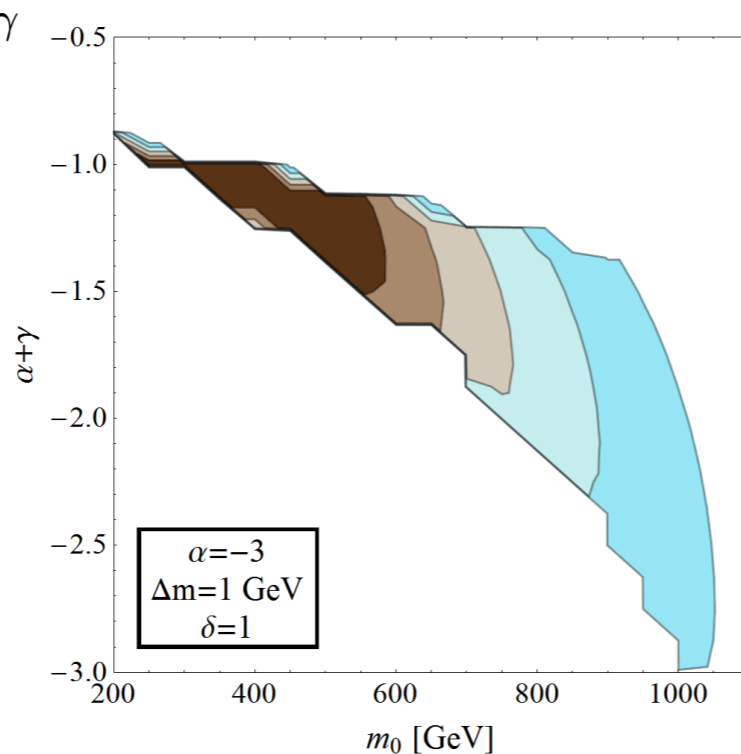
$$m_n = m_0 + n^\delta \Delta m$$

$$\Omega_n = \Omega_0 \left(\frac{m_n}{m_0} \right)^\alpha$$

$$\Gamma_n = \Gamma_0 \left(\frac{m_n}{m_0} \right)^\gamma$$



Dienes, Kumar and Thomas arXiv:1306.2959



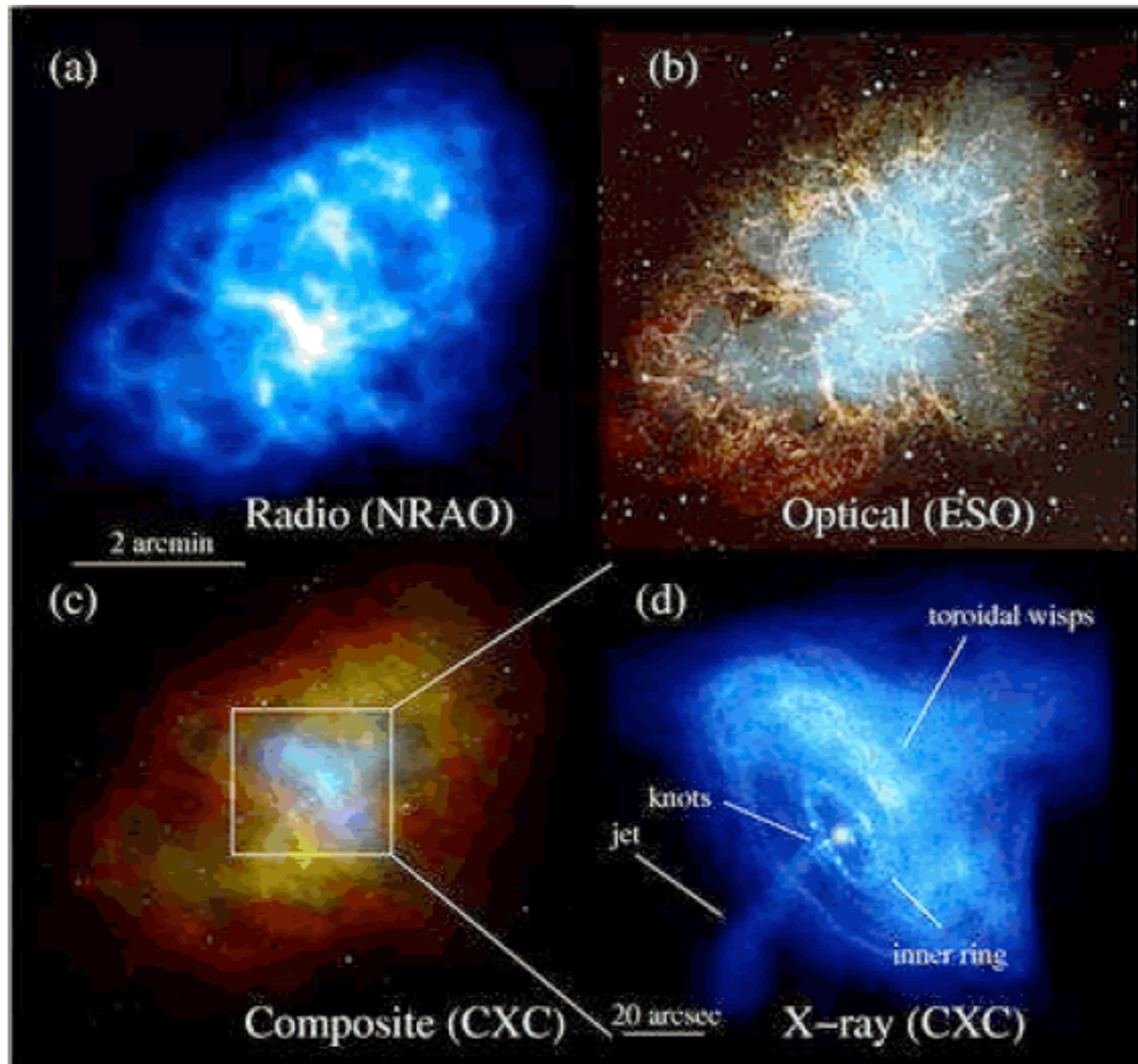
Significance:



FIG. 2: Contours of the minimum significance level with which a given DDM ensemble is consistent with AMS-02 data, plotted within the $(m_0, \alpha + \gamma)$ DDM parameter space for $\alpha = -3$ (left panel) and $\alpha = -2$ (right panel). The colored regions correspond to DDM ensembles which successfully reproduce the AMS-02 data while simultaneously satisfying all of the applicable phenomenological constraints outlined in Sect. IV, while the white regions of parameter space correspond to DDM ensembles which either cannot simultaneously satisfy these constraints or which fail to match the AMS-02 positron-excess data at the 5σ significance level or greater. The slight difference between the results shown in the two panels is a consequence of the differences in the CMB constraints for the two corresponding values of α .

Astrophysical explanation, Contribution from Pulsars

Crab (very young pulsar 10^3 yr)



$$\dot{E} = -\frac{B_s^2 R_s^6 \Omega^4}{6c^3} \approx 10^{31} B_{12}^2 R_{10}^6 P^{-4} \text{ erg s}^{-1}$$

$$\Omega(t) = \frac{\Omega_0}{(1 + t/\tau_0)^{1/2}}$$

$$\mathcal{L} = I\Omega\dot{\Omega} = \frac{1}{2} I\Omega_0^2 \frac{1}{\tau_0} \frac{1}{\left(1 + \frac{t}{\tau_0}\right)^2}$$

$$E_{tot}(t) = \frac{1}{2} I\Omega_0^2 \frac{t}{\tau_0} \frac{1}{1 + \frac{t}{\tau_0}} = 6 \times 10^{43} P_0^{-4} R_{10}^6 B_{12}^2 t_5 \frac{1}{\left(1 + \frac{t}{\tau_0}\right)} \text{ erg,}$$

$$E_{tot} \approx \frac{1}{2} I\Omega_0^2 = 2.2 \times 10^{46} \left(\frac{M_s}{1.4M_\odot}\right) R_{10}^2 P_0^{-2} \text{ erg.}$$

Electrons accel. inside the magnetosphere, produce ICS gamma-rays, which in turn in the presence of strong magnetic fields pair produce electrons positrons further accelerated inside the magnetosphere. In addition electrons and positrons can be accelerated in the termination shock of the pulsar(also of the SNR) and the ISM.

$$\frac{\partial \rho}{\partial t} = \frac{\partial}{\partial E} (b(E)\rho) + \frac{\partial}{\partial x^i} \left(D(E) \frac{\partial}{\partial x^i} \rho \right) + Q(\mathbf{x}, E, t),$$

$$G(\mathbf{x}, E, t; \mathbf{x}_0, E_0, t_0) = \frac{1}{b(E)} \frac{1}{(4\pi\lambda)^{3/2}} e^{-\frac{(\mathbf{x}-\mathbf{x}_0)^2}{4\lambda}} \cdot \delta(t - t_0 - \tau) \theta(E_0 - E). \quad (12)$$

$$Q_{\text{pulsar}}(\mathbf{x}, E, t) = Q(E) \frac{1}{\tau} \left(1 + \frac{t}{\tau} \right)^{-2} \theta(t) \delta(\mathbf{x})$$

$$Q(E) = Q_0 E^{-n} e^{-\frac{E}{M}}$$

Malyshev, Cholis, Gelfand, PRD 2009

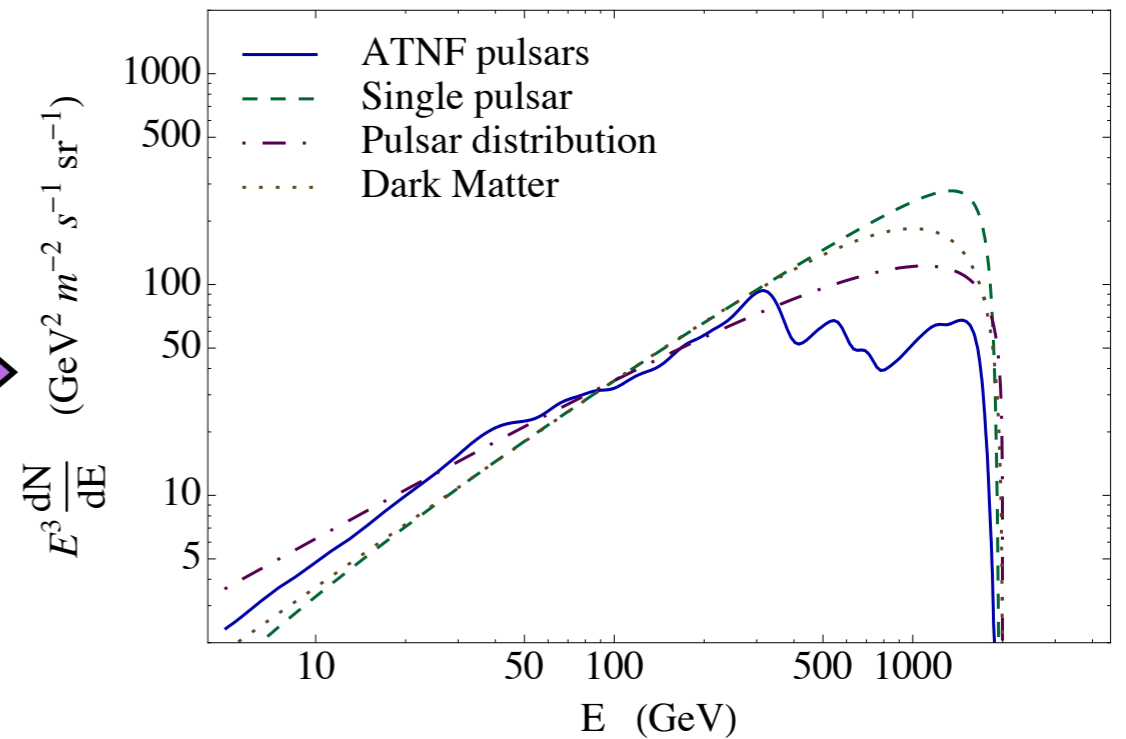
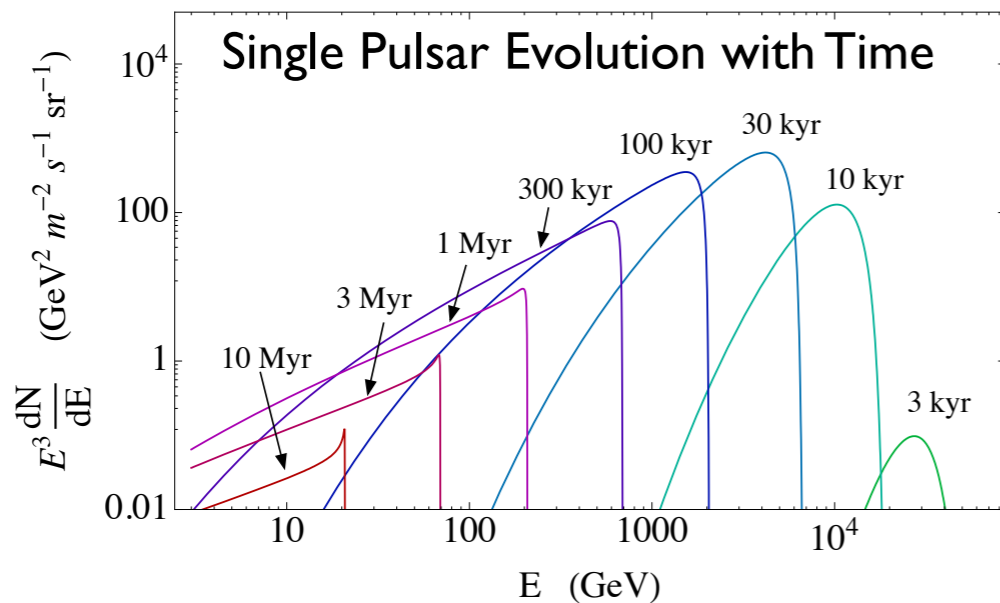
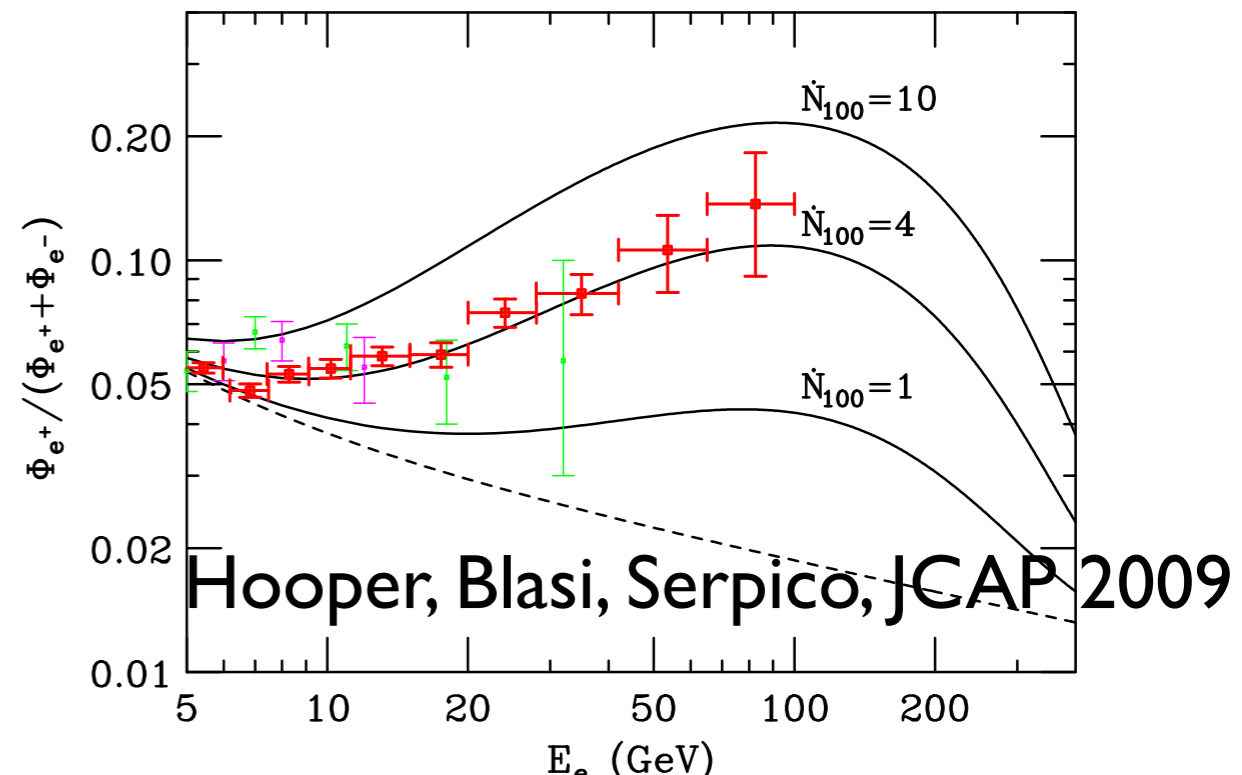
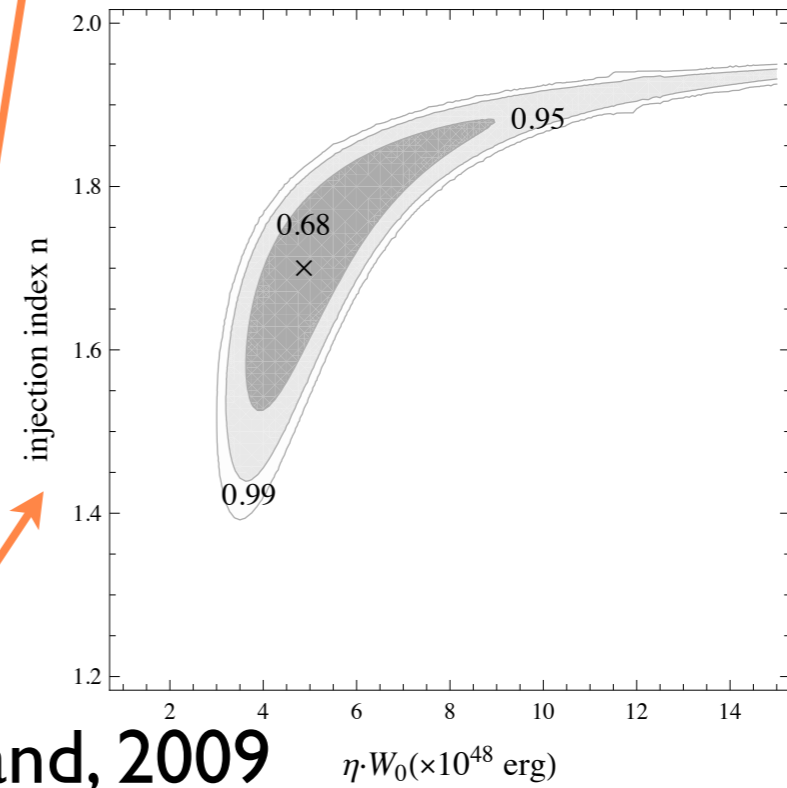
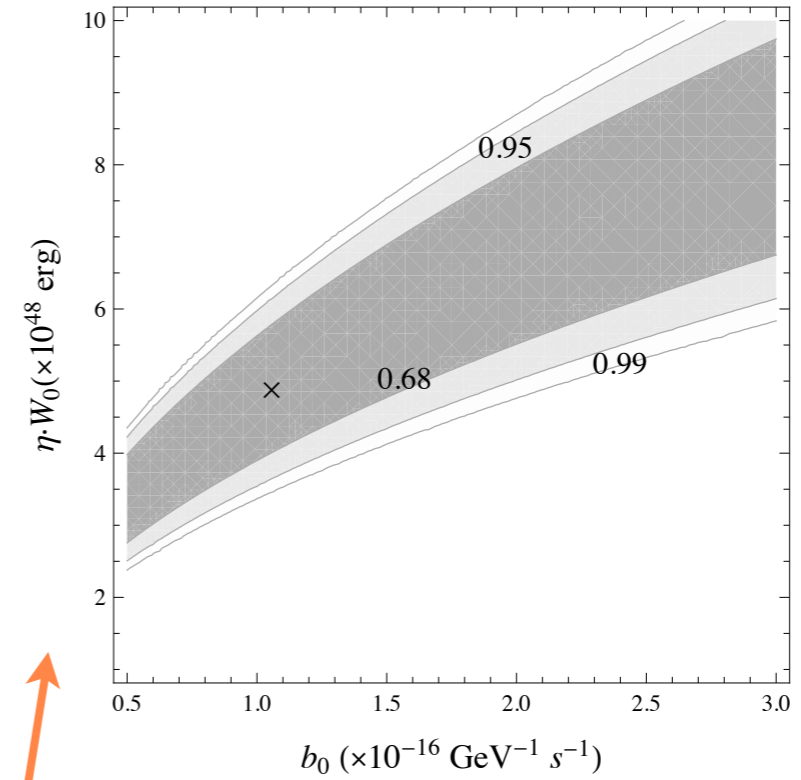
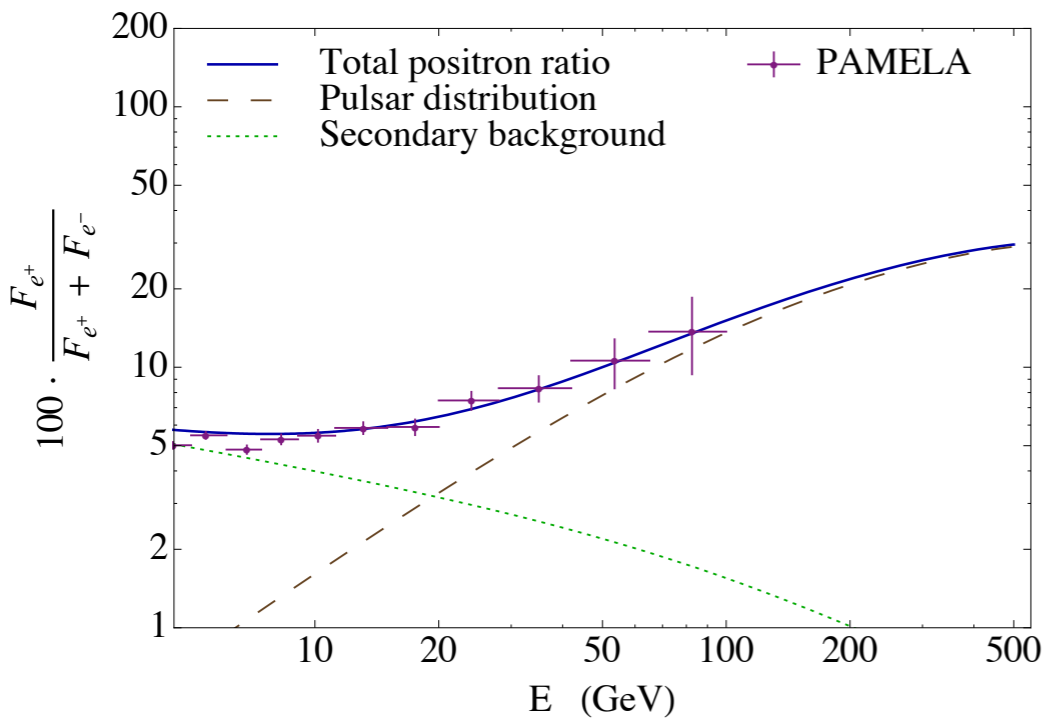
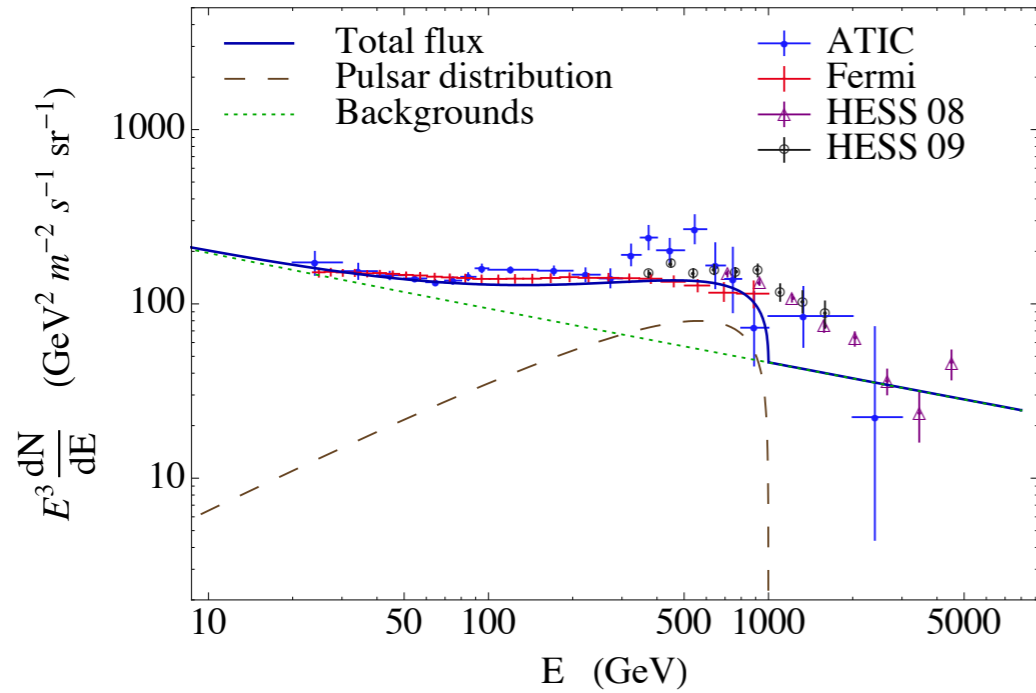


FIG. 1: Time evolution of e^+e^- flux on the Earth from a pulsar at a distance of 1 kpc with $\eta W_0 = 3 \times 10^{49}$ erg, an injection index $n = 1.6$, and an injection cutoff $M = 10$ TeV. The diffusion and energy losses are described in Sec. II A. We assume the delta-function approximation for the emission from the pulsar, $Q(\mathbf{x}, E, t) = Q(E)\delta(\mathbf{x})\delta(t)$. The flux from a young pulsar (the 3 kyr curve on the right) has an exponential suppression because the electrons have not had enough time to diffuse from the pulsar to the Earth. The cutoff moves to the left due to cooling of electrons and becomes sharper. After reaching a maximal value, the flux decreases since the electrons diffuse over a large volume.



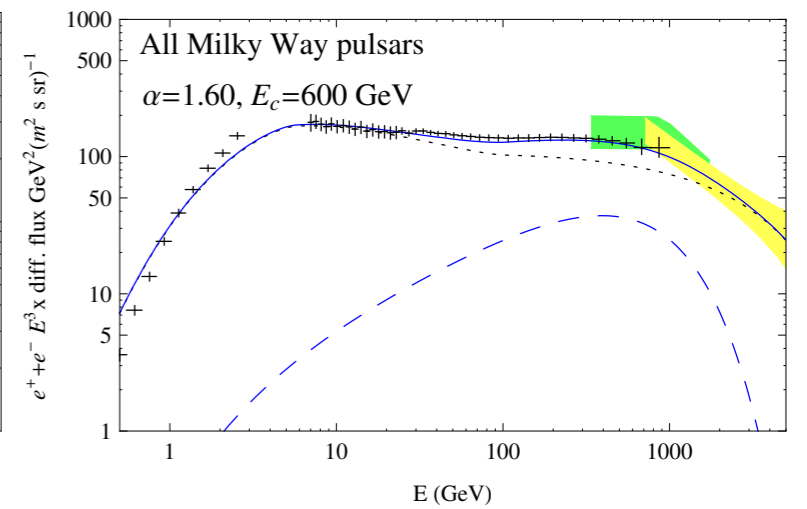
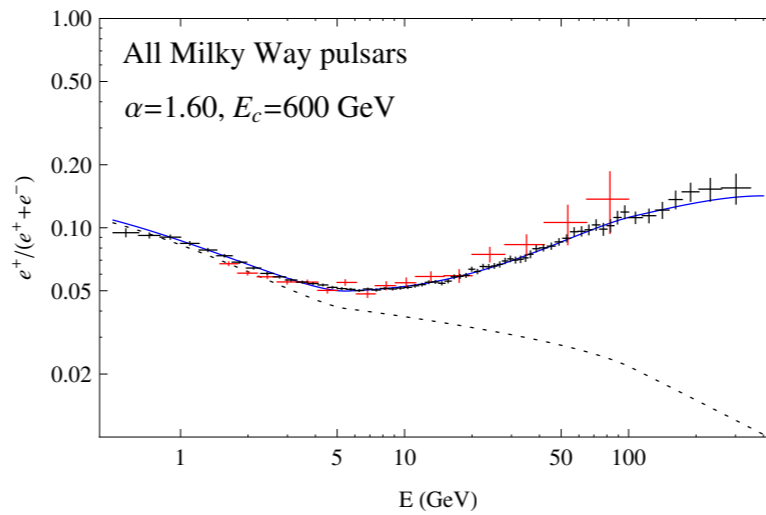
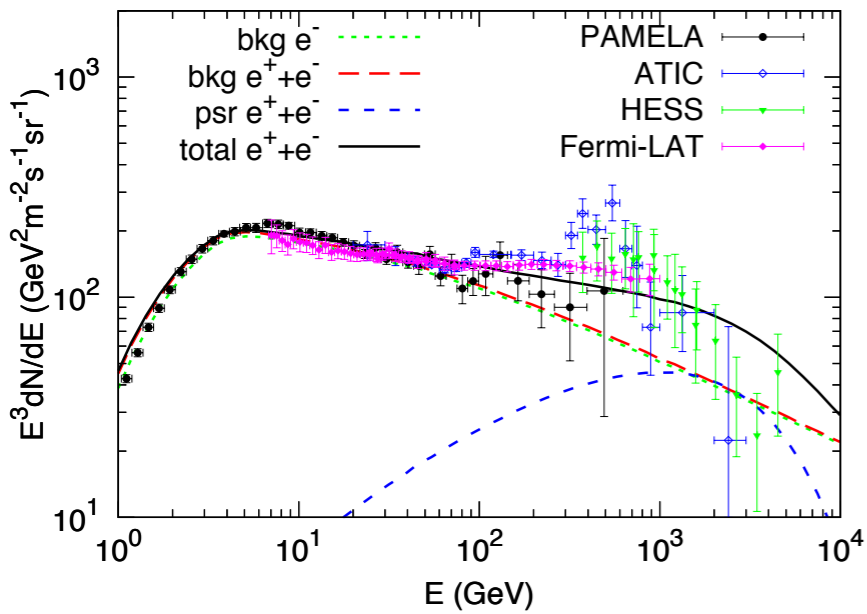
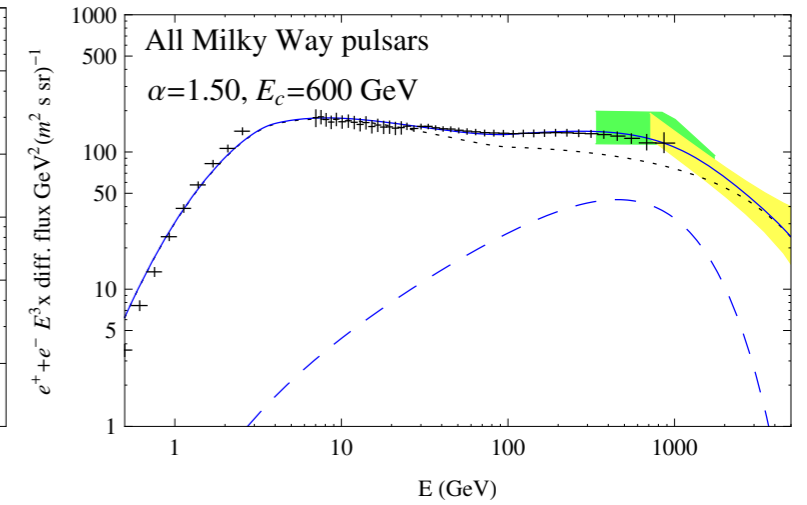
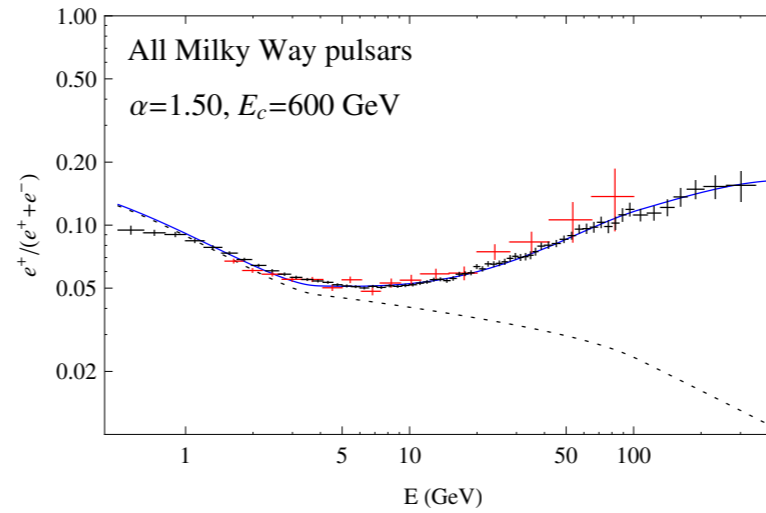
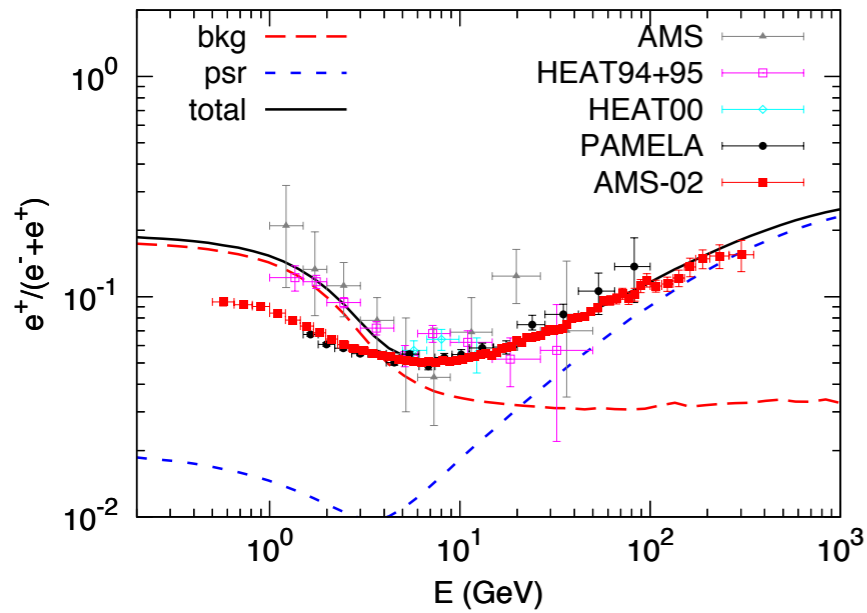


Malyshev, IC, Gelfand, 2009

Constrain combined propagation and pulsar distribution properties

Pulsars With AMS

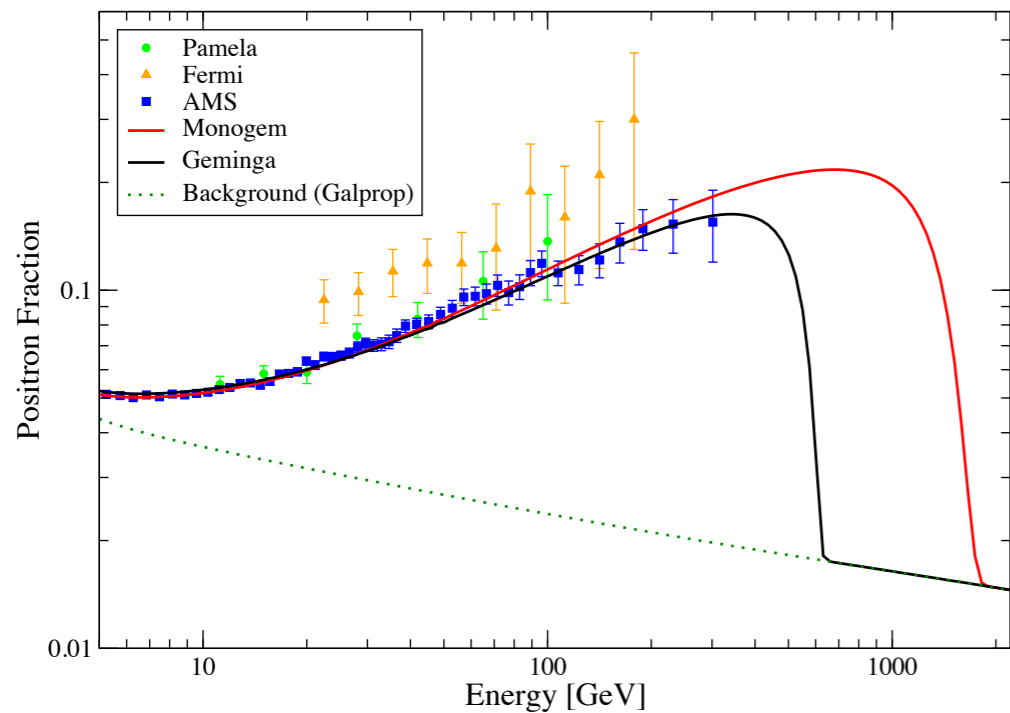
From galactic pulsars (within few kpc)



Yuan et al arXiv:1304.1482

IC, Dan Hooper, PRD 2013

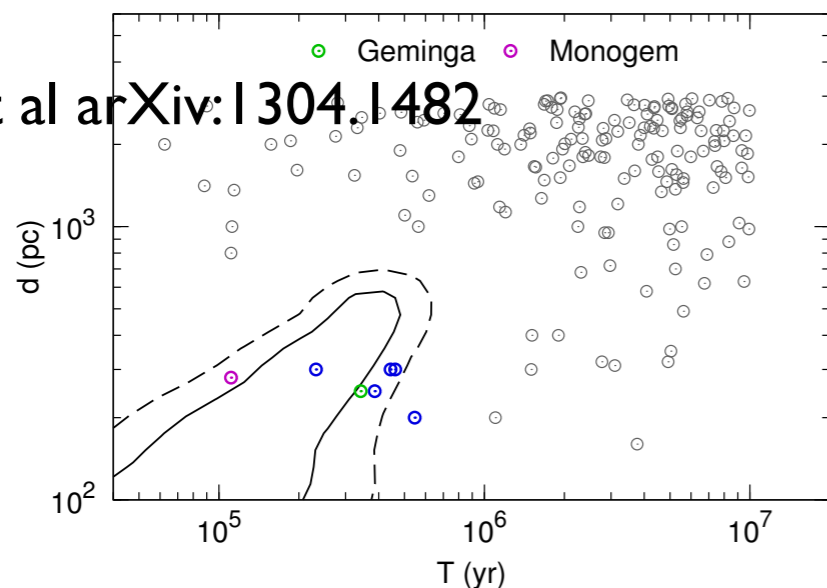
From close by pulsars (within few 100 pc)



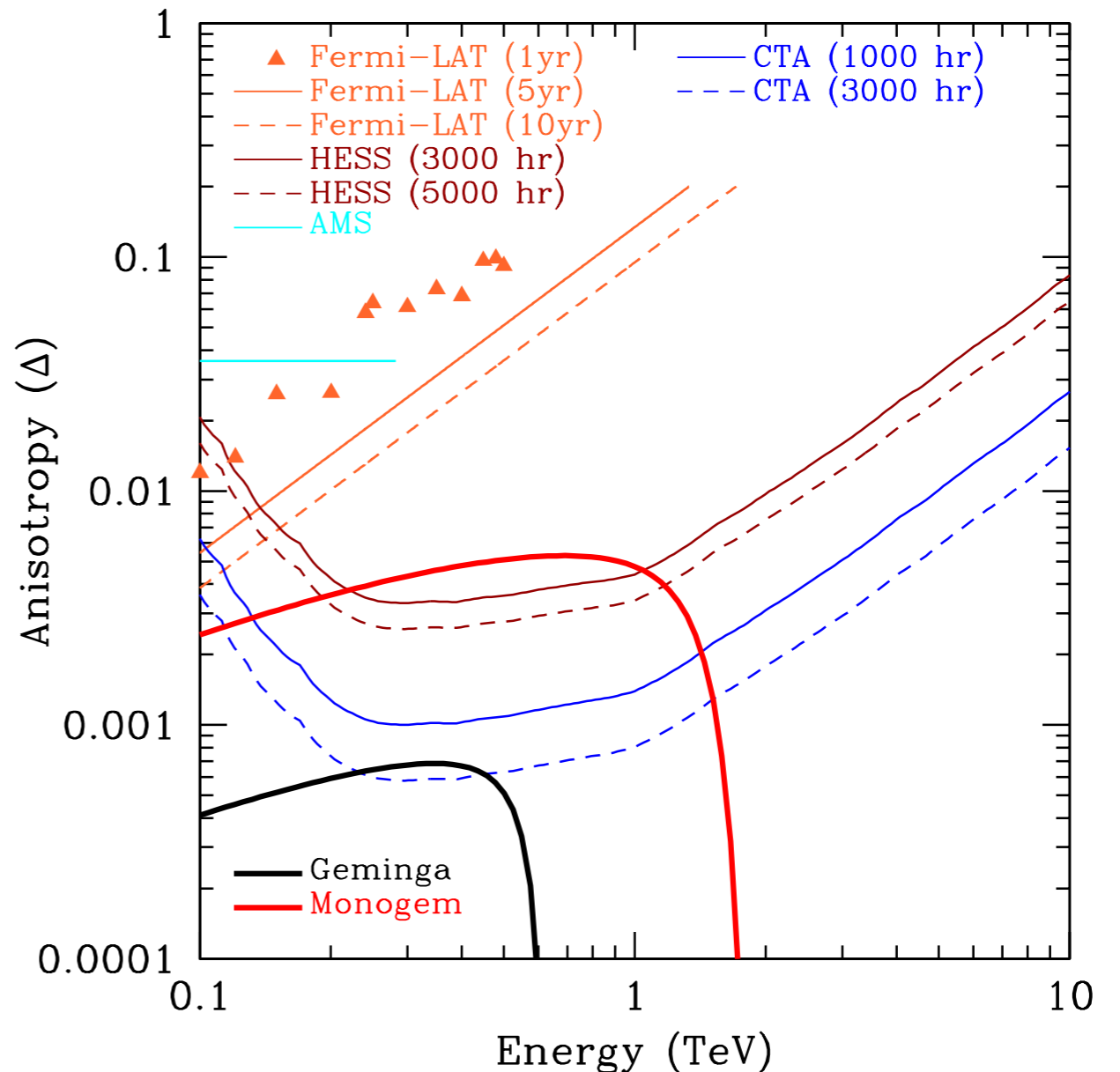
Linden, Profumo, arXiv:1304.1791

$$\Delta = \frac{N_f - N_b}{N_f + N_b} = \frac{N_{psr,f} - N_{psr,b}}{N_{psr,f} + N_{psr,b} + 2(N_{e,iso} + N_p)}$$

Yuan et al arXiv:1304.1482

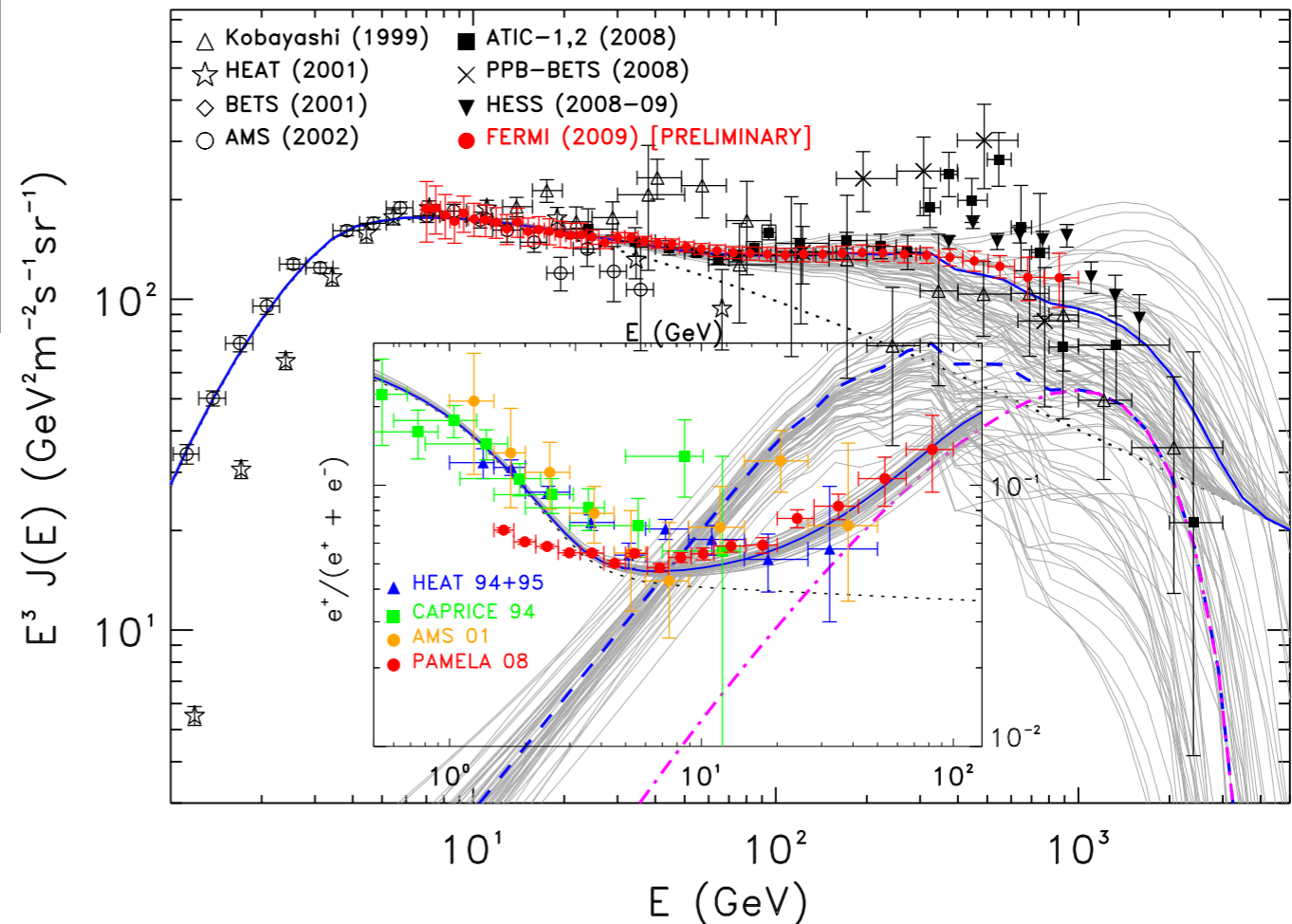
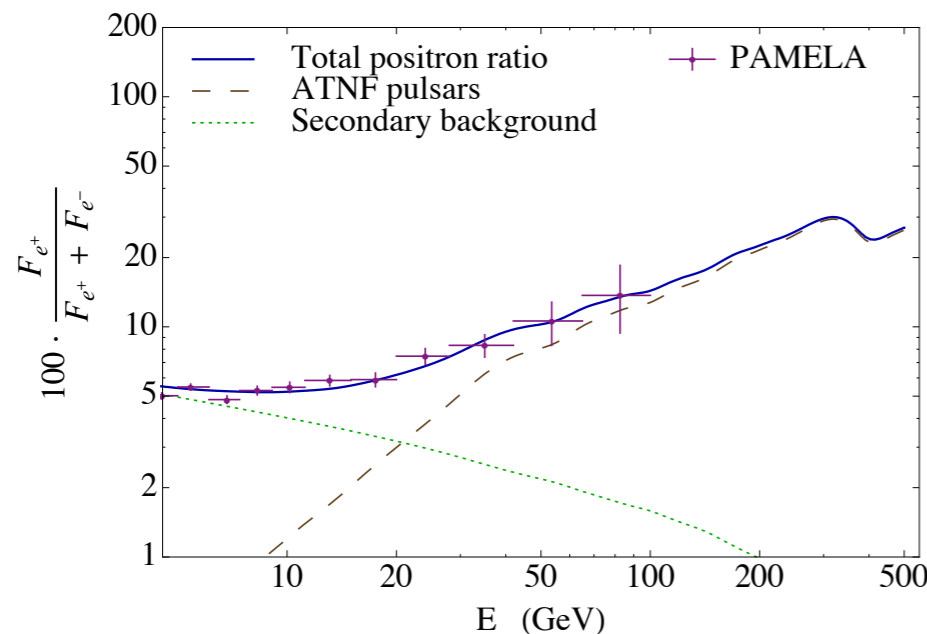
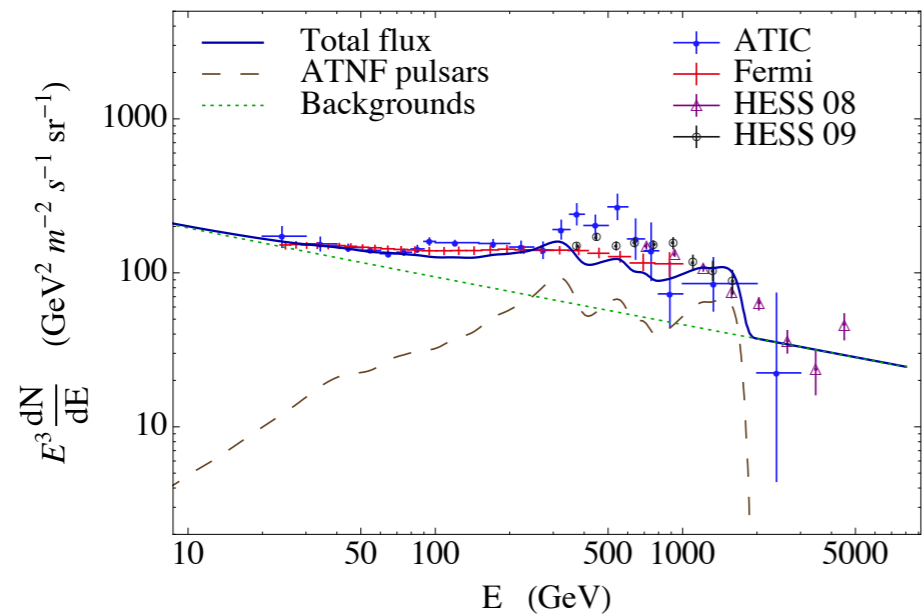


Individual pulsar sources could also cause **anisotropy** in the observed positron spectra. Assuming we have a candidate pulsar source we can point a detector towards and away from the source.



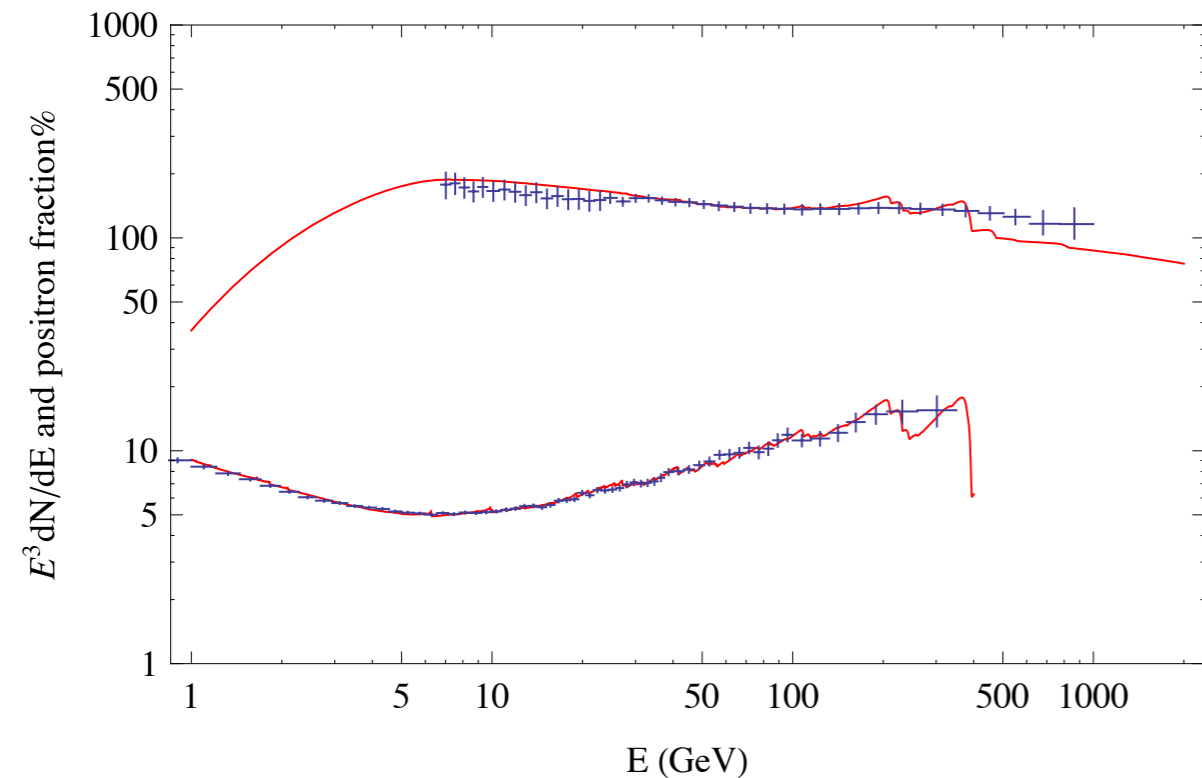
So Pulsars Very Appealing But... not there yet...

- See positive/negative bumps at higher energy electrons +positrons. One bump/cut-off: DM, Many:pulsars

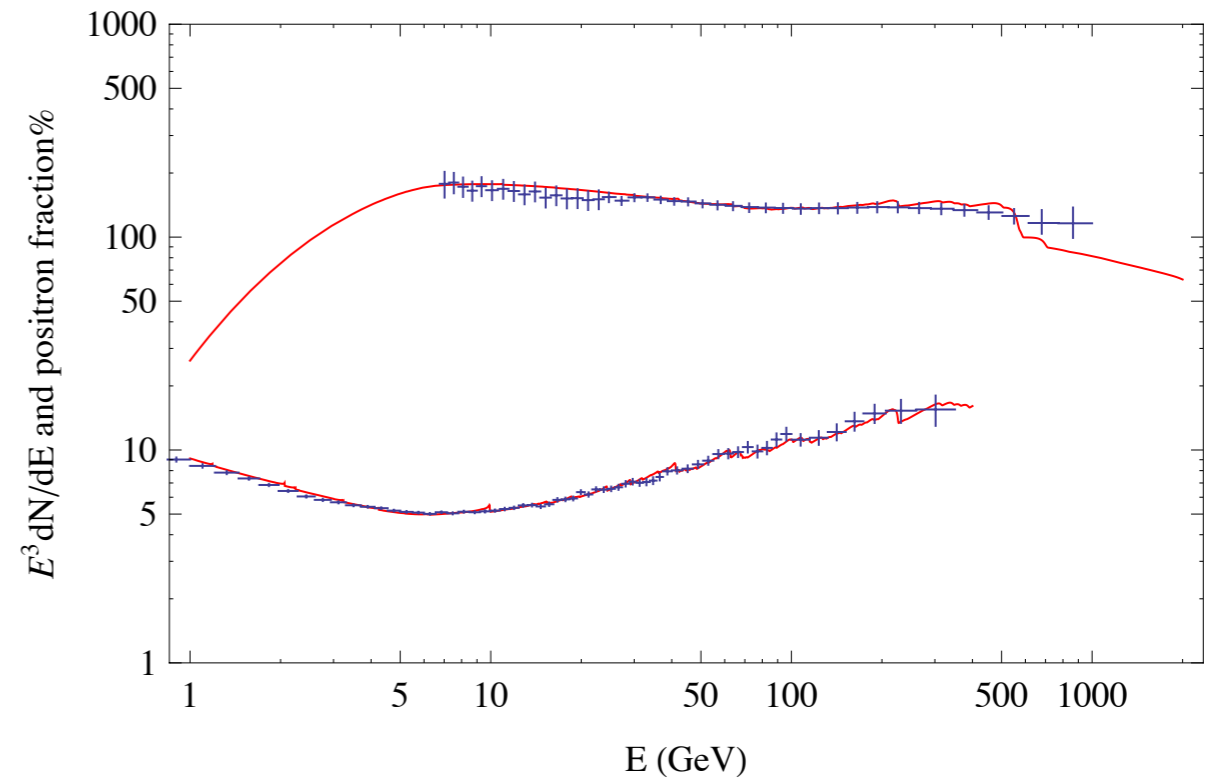


Fermi Coll, 2009

Search For significant bumps and wiggles in the higher energy CR leptonic spectra

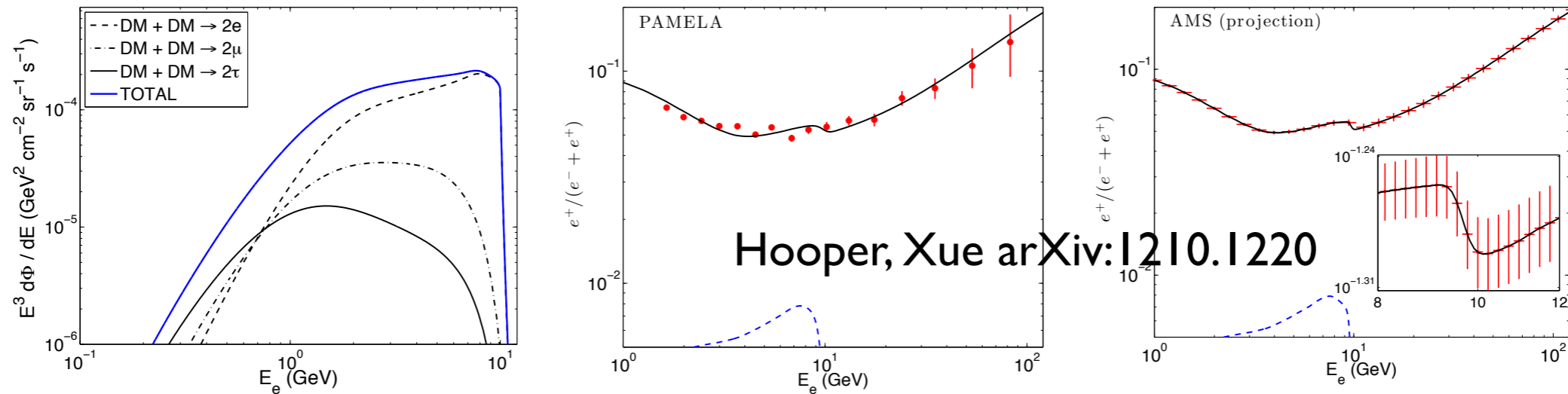


VS

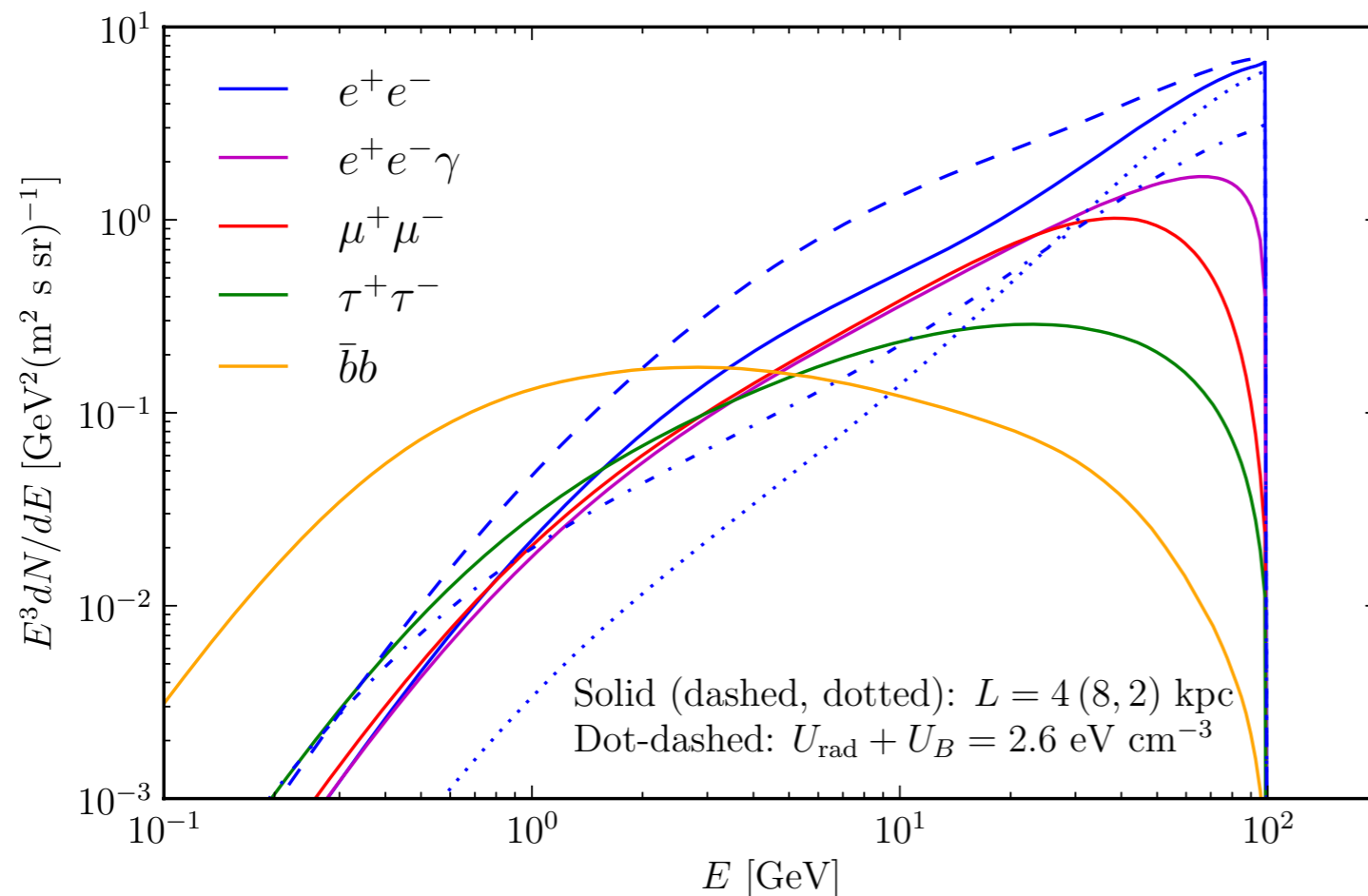


Both come from many pulsar realizations...
We need to understand the significance of spectral features

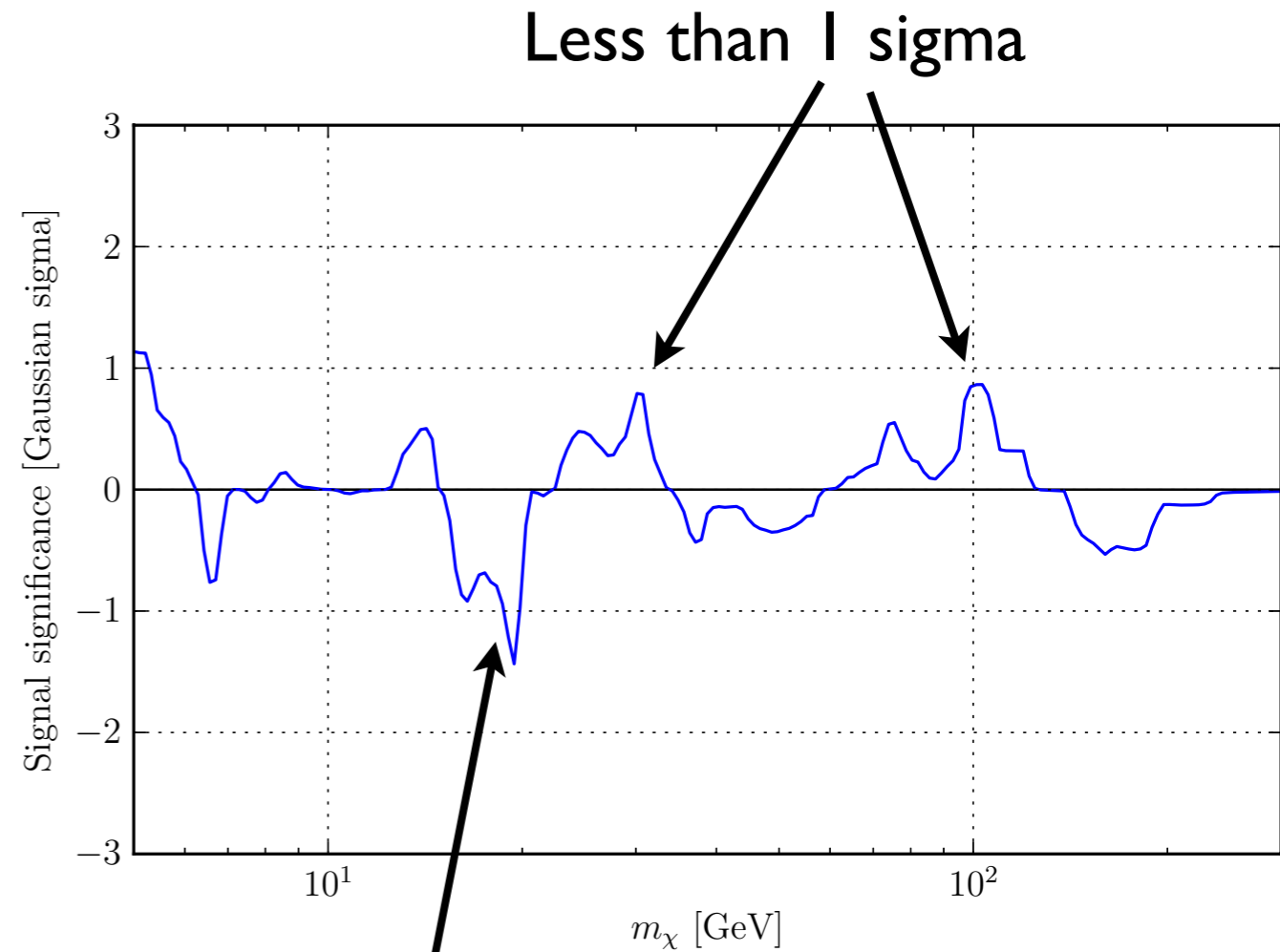
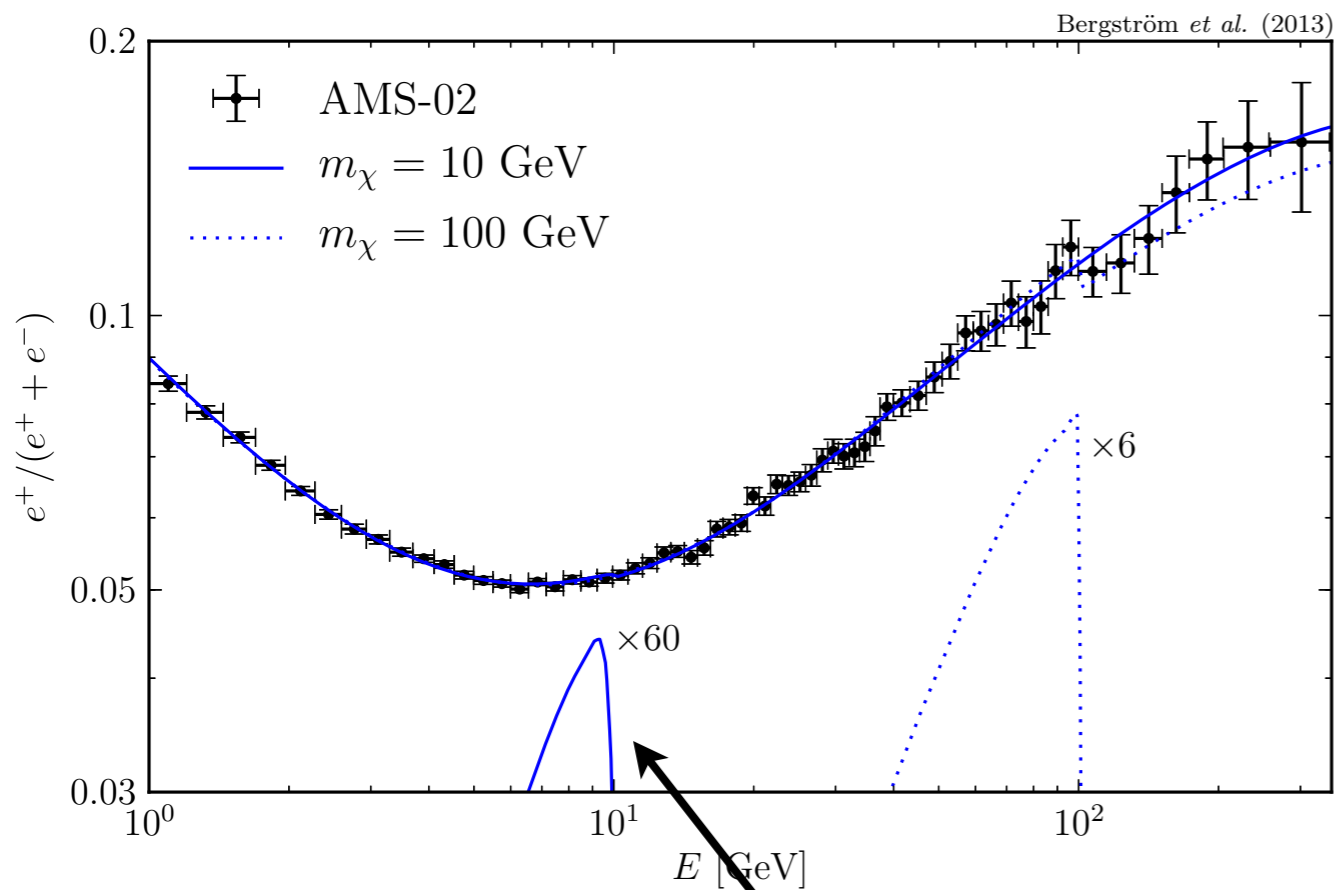
Search for spectral features



The AMS positron fraction lacks any obvious spectral feature up to 350 GeV, thus we can place strong limits on light leptophilic DM.



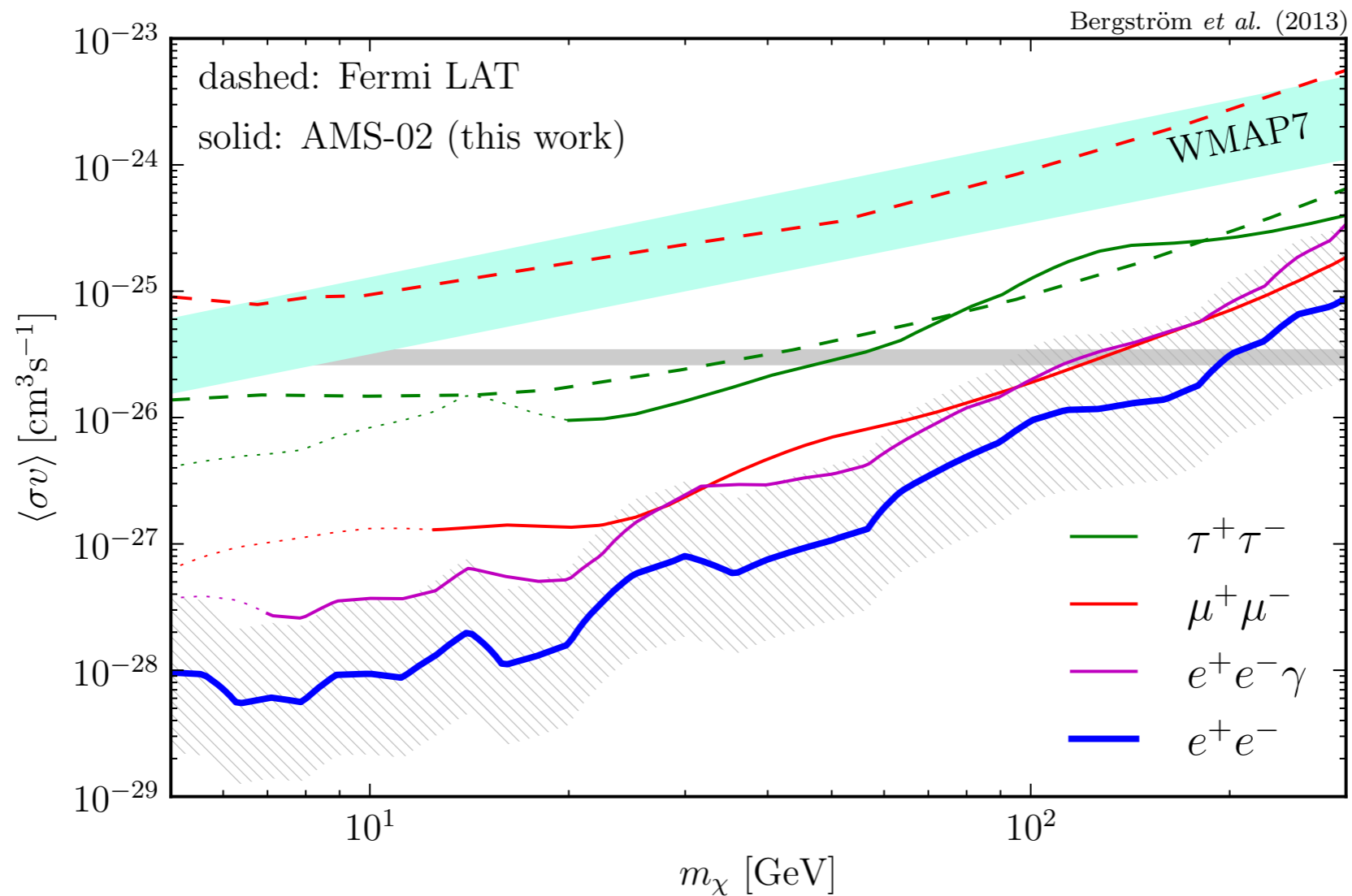
Lars Bergstrom, Torsten Bringmann, IC, Dan Hooper, Christoph Weniger, PRL 2013
 (arXiv:1306.3983)



AMS parametrization (**not** strongly motivated on physical understanding of cosmic ray production sources):

$$\Phi_{e^+} = C_{e^+} E^{-\gamma_{e^+}} + C_s E^{-\gamma_s} e^{-E/E_s}$$

$$\Phi_{e^-} = C_{e^-} E^{-\gamma_{e^-}} + C_s E^{-\gamma_s} e^{-E/E_s}$$



The absence of spectral features in the AMS positron fraction gives limits on light leptophilic DM that are **10-100 times stronger** than current limits from CMB, or from dSph (similarly for the GC)

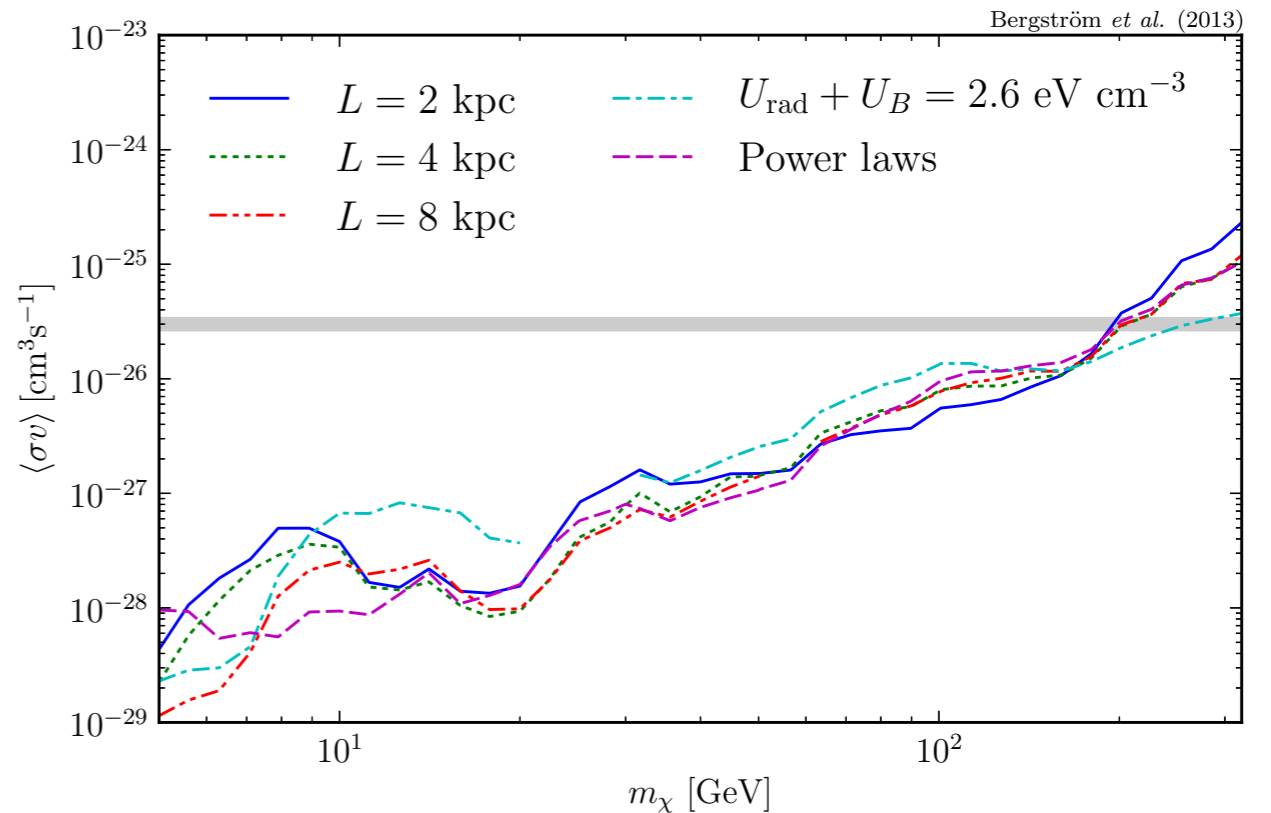
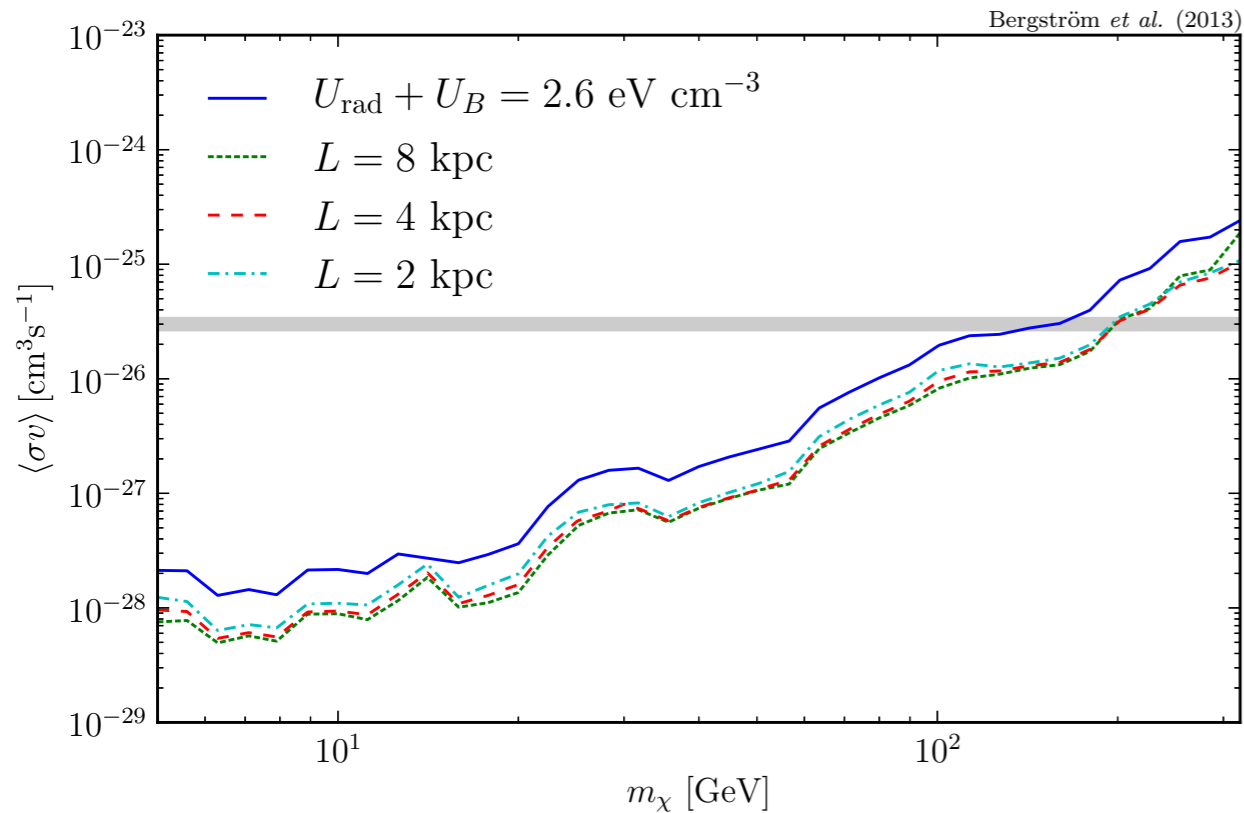
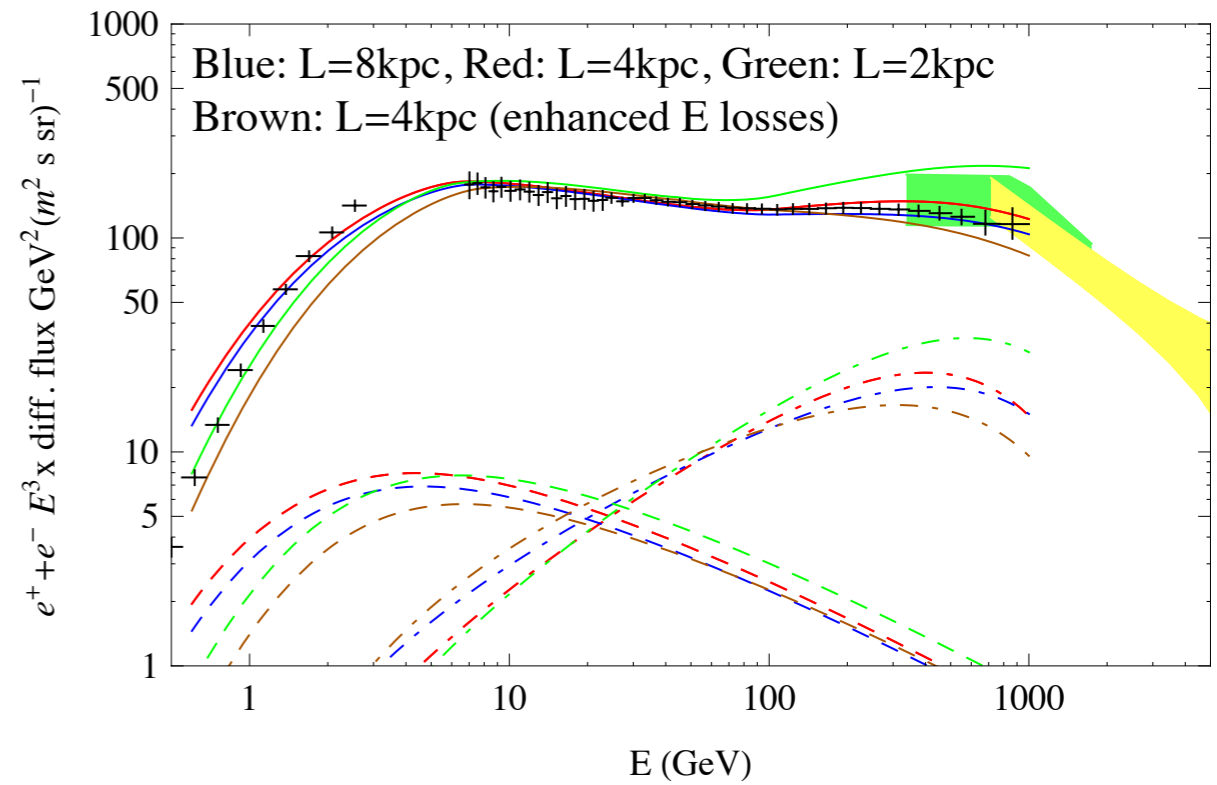
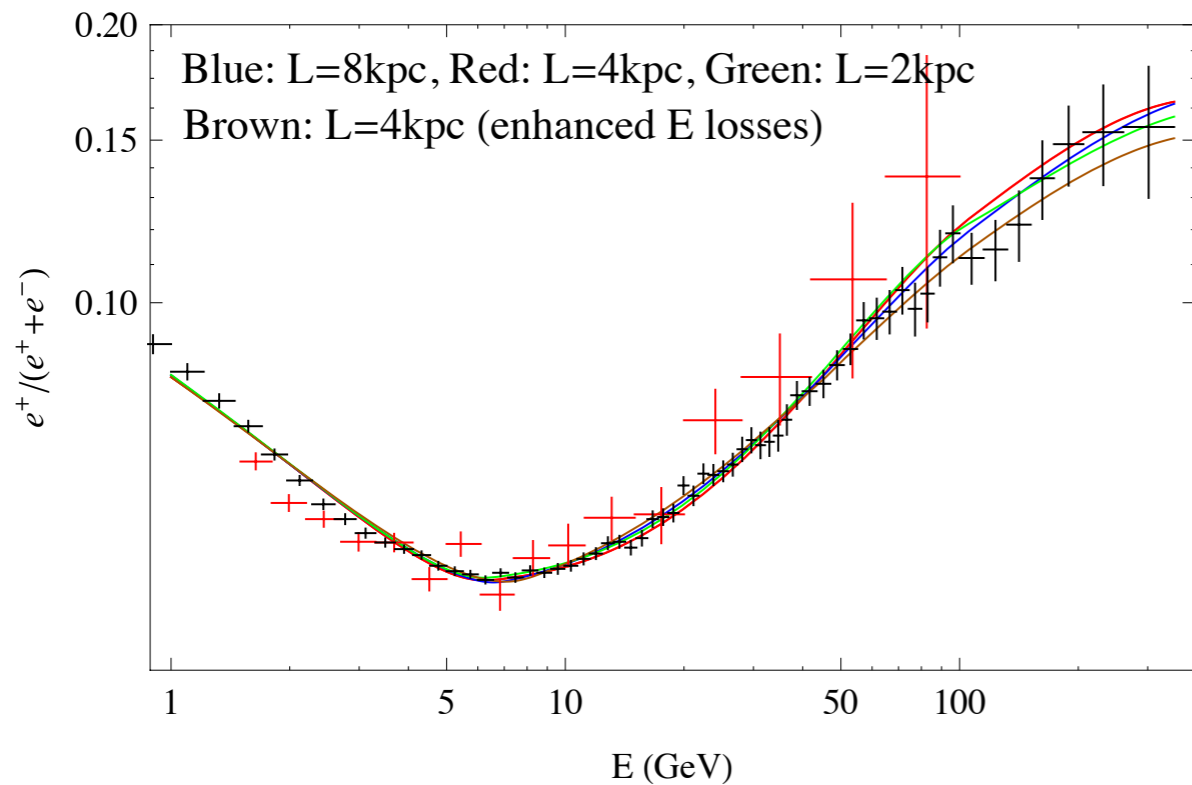
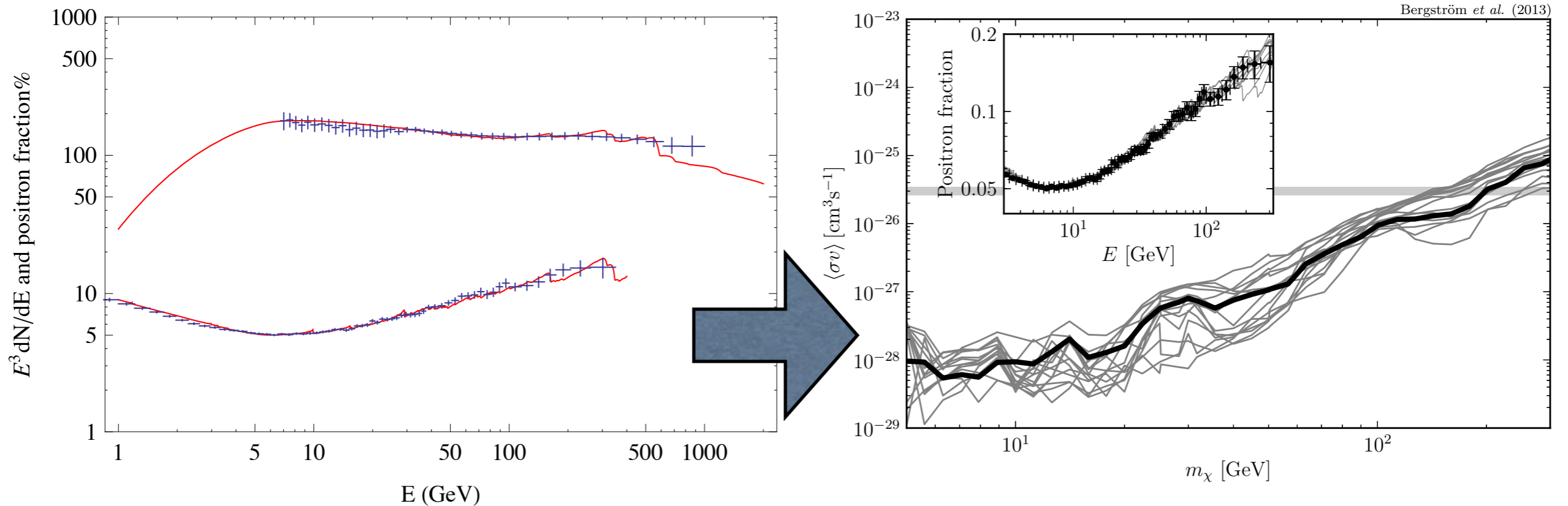


FIG. 4. *Left panel:* Limits obtained when different propagation models for the DM signal are adopted, using the power-law background model adopted in the main text. *Right panel:* Limits derived using different, physically motivated, background models. In both frames, the results are for the case of DM annihilations to e^+e^- .



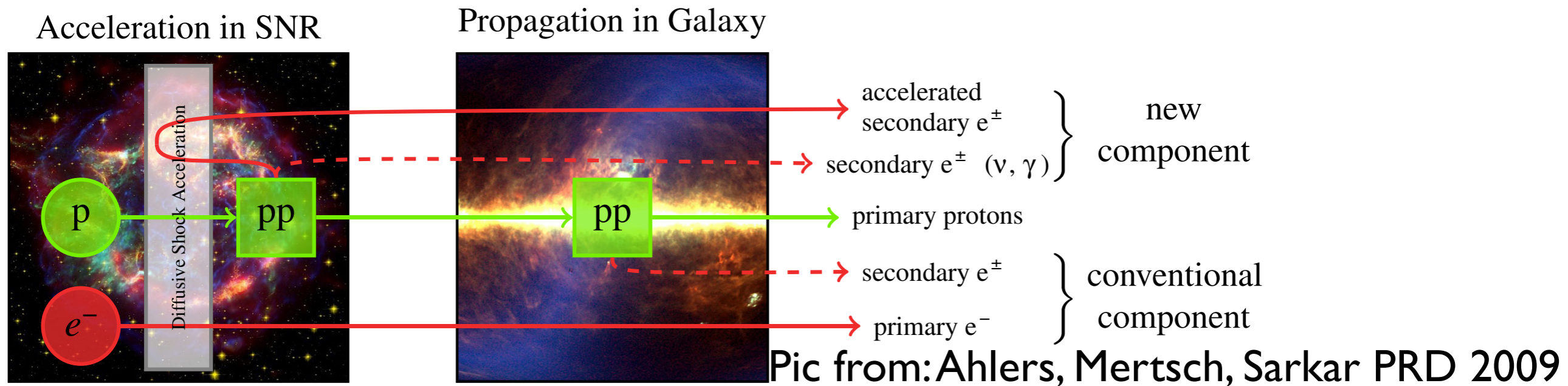


Potential dips in the positron fraction spectrum from astrophysics can impact the limits by a factor of 3. In addition, different propagation conditions due to energy losses in the Galaxy can affect the limits by a factor of 2. Also a factor of ~ 2 from local DM density estimation.

- Also all CR heavy CR nuclei species that will help us out in breaking the degeneracies between DM models/pulsar models and CR galactic propagation

A third option: A hard CR Secondary component from Stochastic Acceleration inside SNRs

Blasi, PRL 2009, Mertsch & Sarkar PRL 2009



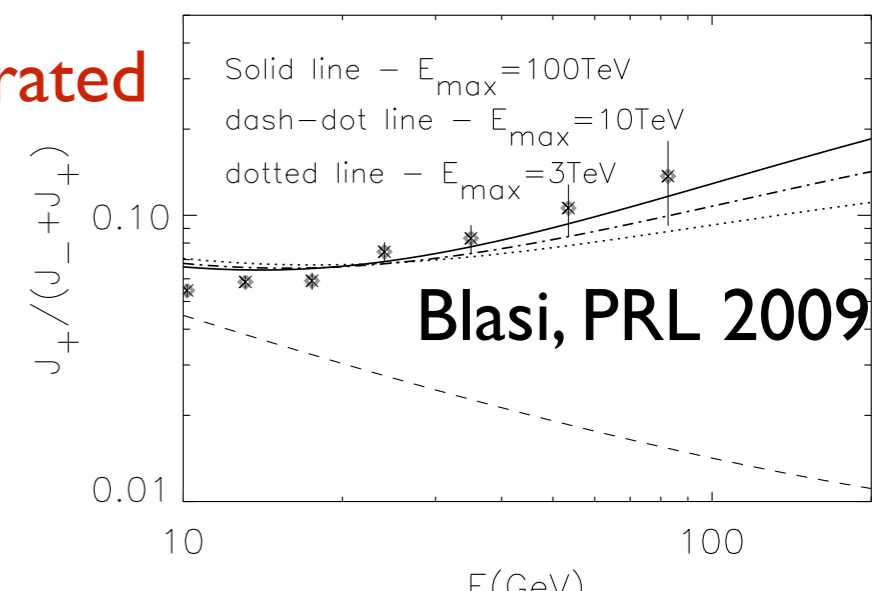
Interplay of three typical timescales for CRs: Spallation, Escape and Acceleration inside the Sources.

If: $\tau_{A \rightarrow B}^{spall} < \tau_A^{esc}$, then we have secondaries produced inside the acceleration region

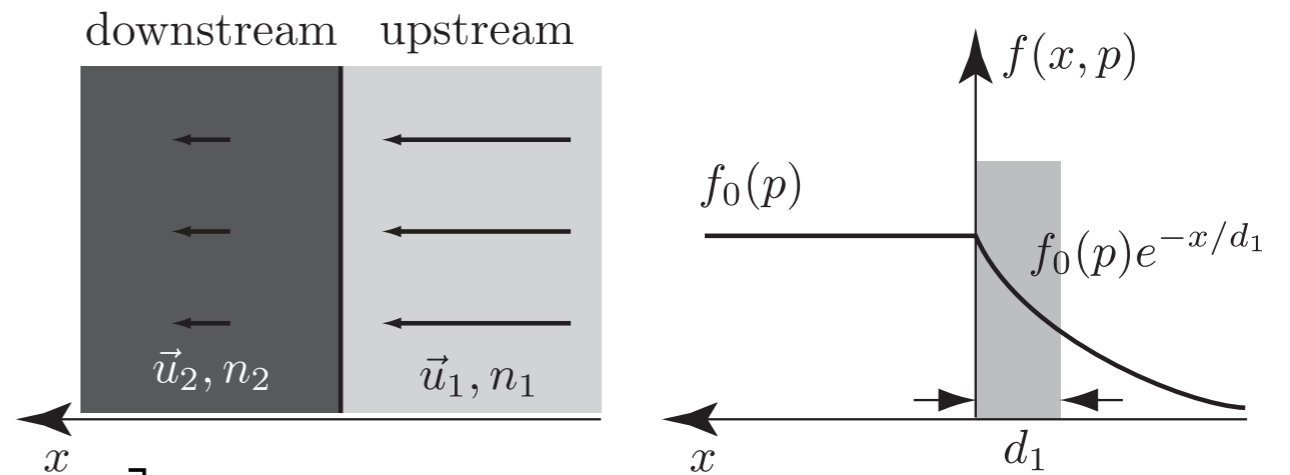
If: $\tau_{acc} < \tau^{spall}$, then secondaries are efficiently accelerated

So: $Acc^A \rightarrow Spall^{A \rightarrow B} \rightarrow Acc^B \rightarrow$

Propagation \rightarrow *Observation*



Some details on the accelerated secondary CRs:



Source term **inside** the SNR:

$$Q_i(E_{kin}) = \sum_j N_j(E_{kin}) \left[\sigma_{j \rightarrow i}^{sp} \beta c n_{gas} + \frac{1}{E_{kin} \tau_{j \rightarrow i}^{dec}} \right]$$

Propagation **inside** the SNR (diffusion, advection, source, decay/spallation and adiabatic E losses):

$$v \frac{\partial f_i}{\partial x} = D_i \frac{\partial^2 f_i}{\partial x^2} + \frac{1}{3} \frac{dv}{dx} p \frac{\partial f_i}{\partial p} - \Gamma_i f_i + q_i$$

Bohm diffusion: $D_i^{\pm}(E) = \frac{K_B r_L(E) c}{3} = 3.3 \times 10^{22} K_B B^{-1} E Z_i^{-1} \text{cm}^2 \text{s}^{-1}$

Thus the source term of SNR CR changes: $f_i^+(x, p) = f_i(0, p) + \frac{q_i^+(0, p) - \Gamma_i^+(p) f_i(0, p)}{v^+} x$

and:

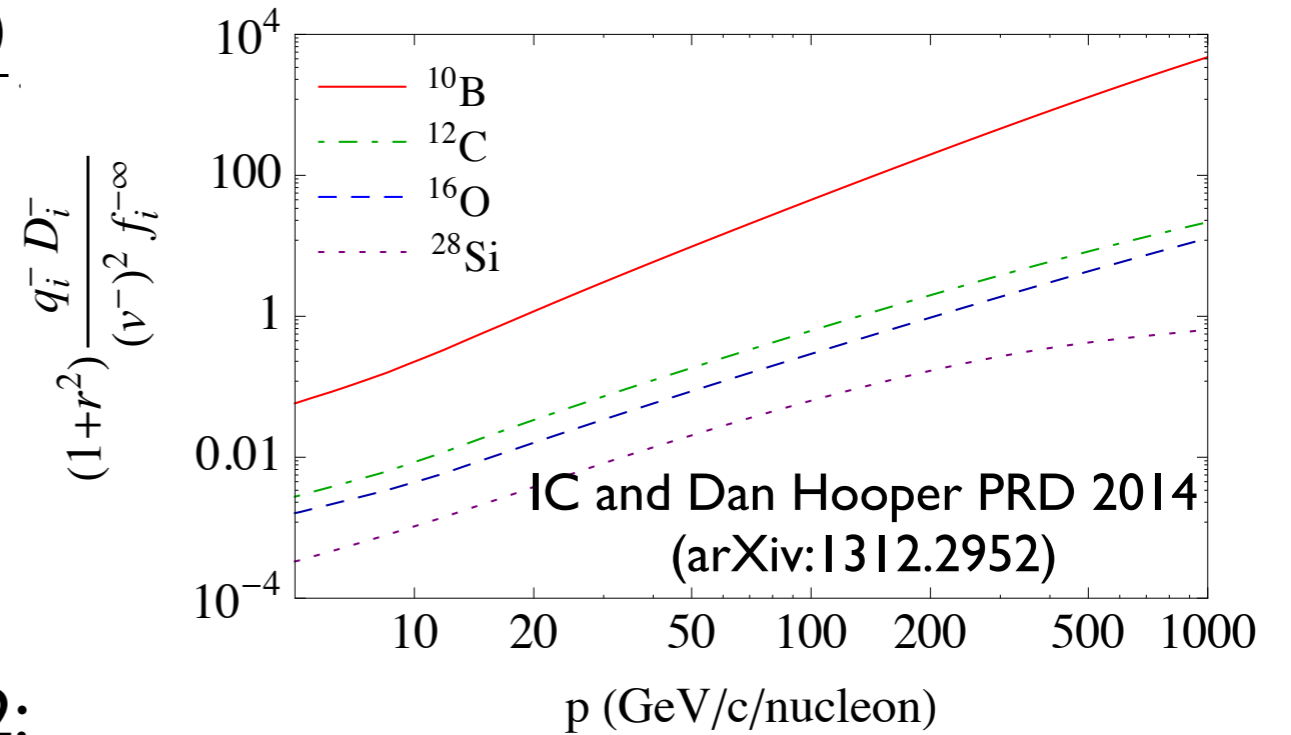
$$f_i(0, p) = \int_0^p \frac{dp'}{p'} \left(\frac{p'}{p} \right)^{\gamma} e^{-\gamma(1+r^2)(D_i^-(p) - D_i^-(p')) \Gamma_i^-(p) / (v^-)^2} \gamma [(1+r^2) \frac{q_i^-(0, p') D_i^-(p')}{(v^-)^2} + Y_i \delta(p' - p_0)]$$

The impact of an individual SNR: $N_i(E) = 16\pi^2 \int_0^{v^+ \tau^{SN}} dx p^2 f_i^+(x, p) (v^+ \tau^{SN} - x)^2$

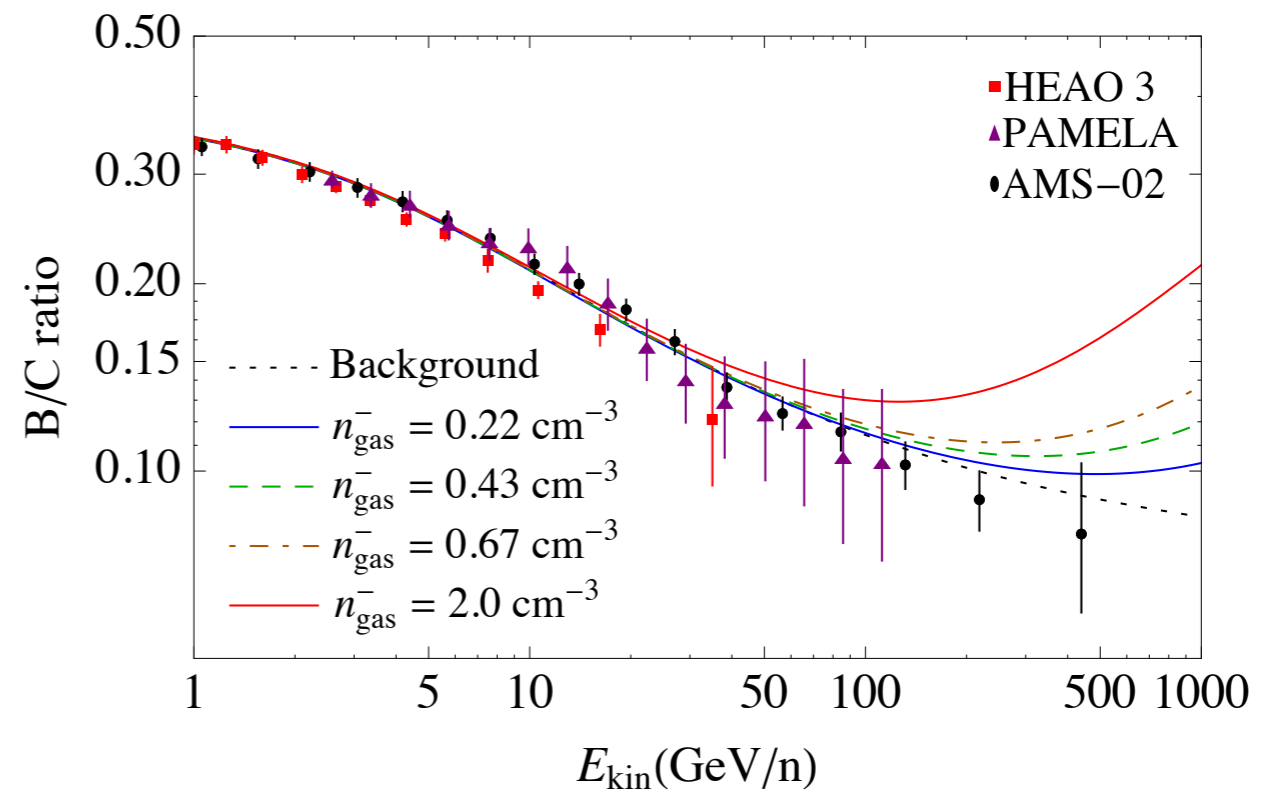
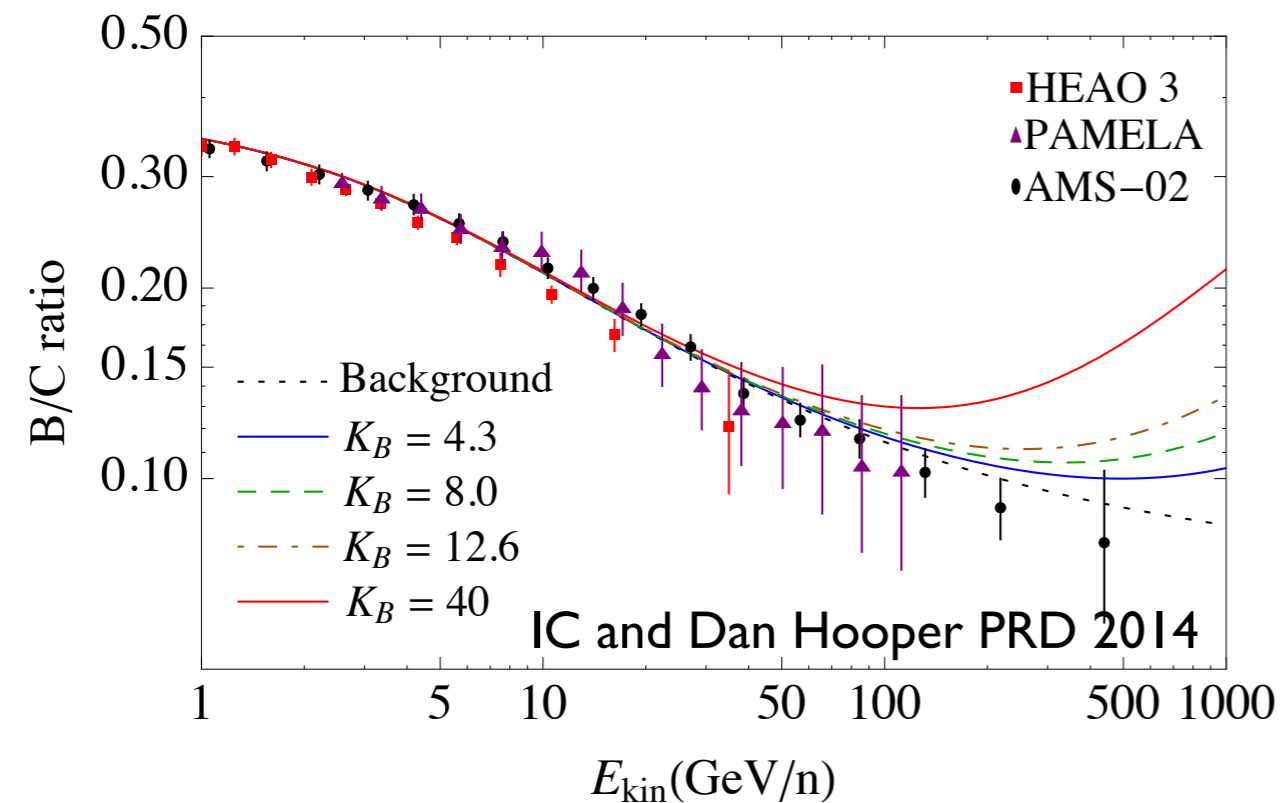
Accounting for all galactic SNRs and including propagation effects:

$$\mathcal{N}_i(E) = \frac{\sum_{j>i} (\Gamma_{j\rightarrow i}^{sp} + 1/(E_{kin} \tau_{j\rightarrow i}^{dec})) \mathcal{N}_j(E) + R_{SN} N_i(E)}{\Gamma_i(E) + 1/\tau_i^{esc}(E)}$$

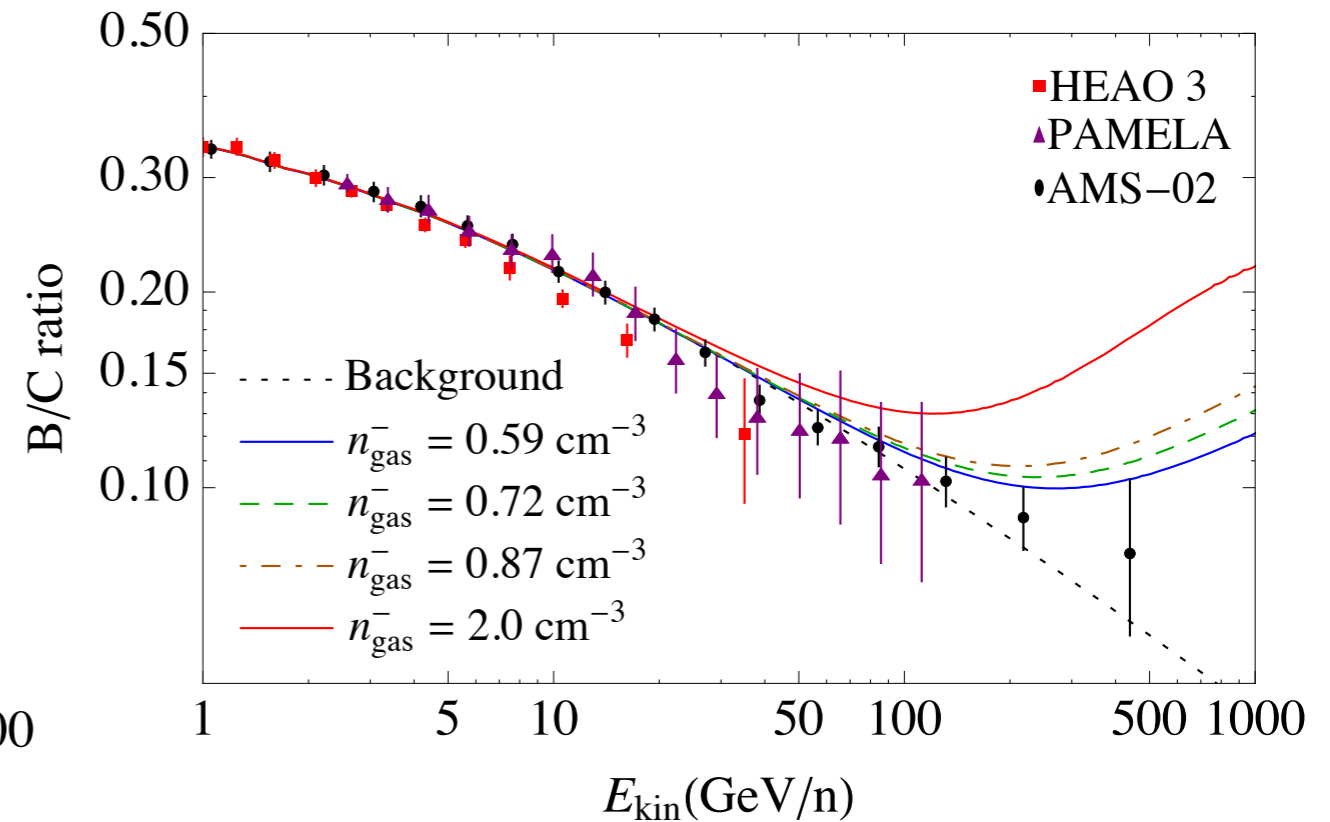
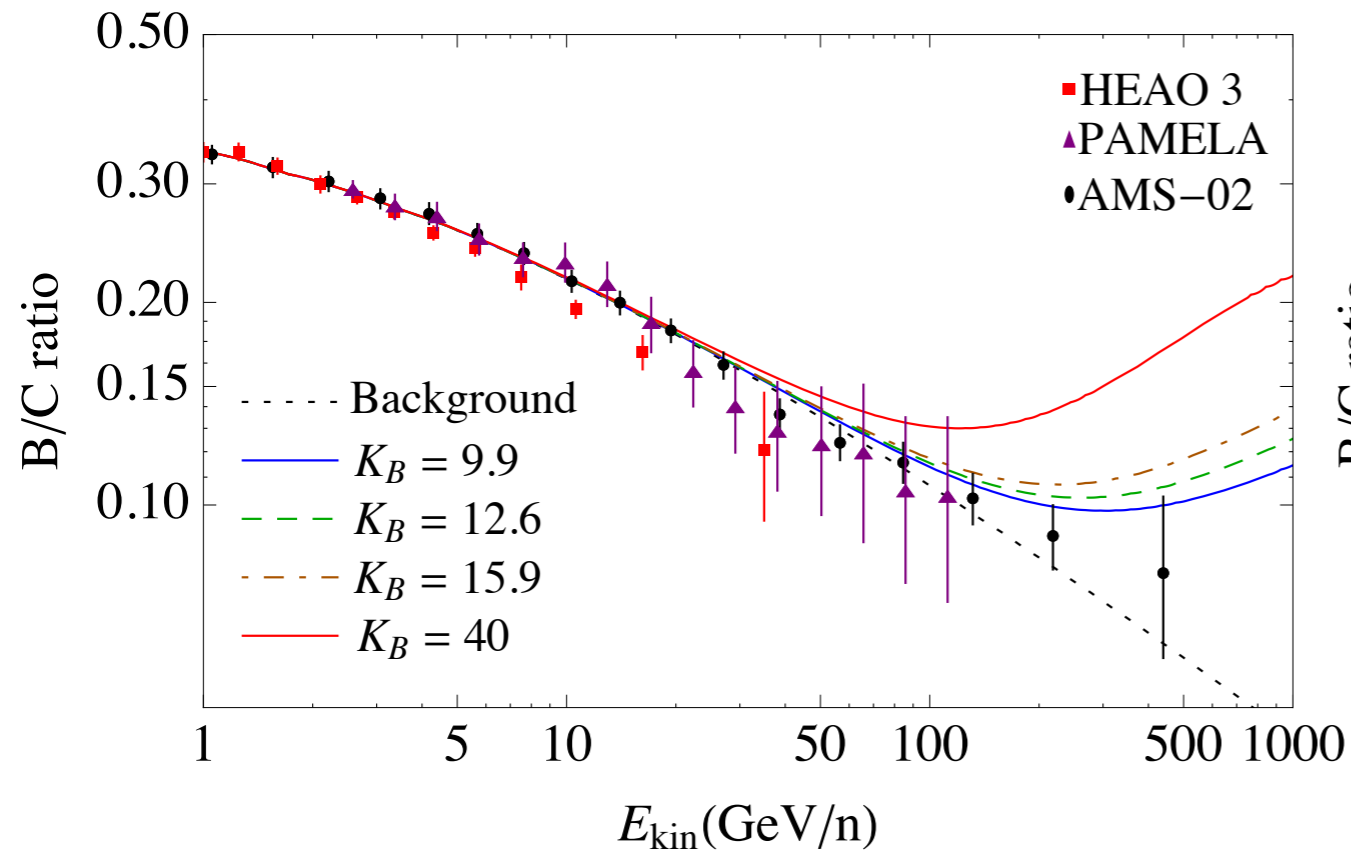
The impact of this additional secondary component is more evident for high E, light nuclei:



Thus a rise in other secondary/primary CR ratios should be observed with AMS-02:

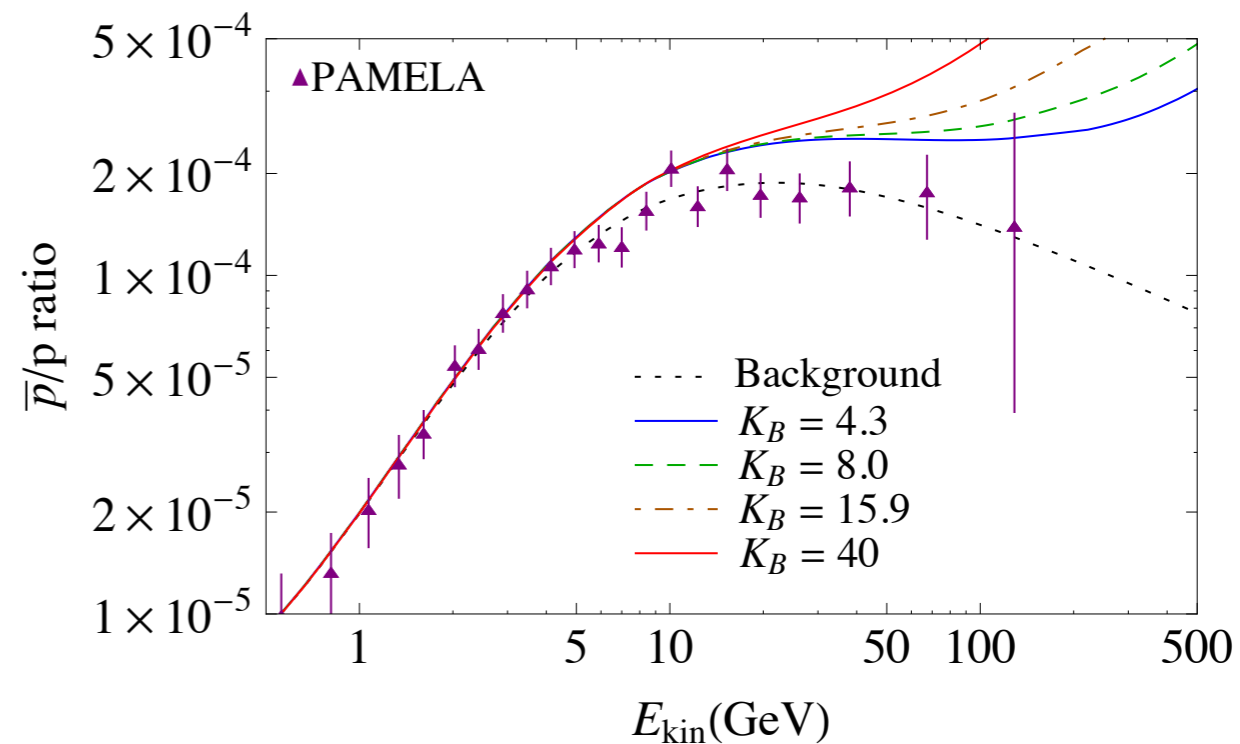
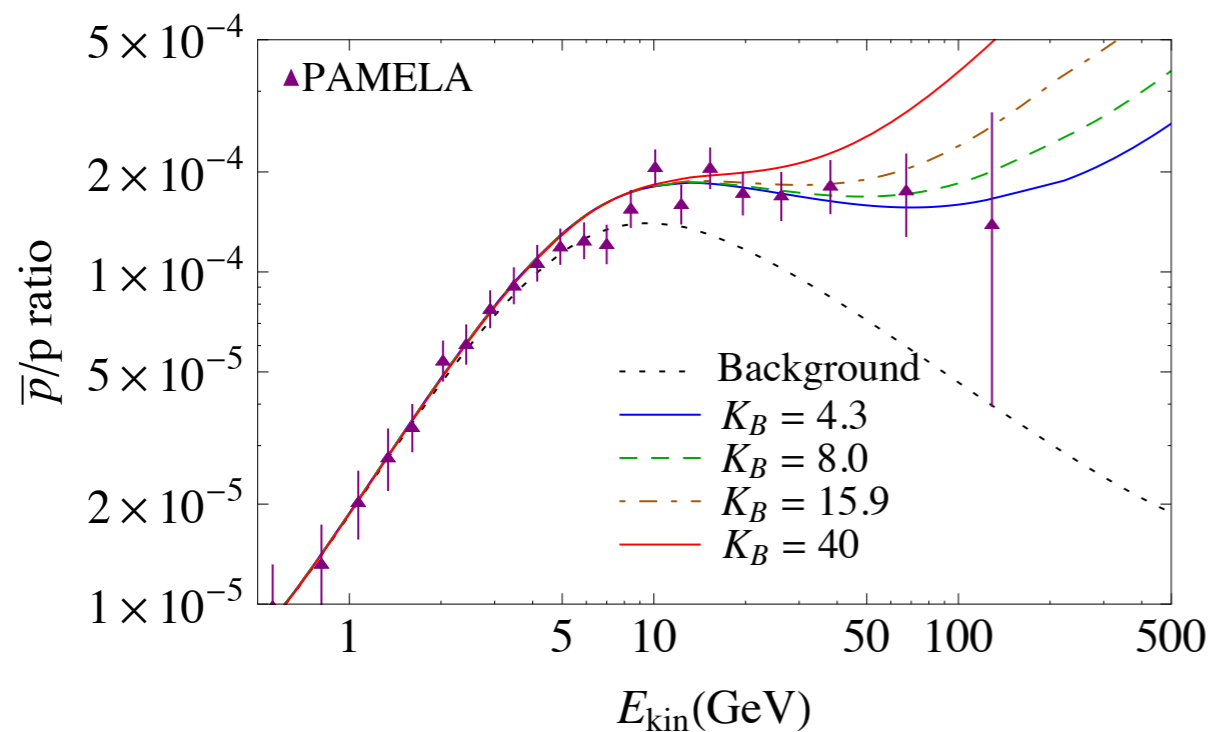


Including uncertainties in the background:

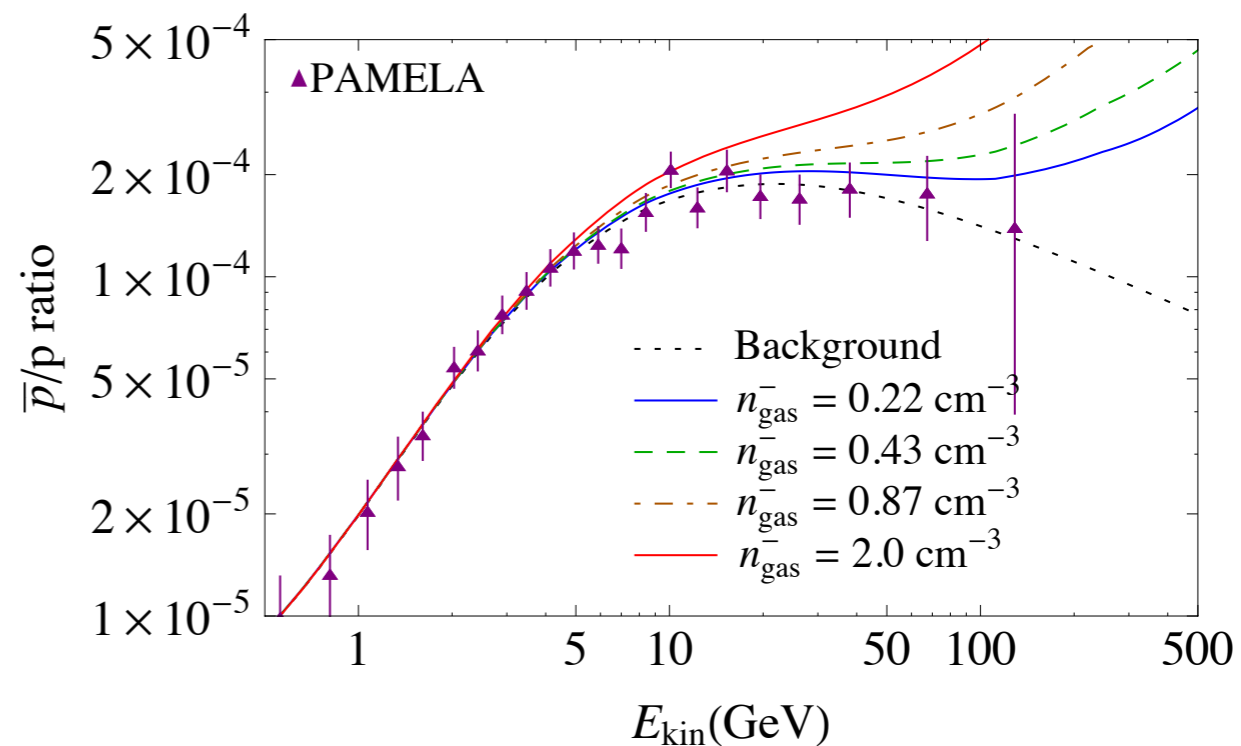
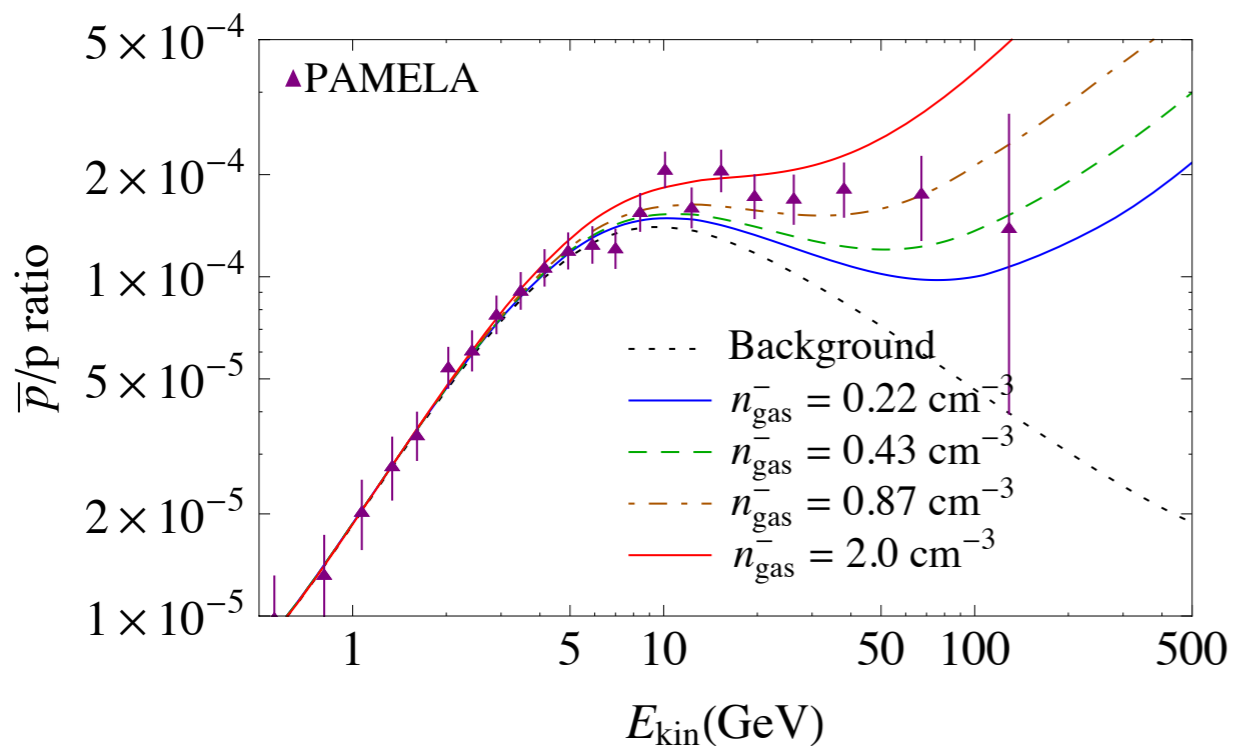


Even after including background uncertainties, the current measurement of the Boron to Carbon ratio, by AMS, severely constrains the acceleration of secondary CRs inside supernova remnants.

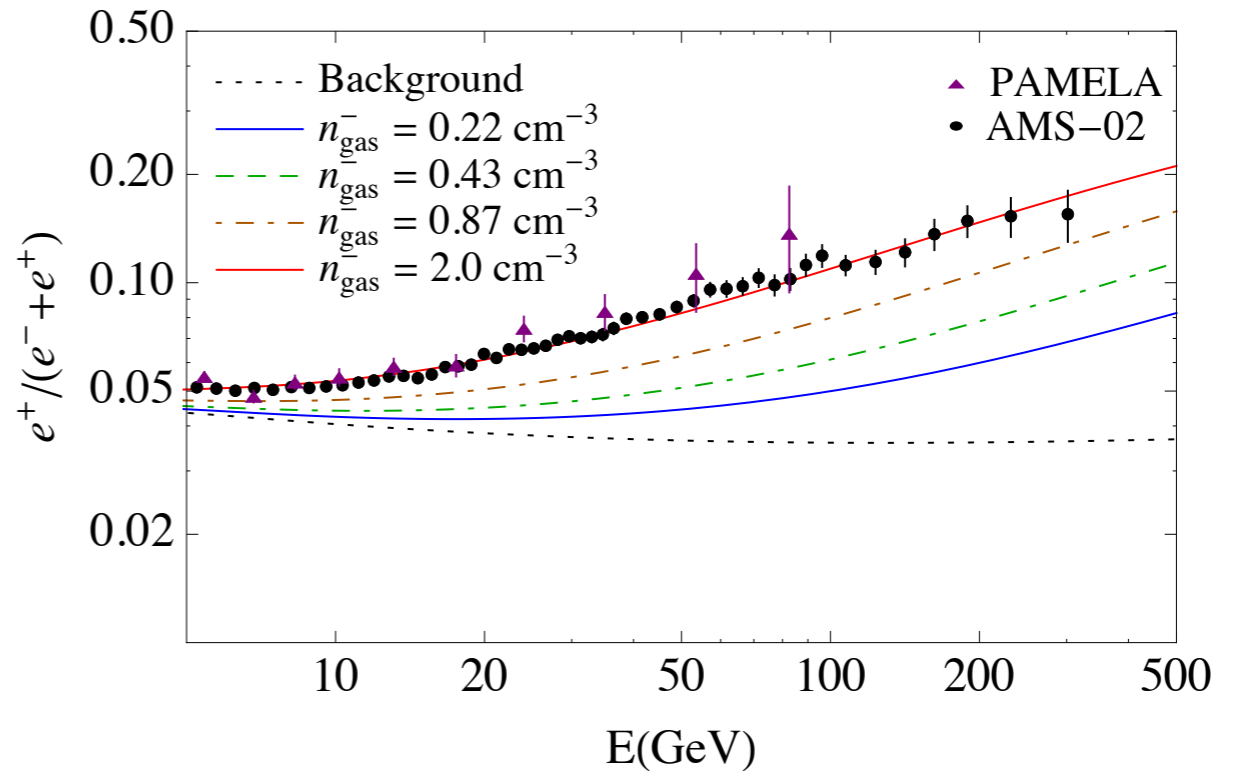
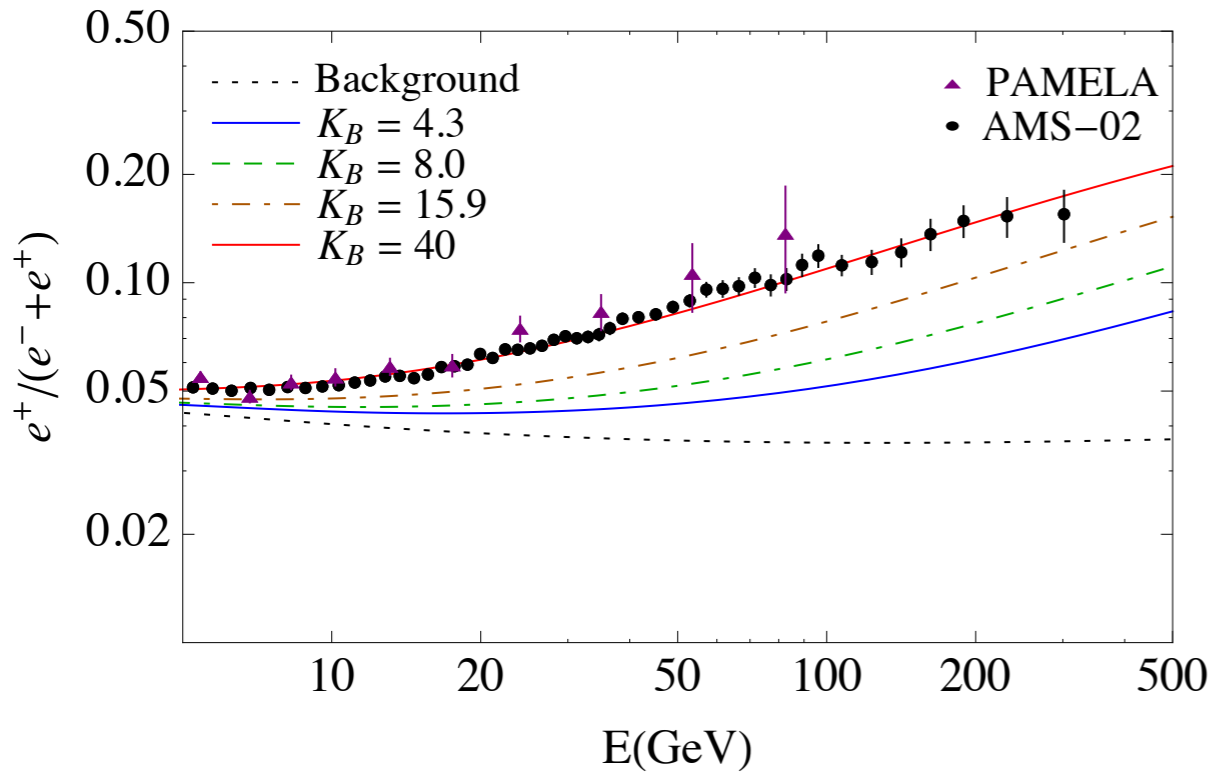
Antiprotons



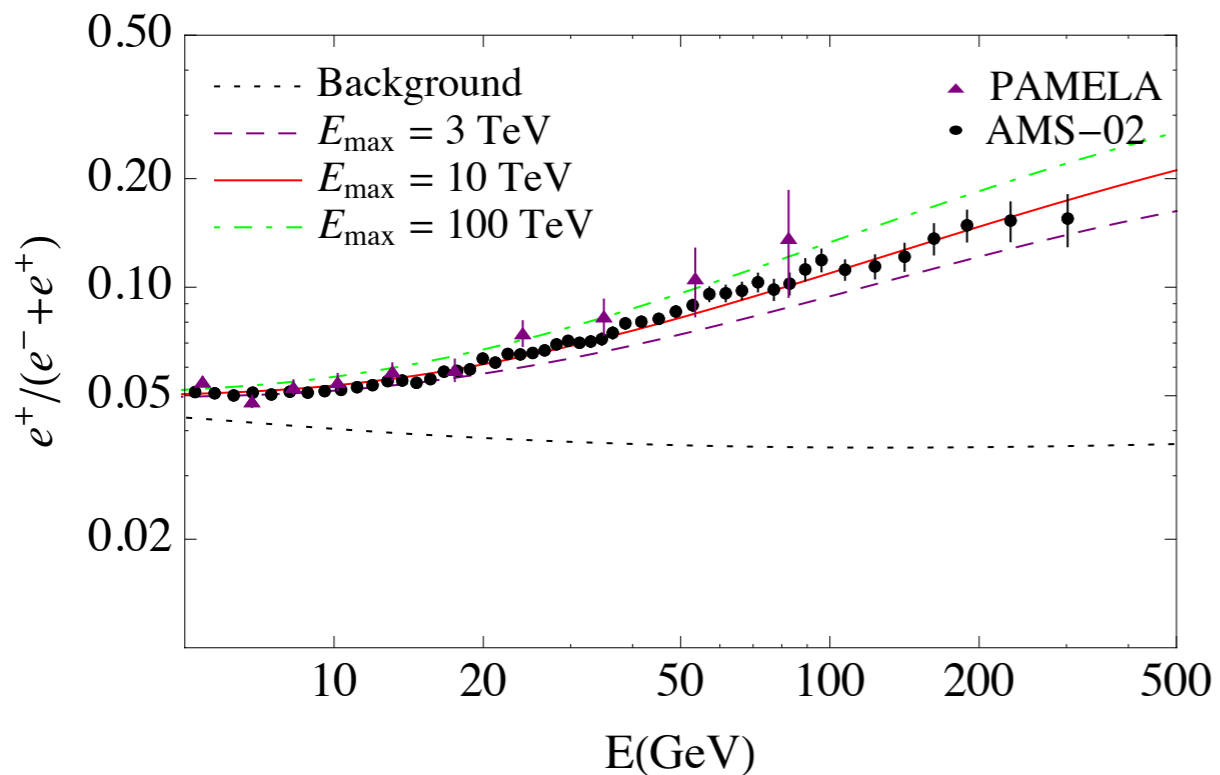
Antiprotons background uncertainties are still large,
(mainly in the high energy production cross-section)



Positrons



Thus secondary CRs inside SNRs can NOT explain the positron fraction excess even for optimistic cases of energy losses inside the SNRs:



Thank you